Turun yliopisto
University of Turku

METAL-ION-BINDING OLIGONUCLEOTIDES: HIGH-AFFINITY PROBES FOR NUCLEIC ACID SEQUENCES

Sharmin Taherpour

University of Turku

Faculty of Mathematics and Natural Sciences
Department of Chemistry
Laboratory of Organic Chemistry and Chemical Biology

Custos

Doctor Tuomas Lönnberg
Department of Chemistry
University of Turku
Turku, Finland

Reviewed by

Professor Doctor Jens Müller
Institute of Inorganic and
Analytical Chemistry, Westfälische
Wilhelms University of Münster
Münster, Germany

Professor Doctor Frank Seela
Institute of Chemistry
University of Osnabrück
Osnabrück, Germany

Opponent

Professor Mikko Oivanen
Department of Chemistry
University of Helsinki
Helsinki, Finland

ABSTRACT

Small non-coding RNAs have numerous biological functions in cell and are divided into different classes such as: microRNA, snoRNA, snRNA and siRNA. MicroRNA (miRNA) is the most studied non-coding RNA to date and is found in plants, animals and some viruses. miRNA with short sequences is involved in suppressing translation of target genes by binding to their mRNA post-transcriptionally and silencing it. Their function besides silencing of the viral gene, can be oncogenic and therefore the cause of cancer. Hence, their roles are highlighted in human diseases, which increases the interest in using them as biomarkers and drug targets. One of the major problems to overcome is recognition of miRNA. Owing to a stable hairpin structure, chain invasion by conventional Watson-Crick base-pairing is difficult. One way to enhance the hybridization is exploitation of metal-ion mediated base-pairing, *i. e.* oligonucleotide probes that tightly bind a metal ions and are able to form a coordinative bonds between modified and natural nucleobases. This kind of metallo basepairs containing short modified oligonucleotides can also be useful for recognition of other RNA sequences containing hairpin-like structural motives, such as the TAR sequence of HIV. In addition, metal-ion-binding oligonucleotides will undoubtedly find applications in DNA-based nanotechnology. In this study, the 3,5-dimethylpyrazol-1-yl substituted purine derivatives were successfully incorporated within oligonucleotides, into either a terminal or non-terminal position. Among all of the modified oligonucleotides studied, a 2-(3,5-dimethylpyrazol-1-yl)-6-oxopurine base containing oligonucleotide was observed to bind most efficiently to their unmodified complementary sequences in the presence of both Cu^{2+} or Zn^{2+}. The oligonucleotide incorporating 2,6-bis(3,5-dimethylpyrazol-1-yl)purine base also markedly increased the stability of duplexes in the presence of Cu^{2+} without losing the selectivity.

Key words: non-coding RNA, microRNA, modified oligonucleotide, hybridization, metal-ion-mediated base pair

TIIVISTELMÄ

Pienillä ei-koodaavilla RNA-molekyyleillä, kuten microRNA, snoRNA, snRNA ja siRNA, on lukuisia biologisia toimintoja solussa. MicroRNA (miRNA) on eniten tutkittu ei-koodaava RNA. Sitä esiintyy sekä kasveissa, että eläimissä ja jopa viruksissa. Lyhyet miRNA-molekyylit estävät kohdegeenin ohjaaman proteiinisynteesin sitoutumalla geenin koodaamaan lähetti-RNA:han. Niiden toiminta voi, viraalisen geenin vaientaminen lisäksi, olla myös onkogeeninen ja siis jopa syöpää aiheuttava. miRNA:n yhteys ihmisen sairauksiin tekee niistä kiinnostavia biomarkkereita ja lääkekehityksen kohteita. Yksi suurimmista ongelmista on miRNA tunnistaminen. Koska niillä on pysyvä hiusneularakenne, invaasio tavanomaisilla Watson-Crick emäspariutumiseen perustuvilla koettimilla on vaikeaa. Yksi tapa parantaa hybridisaatiota on hyödyntää metalli-ionin välittämää emäspariutumista, ts. oligonukleotidikoettimia, jotka sitovat tiukasti metalli-ioneja ja pystyvät muodostamaan koordinoivia sidoksia modifioitujen ja luonnollisten nukleoemäksien välillä. Tällaiset metallo emäsparin sisältävät lyhyet modifioidut oligonukleotidit voivat myös olla käyttökelpoisia sellaisten RNA-sekvenssien tunnistamisessa, jotka sisältävät hiusneula-rakenteita ja pullistumia, kuten HIV:n TAR sekvenssi. Lisäksi metalli-ionin sitovat oligonukleotidit voivat olla potentiaalisia sovelluksia DNA-pohjaisessa nanoteknologiassa. Tässä tutkimuksessa, 3,5-dimetyylipyratsol-1-yyli substituoitu puriini-johdos liitettiin onnistuneesti oligonukleotidisekvenssiin, joko terminaaliseen tai ei-terminaaliseen asemaan. Kaikista tutkituista modifioiduista oligonukleotideista, 2-(3,5-dimetyylipyratsol-1-yyli)-6-oksopuriiniemäksen sisältävän oligonukleotidin havaittiin sitoutuvan tehokkaimmin modifioimattomaan komplementaariseen sekvenssiin, kun läsnä oli joko Cu^{2+} tai Zn^{2+} ioni. Oligonukleotidi, joka sisälsi 2,6-bis (3,5-dimetyylipyratsol-1-yyli) puriiniemäksen, lisäsi myös merkittävästi dupleksin stabiilisuutta menettämättä selektiivisyyttä Cu^{2+}:n läsnä ollessa.

Asiasanat: ei-koodaava RNA, microRNA, modifioitu oligonukleotidi, hybridisaatio, metalli-ioni-välitteinen emäspari

PREFACE

This thesis is based on experimental work carried out in the Laboratory of Organic Chemistry and Chemical Biology at the Department of Chemistry, University of Turku during the years 2010-2015. The financial support of Academy of Finland and Department of Chemistry are gratefully acknowledged.

First of all, I wish to express my deepest gratitude to my supervisor Dr. Tuomas Lönnberg for giving me a chance to work as a PhD student in the field of nucleic acids under his continual guidance and limitless support. His valuable advices, an excellent knowledge of synthetic Chemistry, in particular in Oligonucleotide Chemistry and skills in scientific writing have made this thesis to become reality. I am also very grateful to Professor Harri Lönnberg for his brilliant experience of Organic Chemistry and for his optimism and encouraging guidance. Without his continuous support and amazing science this work would never have been completed.

I wish to thank Professor Jorma Arpalahti for his skill and helpful advices in Bioinorganic Chemistry systems. I am very thankful to my collaborator Oleg Golubev for his contribution to the paper III included in this thesis.

I am indebted to Professor Frank Seela and Professor Jens Müller for their careful reviewing of my thesis. I am also thankful to Professor Mikko Oivanen for accepting to be my opponent.

My special thanks is reserved for my closest friend Dr. Heidi Korhonen for her great support and encouragements and all the joyful moments inside and outside the work. You are not only the closest friend to me, but also very precious to me just like a family member. I am also truly grateful to my closest coworker Dr. Emilia Kiuru for her friendship and importing a positive working atmosphere. It is really easy to approach you and share with you my joys and worries.

I would also like to thank Dr. Päivi Poijärvi-Virta, Dr. Helmi Neuvonen, Dr. Satu Mikkola, Dr. Mikko Ora, Dr. Pasi Virta for being good teachers and supervisors during my MSc and PhD degree times.

My warm gratitude goes to all the present and former co-workers in the Laboratory of Organic Chemistry and Chemical Biology for creating a nice working environment: Dr Anu Kiviniemi, Lotta Granqvist, Dr Tuomas Karskela, Marika Karskela, Dr. Anna Leisvuori Dr. Teija Niittymäki, Maarit Laine, Dr. Diana Florea-Wang, Dr. Alejandro Gimenez Molina, Satish Jadhav, Ville

Turku, September 2015

Sharmin Taherpour

CONTENTS

LIST OF ORIGINAL PUBLICATIONS

This thesis is based on the following publications (I-IV):

I Taherpour, S., Lönnberg, T.: Metal Ion Chelates as Surrogates of Nucleobases for the Recognition of Nucleic Acid Sequences: The Pd^{2+} Complex of 2,6-Bis(3,5-dimethylpyrazol-1-yl)purine Riboside. *J. Nucleic Acids*, **2012**, 2012, article ID 196485.

II Taherpour, S., Lönnberg, H., Lönnberg, T.: 2,6-Bis(functionalized)purines as metal-ion binding surrogate nucleobases that enhance hybridization with unmodified 2'-*O*-methyl oligoribonucleotides. *Org. Biomol. Chem.*, **2013**, 11, 991-1000.

III Taherpour, S., Golubev, O., Lönnberg, T.: Metal-ion-mediated base pairing between natural nucleobases and bidentate 3,5-dimethylpyrazolyl-substituted purine ligands. *J. Org. Chem.*, **2014**, 79, 8990-8999.

IV Taherpour, S., Lönnberg, T.: Fluorescence probing of metal-ion-mediated hybridization of oligonucleotides. *RSC Adv.*, **2015**, 5, 10837-10844.

ABBREVIATIONS

A	adenosine
Ac	acetyl
AU	absorption unit
C	cytidine
CD	circular dichroism
COSY	correlation spectroscopy
CPG	controlled pore glass
dC	2´-deoxycytidine
DCA	dichloroacetic acid
DIPEA	*N,N*-diisopropylethylamine
DMF	*N,N*-dimethylformamide
DMTr	4,4´-dimethoxytrityl (4,4´-dimethoxytriphenylmethyl)
DMSO	dimethyl sulfoxide
DNA	deoxyribonucleic acid
DLS	dynamic light scattering
ESI	electrospray ionization
FRET	fluorescence resonance energy transfer
G	guanosine
HBTU	*O*-(benzotriazol-1-yl)-*N,N,N´,N´*-tetramethyluronium hexafluoro-phosphate
HIV	human immunodeficiency virus
HMBC	heteronuclear multiple bond correlation
HPLC	high performance liquid chromatography
HSQC	heteronuclear single quantum coherence
MeCN	acetonitrile
MS	mass spectrometry
NMR	nuclear magnetic resonance
ON	oligonucleotide
ORN	oligoribonucleotide
PMT	photomultiplier tube
Py	pyridine
RNA	ribonucleic acid
RP	reversed phase
T	thymidine
T_m	melting temperature
TAR	trans-activating response element
TBDMS	*tert*-butyldimethylsilyl
TEA	triethylamine
TEAA	triethylammonium acetate
TFA	trifluoroacetic acid
THF	tetrahydrofuran
Tr	trityl
U	uridine
UV	ultraviolet

1. INTRODUCTION

1.1 Structure and biological role of nucleic acids

Nucleic acids, DNA (deoxyribonucleic acid) and RNA (ribonucleic acid) are linear biopolymers that play an important role in encoding, transmitting and expressing genetic information for protein synthesis. While DNA appears to serve as a relatively passive storage for this information, the biological functions of RNA are much more diverse. In particular, the various types of small non-coding RNA[1-7] molecules have recently attracted interest as potential targets for diagnostics and chemotherapy.[8-22]

Nucleic acid is a polymer that is formed from nucleotides, which consist of a pentose sugar, a phosphate group and a nucleobase moiety. The main difference between the two types of nucleic acids resides in the structure of the sugar moiety: with DNA 2´-deoxyribose and with RNA ribose. The nucleobases are either purine (adenine and guanine) or pyrimidine bases (thymine, cytosine and uracil). Three nucleobases: adenine, cytosine, and guanine are common to both DNA and RNA, whereas thymine occurs in DNA and uracil correspondingly in RNA. The nucleobase is connected to C1´ of the pentose sugar through an N-glycosidic linkage from a nucleobase ring nitrogen: N1 for pyrimidines and N9 for purines. The nucleosides are, in turn, linked to each other through 3´,5´-phosphodiester linkages (Figure 1).
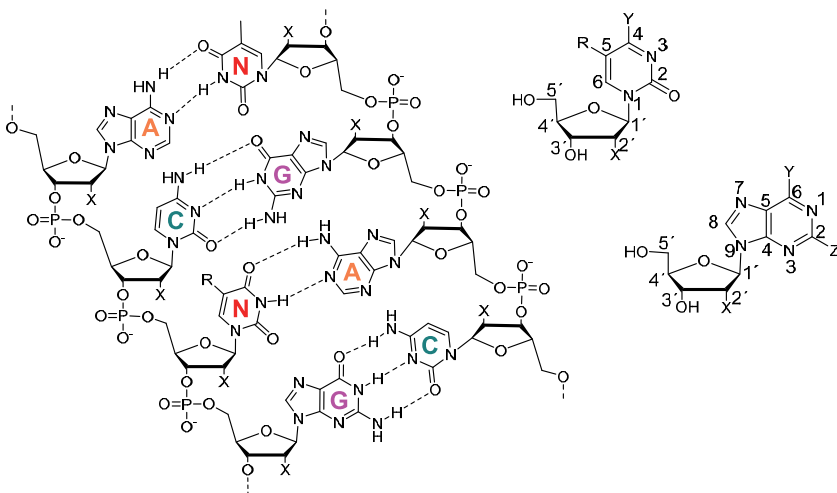
Figure 1. *The double-stranded structure of DNA (or RNA) and hydrogen bonding of the Watson-Crick base-pairing. DNA: X = H, N = T (R = CH₃); RNA: X = OH, N = U (R = H); Y or Z = NH₂ or O; A = Adenine; G = Guanine; C = Cytosine; U = Uracil; T = Thymine*

1.1.1 Watson-Crick base pairing

The hybridization of DNA into a double helix, as well as the transcription of genetic information from DNA to RNA is controlled by Watson-Crick base pairing. Adenine recognizes thymine or uracil and guanine recognizes cytosine by formation of two and three hydrogen bonds, respectively (Figure 1). Although base-stacking plays a more important role in stabilizing the double-helical secondary structure,[23] Watson-Crick base pairing accounts for the high fidelity of the recognition of specific nucleic acid sequences.

1.2 Metal-ion-mediated base pairing

In metal-ion-mediated base pairing, a specific hydrogen bond is replaced with two coordinative covalent bonds. An electronegative atom within the nucleobases (or their surrogates) on opposite strands donates an electron pair to a common metal ion. This donor atom is usually nitrogen, but it may also be oxygen (Scheme 1). While this kind of metal-ion-mediated bonding is weaker than real covalent bonds, it still is much stronger than hydrogen bonding, the bond energies falling in the range of 10-30 kcal mol^{-1} and 0.7-1.6 kcal mol^{-1}, respectively.[23,24] Accordingly, a remarkable duplex stabilization may take place.

Often the structure of canonical nucleobases has to be modified to achieve duplex stabilization by metal ions. Detailed information on the structure of the ligands and their ability to bind metal ions is required for the design of workable metallo base pairs. It is useful to investigate the structure and stability of the metallo base pairs first at monomeric level. This may be carried out by crystallography,[25] by using DFT (density functional theory) modelling,[26-29] or NBO (natural bond orbital), MIA (metal ion affinity) and QTAIM (quantum theory of atoms in molecules) analysis,[30] or by experiments in solution applying NMR, EPR (electron paramagnetic resonance) and mass spectrometry and UV/Vis spectroscopy.[31-34] Many factors, such as acidity, geometry and coordination type of metal ions affect selecting appropriate metal-ion for a given nucleobase.[26]
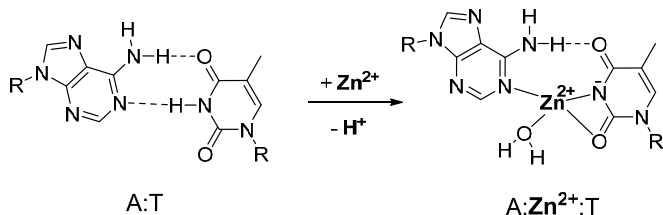
Scheme 1. *Suggested structure by Lee et al. of a base pair formed by specific hydrogen bonds (A:T), and coordination of metal-ion by coordinate covalent bond (A:Zn^{2+}:T);R = sugar.*[35]

1.2.1 Lewis and Brønsted Acidity

The affinity of a given ligand to a given metal ion depends on the Brønsted and Lewis basicities of the donor atom(s). Assuming identical steric factors, more basic ligands form more stable complexes with metal ions. Hard Lewis acids (*e.g.* alkali metals, alkaline-earth metals, lanthanides) favor hard Lewis bases (such as oxygen) and soft Lewis acids (*e.g.* Ag$^+$, Au$^+$, Cd^{2+}, Hg^{2+}, Pd^{2+}, Pt^{2+}, Ru^{2+}) favor soft Lewis bases (such as sulfur and nitrogen). Intermediate metal-ions (*e.g.* Mn^{2+}, Fe^{2+}, Co^{2+}, Ni^{2+}, Cu^{2+} and Zn^{2+}) coordinate reasonably well to both hard and soft bases. As a consequence, soft metal ions coordinate to the endocyclic nitrogen atoms (N3 of cytosine, thymine and uracil and N1 and N7 of guanosine and adenosine) of natural nucleobases (Figure 2).[36] In addition, the oxo substituents are potential exocyclic ligands that can participate in the binding, especially with hard metal-ions. Finally, protons can compete with metal ions for binding to a donor atom. For example, guanine N1 and thymine N3 (Figure 2 and 3) may only coordinate metal ions in their deprotonated form, *i.e.* under sufficiently basic conditions. Under more acidic conditions, the metalation takes place at N7 of guanosine and O4 of thymidine nucleosides (Figure 3).
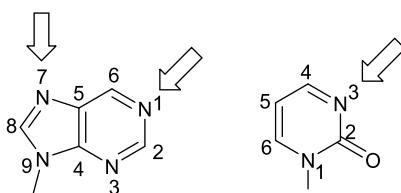
Figure 2. *Purine and pyrimidine structure and their favored coordination sites (indicated by arrows).*
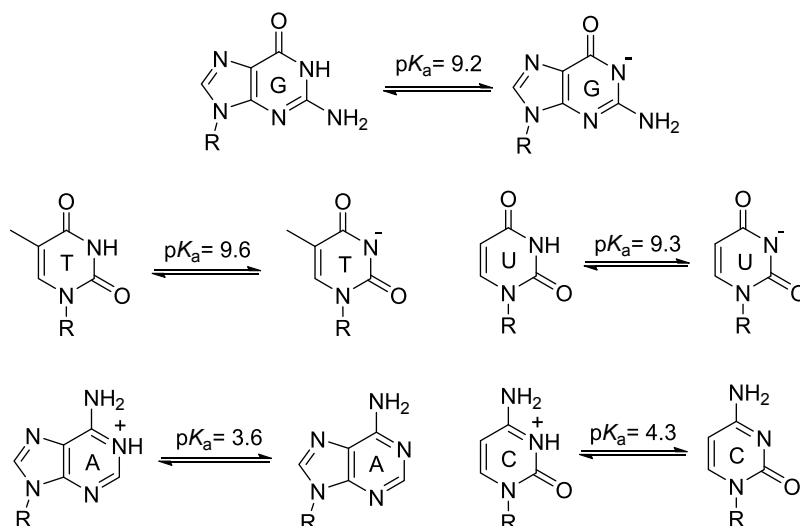
Figure 3. *Acidity constants and protonation/deprotonation features for all natural nucleosides (R = sugar).[36]*

1.2.2 Geometry and mode of coordination

Besides the Brønsted and Lewis basicity of nucleobases, steric factors and coordination geometry are of importance for metallo base pair formation. For example, N1 of adenosine is a poorer ligand for metal ions than N1 of 9-(β-D-ribofuranosyl)purine even though it is more basic.[37] The reason is that the exocyclic 6-amino group of adenine causes a steric hindrance for coordination to N1. Another important aspect is the geometry of the metal- ion-mediated base pairs. The complex should be accommodated within the ideal structure of B-form DNA (or A-form RNA). In particular, due to the planar structure of stacked base-pairs in DNA and RNA, the optimal coordination geometry of a metal ion base pair should be planar. Metallo base pairs deviating from the ideal coplanar orientation induce major destabilizing effects (Figure 4) in the helical structure.[26,38,39]
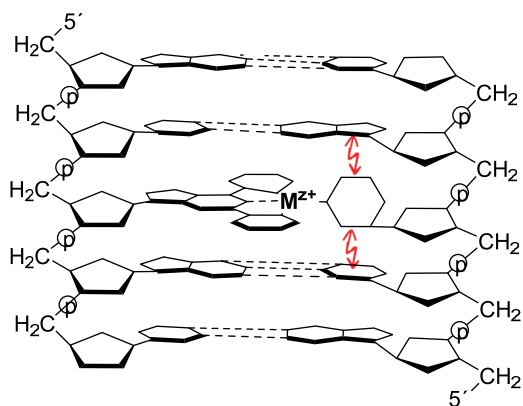
Figure 4. *The perpendicular orientation of a metallo base pair within a double helix decreases the π stacking interaction and destabilizes the duplex.*

The relative orientation of the nucleobases within a metal-ion-mediated base pair is largely dictated by the coordination geometry of the metal ion. In principle, linear, trigonal planar (or trigonal bipyramidal) and square-planar (or octahedral) geometries can be accommodated within the base-stack of a double helical nucleic acid. The metal-ion-mediated base pair can, hence, be formed via (1+1)[40,41], (2+1)[42,43], (2+2)[44,45] or (3+1)[46,47] types of coordination (Scheme 2A-F).[48,49] Of these, only the (2+2) coordination forces the base pair to assume a co-planar conformation. The other coordination types allow rotation about one or more bonds and especially in the case of sterically demanding ligands, a perpendicular conformation may be favored (Schemes 2D-E).[39] On the other hand, hydrogen bonding interactions between the two ligands may stabilize the coplanar conformation (Scheme 2F). Other coordination types such as (3+3), (1+1+1) and (2+2+2) have also been reported but they generally lead to formation of higher-order structures.[50-52]
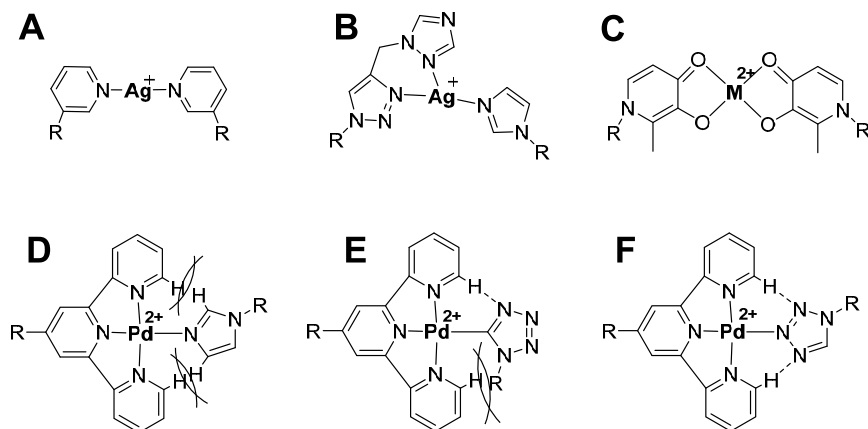
Scheme 2. *Formation of metallo base pair via (1+1)(A), (2+1)(B), (2+2)(C) and (3+1)(D-F) types of coordinaton. Tridentate terpyridine and monodentate imidazole (D) and tetrazole with two different binding modes via Pd^{2+} ion: C1 (E) and N3 (F). R = sugar or methyl.*[39,42,44,51]

1.3 Metal-ion-mediated base pairs within unmodified DNA or RNA

The effect of metal ions on the structure of natural DNA was studied largely in the 1960s with a variety of transition metal-ions such as: Co^{2+}, Ni^{2+}, Mn^{2+}, Cd^{2+}, Zn^{2+}, Cu^{2+}, Hg^{2+}, Ag^+.[53,54] According to potentiometric, UV-spectrophotometric and NMR measurements, only Hg^{2+} [54] and Ag^+ [55,56] were capable of binding strongly to nucleobases without unwinding the double helix or binding to the phosphate groups. The (1+1) coordination of metal-ion is often observed in this case. Divalent metal ions, such as Zn^{2+}, Co^{2+}, and Ni^{2+}, have been reported to mediate base pairing at high pH,[35] *i.e.* under conditions where the metal ion is able to compete with proton for N3 of U/T and N1 of G. Metal-ion-mediated base-pairing has been reported for both Watson-Crick pairs as well as C:C and T:T (or U:U) mispairs.[57-61] The term metal-DNA was first used by Lee *et al*.[49,62] The best-known example of metal ion coordination to unmodified nucleic acids undoubtedly is the crosslinking of DNA by platinum compounds.[63] However, as these compounds tend to distort the DNA double helix rather than form well-defined metallo base pairs within it, they fall beyond the scope of this dissertation.

Incorporation of metal ions within canonical Watson-Crick base pairs at high pH has been demonstrated with divalent Zn^{2+}, Co^{2+}, and Ni^{2+} ions by Lee *et al*.[35,64] The metal ion coordination was studied by NMR titration by tracking the proton signals of N3-H of thymine or N1-H of guanine. In Lee´s model (Figure 5A) one

of the protons, either N3-H of thymine or N1-H of guanine, was replaced by a divalent metal-ion and thus, one positive charge was left on the double helix. Alternative modes for incorporation of metal ions to natural base pairs has been suggested by Lippert *et al.* (Figure 5B)[65] and Alexandre *et al.* (Figure 5C).[66]
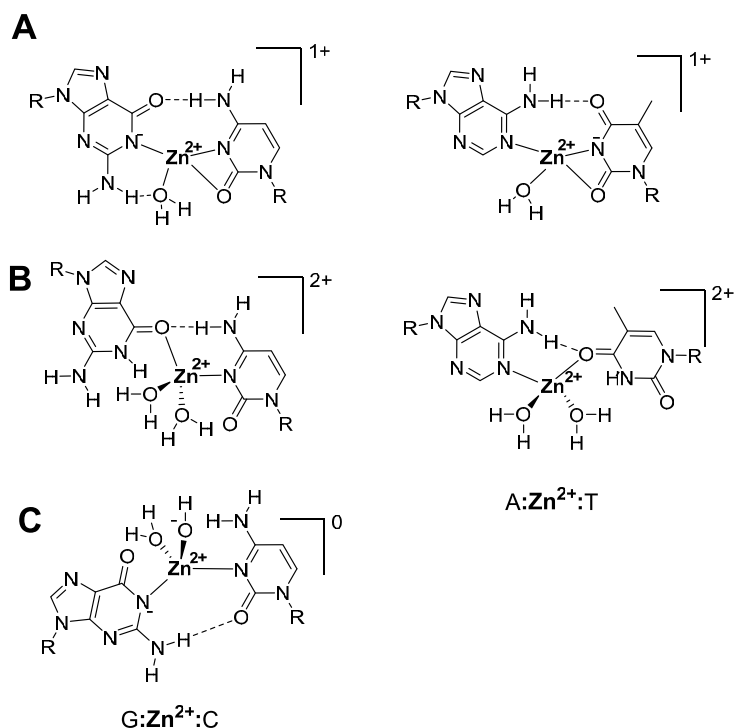
Figure 5. Suggested structures of the natural base pairs in the presence of Zn^{2+} ion according to Lee´s (A), Lippert´s (B) and Alexandre´s (C) model (R = sugar).[35,62,65,66]

The most extensively studied example of a mispair stabilized by a bridging metal ion is the T:Hg⁺:T base pair (Figure 6), first suggested by Katz as early as 1963.[49,57] The formation of T:Hg⁺:T metallo base pairs has since been confirmed by X-ray crystallography.[58,67] Further studies on the coordination of the Hg^{2+} to two thymines were carried out by Ono *et al.* using fluorescence, melting temperature and ESI mass spectrometric measurements.[68-70] The DNA structure was also explored by NMR, using ¹⁵N3-labeled thymine bases, which allowed the measurement of the $^2J_{NN}$ coupling constant.[33,70] By this method, formation of three sequential T:Hg⁺:T base pairs in 3-mer duplex DNA could be confirmed.
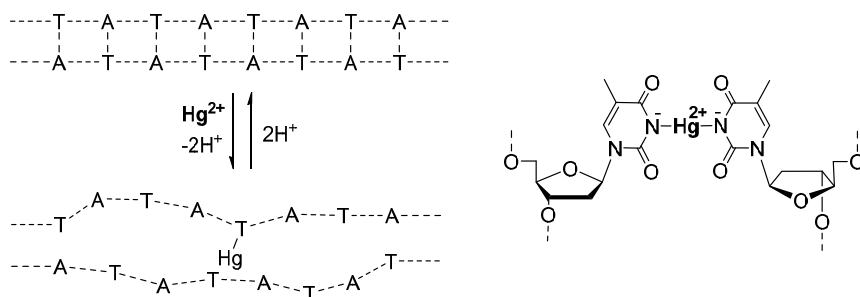
Figure 6. *Suggested model of Katz for formation of metallo base pair T:Hg:T by slippage of the DNA double helix.[49]*
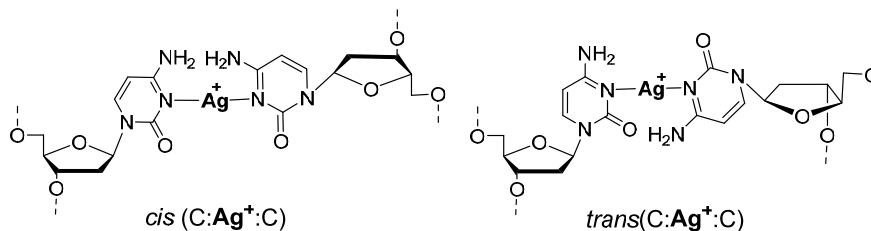
Figure 7. *Suggested model for C:Ag:C base pair with either trans or cis conformations.[71]*

A C:C mispair may also be stabilized by metal ion coordination, but in this case Ag^+, rather than Hg^+, is the preferred metal ion.[60,61] This mismatched metallo base pair occurred either in *trans* (parallel duplex) or *cis* (antiparallel duplex) conformation (Figure 7).[71] The 8-mer DNA oligonucleotide (ON), which contained cytosine bases only, was by CD and UV spectroscopy shown to form $C:Ag^+:C$ base pairs with a parallel orientation of the strands.[31]

RNA has not been explored as much as DNA, most likely because RNA is more susceptible to enzymatic degradation. The first report on a metal-ion-mediated RNA base pair was an Au^{3+}-mediated G:C-base pair, formed by accident during crystallization.[72]

The Müller group incorporated a metal-mediated base pair, $U:Hg^{2+}:U$ within a double-stranded oligoribonucleotide (ORN).[59] The study was carried out with five different RNA structures (Table 1).[59] Some of these ORNs were non-palindromic duplexes containing a window of two or six consecutive uridine

residues in the middle of the sequence (**ON1** and **ON2**) and the rest were partly palindromic (**ON3-ON5**) containing oligo(U) loops of different lengths. The T_m increased in nearly all cases upon addition of Hg^{2+}. The stabilization correlating with the number of uracil bases. The stabilization of non-palindromic duplexes **ON1** and **ON2** results from conversion of U:U-pairs to U:Hg^{2+}:U –pairs, while the palindromic **ON3-ON5** undergo transition from unimolecular hairpin to bimolecular duplex upon formation of the metallo base pairs. To verify this, diffusion-ordered NMR spectroscopy (DOSY NMR) and dynamic light scattering (DLS) methods were used to determine the size of ORN structures in the presence of Hg^{2+}.[34] Hydrodynamic radii (r_H) were measured to distinguish between hairpin and metal-ion-mediated duplex structures (Table 1). After addition of Hg^{2+} ion, **ON3** experienced an increase in the value of r_H by approximately 30% (Scheme 3), while the **ON1** and **ON2** remained unaffected. The results obtained with **ON4** and **ON5** were less clear, suggesting that these oligonucleotides were mixtures of different duplexes.
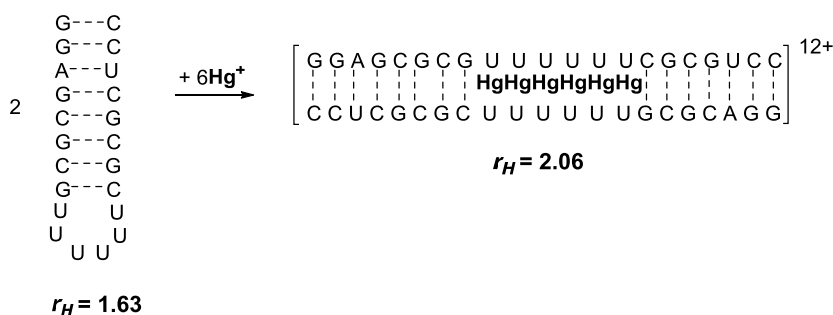
Scheme 3. *Increasing of hydrodynamic radii (r_H) from hairpin structure to double helix upon addition of Hg^{2+} ion.*

Table 1. Hydrodynamic radii r_H of **ON1-ON5** as determined by DLS($r_{H,DLS}$) and DOSY NMR ($r_{H,DOSY}$) before and after addition of 1.2 equiv. of Hg^{2+}. In case the sequence is able to form either hairpin or duplex, theoretical values are given for both conformations.[59]

	Sequence	hair-pin r_H	Du-plex r_H	Without Hg^{2+}		With Hg^{2+}	
				$r_{H, DOSY}$	$r_{H, DLS}$	$r_{H, DOSY}$	$r_{H, DLS}$
ON1	5´-r(GGAGCGCGU$_2$GUCCCUC)-3´ 3´-r(CCUCGCGCU$_2$CAGGGAG)-3´	-	2.21	2.06 ± 0.12	2.13 ± 0.02	2.18 ± 0.33	2.23 ± 0.02
ON2	5´-r(GGAGCGCGU$_6$GUCCCUC)-3´ 3´-r(CCUCGCGCU$_6$CAGGGAG)-3´	-	2.00	2.26 ± 0.11	2.00 ± 0.02	2.36 ± 0.16	1.69 ± 0.02
ON3	5´-r(GGAGCGCGU$_6$CGCGCUCC)-3´	1.43	2.04	1.63 ± 0.10	1.56 ± 0.02	2.06 ± 0.17	2.26 ± 0.05
ON4	5´-r(GGAGU$_{10}$CUCC)-3´	1.17	2.34	1.51 ± 0.35	1.74 ± 0.04	2.18 ± 0.38	2.08 ± 0.05
ON5	5´-r(GGAGU$_{20}$CUCC)-3´	1.82	2.28	1.82 ± 0.10	2.40 ± 0.05	2.81 ± 0.90	2.65 ± 0.06

ON3 evidently underwent conversion from hairpin into an A-type homoduplex through metal-ion-mediated base pairs. This conformational change was further verified by ^1H, ^1H NOESY and $^1J_{HC}$-HSQC spectrometric measurements with ^{15}N and ^{13}C-enriched compounds, and by CD spectroscopy.[59,73,74] Lengthy treatment of the metallated ORNs, **ON1-5**, with a chelating Chelex resin removed Hg^{2+} from the U:Hg^{2+}:U base pairs.[59] The same treatment did not, however, removed Hg^{2+} from the T:Hg^{2+}:T base pair within corresponding DNA duplexes.[33] It was presumed that the base pairs and, hence, the bridging metal ions, are more exposed to solvent in A-type RNA than in B-DNA structure.

1.4 Metal-ion-mediated base pairs within modified DNA or RNA

Numerous modified nucleosides capable of forming metal-ion-mediated base pairs, both homo- and heterodimers, have been described.[26,46,47,49] The potential application area has been anticipated to cover several interesting fields such as: DNAzymes, molecular mechanism of gene mutations related to heavy metal-ions, and creation of molecular nanodevices and medical materials. The diversity of transition metal ions used to bridge the modified nucleobases is almost as numerous, representing various coordination numbers and geometries.

1.4.1 Metal-ion-mediated base pairs with (1+1) coordination

In addition to the T:T, U:U and C:C mispairs described above, several artificial monodentate ligands form Ag^+- or Hg^{2+}-mediated homo-base pairs through linear coordination to the central metal ion.[40,41,75,76] The base pair adopts a coplanar geometry within a double helix (see section 1.2.3)[75] and maintains a B-conformation of the DNA duplex, providing that there is no marked steric repulsion between the modified bases.[41,77] As an example, three 1,2,4-triazole nucleosides were incorporated next to each other within the loop of a hairpin ON (Scheme 4A).[40] Formation of the hairpin structure in the absence of Ag^+ ion was verified by independence of the T_m value of the oligonucleotide on its concentration, as well as by FRET experiments. When 3 equiv. of Ag^+ were added, the hairpin structure was transformed to a double helix by formation of three consecutive triazole:Ag^+:triazole base pairs, as evidenced by conversion of the T_m value to concentration-dependent. Formation of the Ag^+-mediated homo-duplex was additionally verified by FRET, MS and DLS experiments. Addition of Hg^{2+}, on the other hand, destabilized the double helix by 2 °C per equiv. of Hg^{2+}.[40] The destabilization was suggested to result from either the ability of Hg^{2+} to form only a 1:1 complex with triazole, or high affinity of Hg^{2+} to thymine.
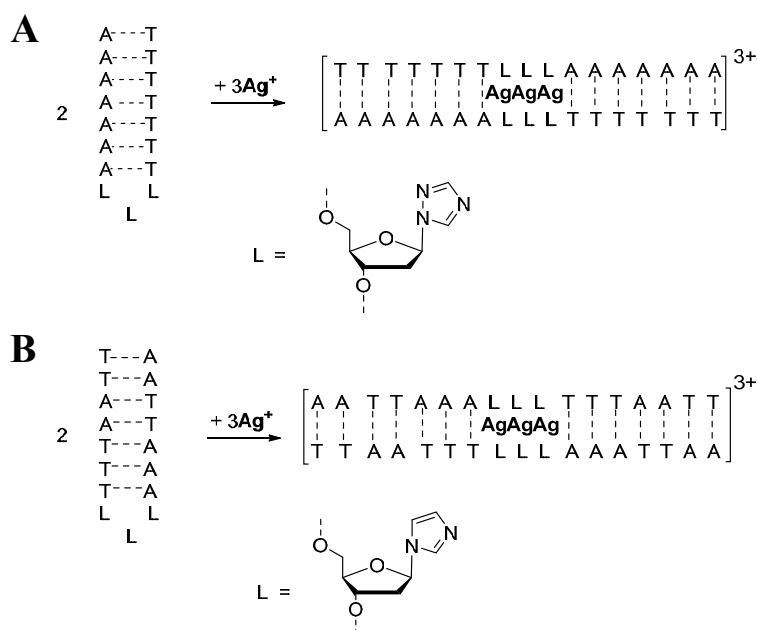
Scheme 4. *Formation of metal-ion-mediated base pairs through either triazole (A) or imidazole (B) nucleobase and simultaneous change of ON from hairpin structure to a regular double helix upon addition of Ag^+.[26,78]*

Similar results were obtained with imidazole nucleosides (Scheme 4B).[78] Incorporation of a methyl group vicinal to the donor nitrogen (position 2 or 4 of the imidazole ligand) was also tolerated (Figure 8A) and, in fact, led to a larger increase in T_m upon addition of Ag+ (**ON6**, Table 2).[41] Finally, two 3-pyridine nucleosides form a similar Ag+-mediated homo-base pair that was slightly stabilizing (Figure 8B and Table 2).[51]
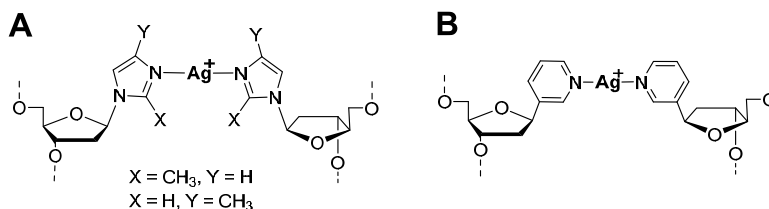
Figure 8. *Ag+-mediated pairs between two unidentate surrogate bases.[41,51]*

Table 2. The effect of various metallo base pairs with (1+1) coordination on the stability of double helices of complementary oligonucleotides.

	Sequences	Modified base pair (X) with metal ion	ΔT_m	*Ref.*
ON6	5´-dTTT GTTTG TTT G**X**TT G(T)$_{10}$/ 3´-dAAACAAACAAAC**X**AAC(A)$_{10}$	(2-Me-Im)$_2$:Ag+ or (4-Me-Im)$_2$:Ag+	+9.0 +8.0	41
ON7	5´-dTTT TTT TTT T **X**TT TTT TTT TT/ 3´-dAAAAAAAAAAA**X**AAAAAAAAA	(3-Py)$_2$:Ag+	+6.8^a +3.8	51
ON8	5´-dGTGACCA**X**TGCAGTG/ 3´-dCACT GGT**X**ACGTCAC	(2-Thiothymine)$_2$:(Ag+)$_2$ (4-Thiothymine)$_2$:(Ag+)$_2$	+23.0^b +23.0^b	79
ON9	5´-dGAGGGA**X**AGAAAG/ 3´-dCT CCCT **X**TCT TTC	(εA)$_2$:(Ag)$_2$	+12.0	76
ON10	5´-dTAGGT**X**AATACT/ 3´-dATCCA**X**TTATGA	(^{ph}ImdC)$_2$:(Ag+)$_2$ (^{me}ImdC)$_2$:(Ag+)$_2$	+38.5^{b,c} +30.0^{b,d}	80
ON10	5´-dTAGGT**X**AATACT/ 3´-dATCCA**X**TTATGA	(^{ph}PyrdC)$_2$:(Ag+)$_2$ (^{me}PyrdC)$_2$:(Ag+)$_2$	+22.5^{b,c} +18.5^{b,c}	32
ON11	5´-dTAGGT**XX**ATACT/ 3´-dATCCA**XX**TATGA	(^{ph}PyrdC)$_2$:(Ag+)$_2$ (^{me}PyrdC)$_2$:(Ag+)$_2$	- >42.5^{b,c}	32

^{a} 3 equiv. of Ag+ ion. ^{b} 2 equiv. of Ag+ ion. ^{c} pH is 7.4 or 9.0. ^{d} pH is 6.0

The linear coordination geometry of Ag+ allows formation of more than one Ag+ bridges between appropriate ligands. As could be expected, such dinuclear metallo base pairs can be highly stable. For example, a single thiopyrimidine homo-base pair with two Ag+ ions (Figure 9A) increased the T_m of a double-helical DNA oligonucleotide (**ON8**) by 23 °C relative to the metal-free duplex.[79]

Recently $1,N^6$-ethenoadenine (εA) was explored as a Ag$^+$-mediated base pair in a DNA system.[76] Two Ag$^+$ ions could bind by (1+1) coordination to the N6 and N7 atoms of this base (Figure 9B) and the duplex (**ON9**) was considerably stabilized (ΔT_m = +12 °C). Similar two silver ion systems exhibiting even greater stabilization have been constructed by using either methyl- (^{me}Pyr-dC) or phenyl-substituted pyrrolocytosine (^{ph}Im-dC and ^{ph}Pyr-dC) as the artificial nucleobase (Figure 9C).[32,80] The best example is ^{ph}Im-dC:^{ph}Im-dC base pair which stabilize the DNA duplex (**ON10**) by +38.5 °C upon addition of 2 equiv. Ag$^+$ under neutral and basic conditions. The duplex **ON10** is also markedly stabilized by metallo base pair ^{ph}Pyr-dC:(Ag$^+$)$_2$:^{ph}PyrdC (Table 2) under the same conditions. When conditions are changed to slightly acidic, the ^{ph}Im-dC:(Ag$^+$)$_2$:^{ph}ImdC base pair still retains the high stability (ΔT_m = +30 °C), but with ^{ph}PyrdC:(Ag$^+$)$_2$:^{ph}PyrdC only very modest change was observed (ΔT_m = +2.5 °C). Apparently N9 is deprotonated much more easier in ^{ph}Im-dC compared to N7 deprotonation of ^{ph}PyrdC. One ^{ph}Pyr-dC:(Ag$^+$)$_2$:^{ph}Pyr-dC base pair stabilized the double helix (**ON10**) more than one ^{me}Pyr-dC:(Ag$^+$)$_2$:^{me}Pyr-dC base pair. However, the situation was reversed, when two sequential metallo base-pairs were incorporated in the middle of **ON11** (Table 2). Interestingly, both modified ^{ph}Im-dC and ^{ph}Pyr-dC bases were paired with G in the middle of duplex **ON10** and stabilized the helix in the absence of metal ion more than the natural Watson-crick base pair (C:G). But the effect of Ag$^+$ ion is negligible. The ^{ph}Im-dC:C and ^{ph}Pyr-dC:C base pairs were not as stable as with G in the absence of metal ion, but show some stability of duplex after addition of Ag$^+$ (ΔT_m = 10.5 °C and +3.5 °C, respectively).
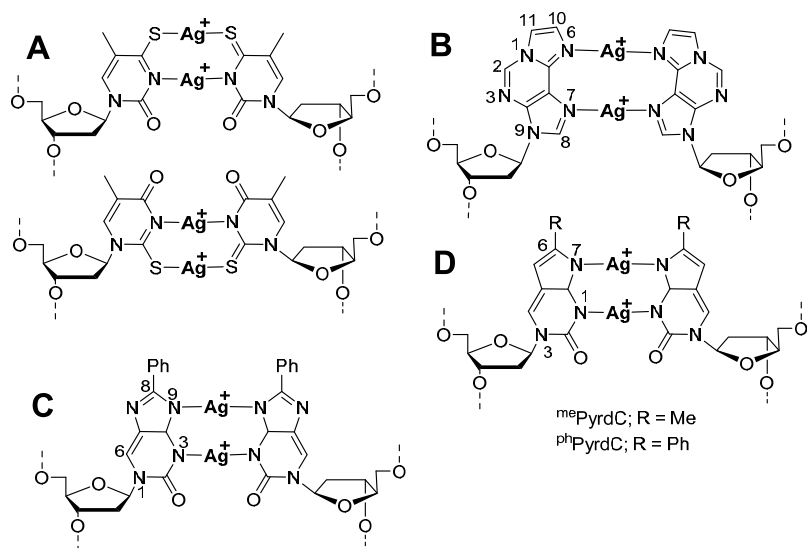
Figure 9. *Metallo base pairs with (1+1) coordination of two metal-ions.*[32,76,79]

1.4.2 Metal-ion-mediated base pairs with (2+1) coordination

Ag^+ also forms trigonal-planar complexes but these have been less widely exploited in studies on metal-ion-mediated base pairing. Only very recently, the first artificial metallo base pair with (2+1) coordination was introduced. This Ag^+-mediated base pair was formed between 4-[(1*H*-1,2,4-triazol-1-yl)methyl]-1*H*-1,2,3-triazole (TriTri), containing two triazole rings, and imidazole (Figure 10A).[42] None of the other metal ions (Au^{3+}, Cu^{2+}, Co^{3+}, Cr^{3+}, Fe^{2+}, Hg^{2+}, Mn^{2+}, Ni^{2+} and Zn^{2+}) screened offered comparable stabilization. Furthermore, when imidazole in the middle of duplex **ON12** was replaced with either cytosine or thymine, the stabilizing effect of Ag^+ was much more modest (Table 3), but addition of Ni^{2+} then reasonably stabilized the double helix. Analogous structures featuring pyrazole (TriPyr, Figure 10B) or pyridine (TriPy, Figure 10C) in place of the 1,2,3-triazole ring were also tested.[43] When incorporated within a 13-mer double-stranded oligonucleotide (**ON13**), the highest stabilization was achieved with the TriPy:Ag^+:imidazole pair (Table 3).
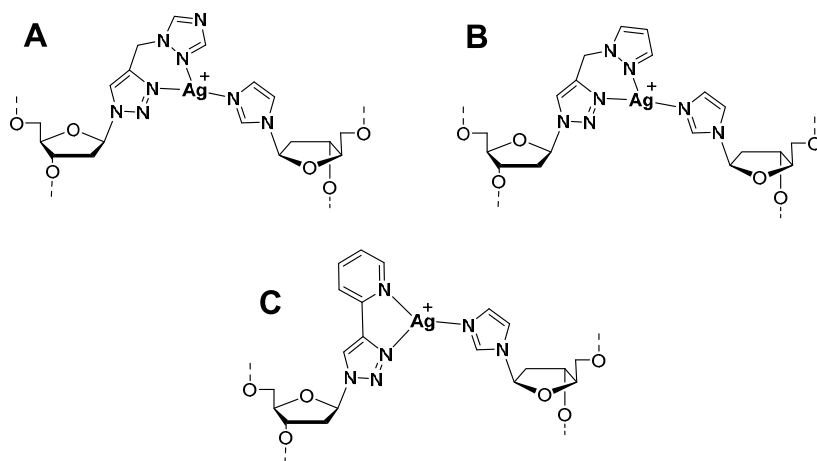
Figure 10. *Metallo base pairs with (2+1) coordination of metal-ion.*[42,43]

Table 3. The effect of various metallo base pairs with (2+1) and (2+2) coordination on the stability of double helices of complementary oligonucleotides.

	Sequences	Mod. base (X)	Mod. base (Y)	ΔT_m X:X	X:Y	Ref
ON12	5′-dGAGGGA**X**AGAAAG/ 3′-dCT CCC T**Y**T CT TTC	TriTri*	Im	+2.1[a,f]	+0.1[b]/+6.0[c]	42 43
ON13	5′-dAGAAAG**X**GAGGGA/ 3′-dTC T TT C**Y**CT CCCT	TriPy	Im	+1.4[a]	+12.6[a]	43
ON13	5′-dAGAAAG**X**GAGGGA/ 3′-dTC TT TC **Y**CT CCCT	TriPyr	TriPy	+2.8[a]	+7.4[a]	43
ON14	5′-dCACATTA**X**TGTTGTA/ 3′-dGTGTAAT**X**ACAACAT	H	-	+13.1	-	44
ON15	5′-dAGTCG**X**CGACT/ 3′-dTCAGC**X**GCTGA	5-MeBPy	-	+7.5	-	89
ON16	5′-dCTTT CT**X** TCCCT/ 3′-dGAAAGA**X**AGGGA	Pur[P]	-	+17.6[c]/+2.9[b]	-	90
ON16	5′-dCTTT CT**X** TCCCT/ 3′-dGAAAGA**X**AGGGA	Pyr[P]	-	+16.5[c]/+2.1[b]	-	45
ON14	5′-dCACATTA**X**TGTTGTA/ 3′-dGTGTAAT**X**ACAACAT	Pur[C]	-	+8.3[c]/+22.7[b]	-	91
ON14	5′-dCACATTA**X**TGTTGTA/ 3′-dGTGTAAT**X**ACAACAT	Salen	-	+13.8[d]/+41.3[e]	-	93

[a]with Ag$^+$; [b]with Cu^{2+}; [c]with Ni^{2+}; [d]1.3 equiv. of Cu^{2+}.[e]Addition of 100 μM ethylenediamine with 1 equiv. Cu^{2+}; [f]The sequence is the same as with TriPyr.*Additionally, TriTri:C bases with Cu^{2+} (+0.6) or Ag$^+$ (+1.4), TriTri:T bases with Cu^{2+} (+0.3) or Ag$^+$ (+2.0).

1.4.3 Metal-ion-mediated base pair with (2+2) coordination

Most artificial metal-ion-mediated base pairs described in the literature are based on (2+2) coordination.[48,49] In the case of metal ions with square-planar coordination environment, this coordination type forces the base pair to adopt a coplanar conformation even at the monomer level. The most widely utilized among such metal ions are Cu^{2+}, Ni^{2+}, Pd^{2+} and Pt^{2+}.[48] The first example of a modified nucleoside engaged in metal-ion-mediated base pair with (2+2) coordination was published by Tanaka and Shionoya in 1999 (Figure 11A).[81] Initially, an *O*-phenylenediamine complex with Pd^{2+} was synthesized, followed by similar derivatives with Cu^{2+} and B^{3+}.[81-84] These artificial metallo base pairs were only studied at the monomer level. The isosteric Cu^{2+}-mediated 3-hydroxypyridin-4-one (**H**) homo-base pair (Figure 11B) was, in turn, embedded into a number of different ON duplexes.[44,85] As many as five consecutive metallo base pairs could be accommodated within a single 7-mer ON, as confirmed by UV and CD titrations and EPR and mass spectrometry.[85] According to the EPR data, the Cu^{2+} ions were ferromagnetically coupled on top of each other, with a distance of 3.7 Å (the respective value for unmodified B-type DNA is 3.3-3.4 Å). When the 3-position of 2-pyridone was substituted by sulfur, soft metal ions such as Pd^{2+}, Pt^{2+} or Ni^{2+} formed stable base pairs at monomeric level.[86]

Additionally, derivatives of 2,2′-bipyridine (BPy), where the base was attached either directly or via a methylene group to the anomeric carbon, have been studied.[87-89] The BPy:BPy pair significantly stabilized a 19-mer DNA duplex in the absence of metal ion,[87] but addition of metal ions resulted in destabilization (Figure 11C).[88] By contrast, 5-methyl-2,2′-bipyridine stabilized a 11-mer DNA helix (**ON15,** Table 3) by 7.5 °C upon addition of Cu^{2+} ion (Figure 11D).[89] The related pyridyl-substituted derivatives (Pur^P and Pyr^P) of the natural nucleobases adenine and cytidine (Figure 11, E and F) markedly enhanced hybridization of **ON16** duplex through Ni^{2+}-mediated homo-base pairing (Table 3).[45,90] This effect was not observed with the other divalent metal ions screened (Co^{2+}, Cu^{2+}, Zn^{2+}, Fe^{2+} and Mn^{2+}).
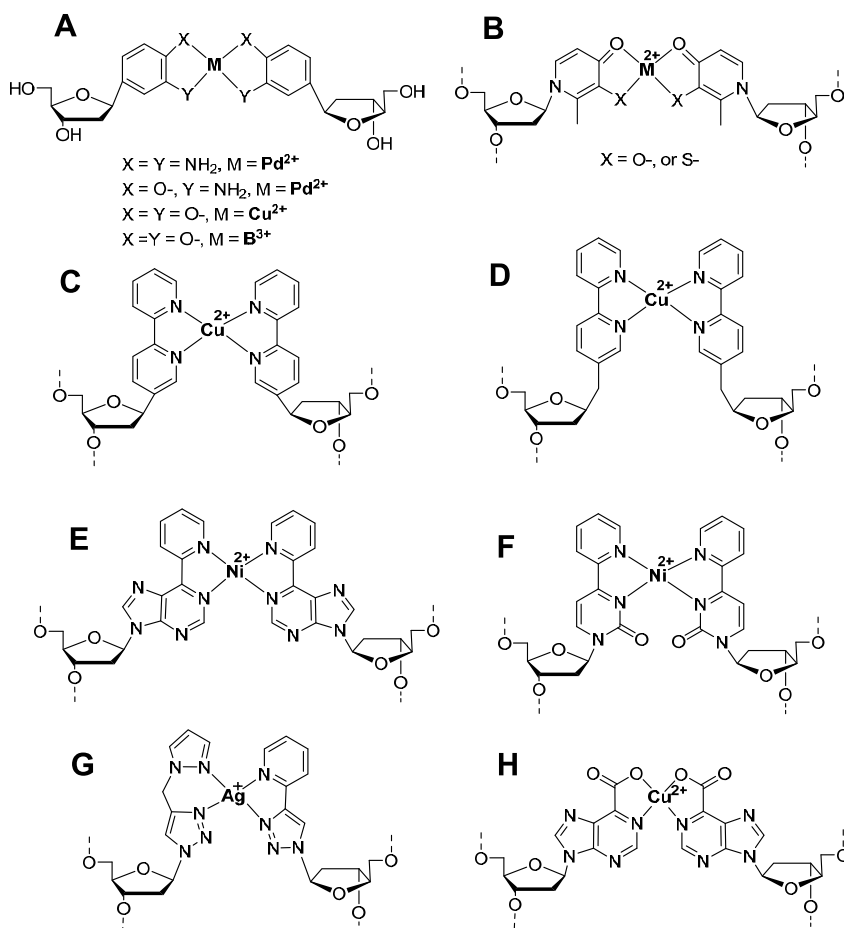
Figure 11. *Metallo base pairs with (2+2) coordination of metal-ion.* [43-45,81,87-91]

Finally, this type of coordination has been recently studied with TriPyr:Ag^+:TriPy (Figure 11G) and Pur^C:Cu^{2+}:Pur^C (Pur^C = 6-carboxypurine) (Figure 11H) base pairs.[43,91] The TriPyr:Ag^+:TriPy metallo base pair reasonably stabilized **ON13** duplex (Table 3), but none of the other metal ions screened (Hg^{2+}, Cu^{2+}, Zn^{2+} and Ni^{2+}) had any significant stabilizing effect.[43] By contrast, Pur^C:Pur^C base pair that was markedly stabilized by Cu^{2+} (ΔT_m = 22.7 °C for a 9-mer DNA duplex **ON14,** Table 3) was moderately stabilized also by other metal ions, such as Ni^{2+}, Zn^{2+}, Co^{2+}, Fe^{2+}, Fe^{3+}, Hg^{2+} and Mg^{2+} (ΔT_m = +5-8 °C). In this case, Mn^{2+} and Ag^+ were inefficient.[91]

An innovative and unusual type of metal-ion-mediated base pair based on (2+2) coordination of Cu^{2+} to two nucleosides derived from salicylaldehyde was presented by the Carell laboratory.[92] Two of these modified nucleosides were placed opposite to each other in the middle of a 15-mer double-helical DNA ON. The duplex with a melting point of 41.1 °C, exhibited ΔT_m of +13.8 upon addition of Cu^{2+} ion. This stabilization by Cu^{2+} is comparable to the effect of the **H**:Cu^{2+}:**H** base pair within the same double-stranded DNA (**ON14**), examined by Tanaka *et al* (ΔT_m = 13 °C).[44] The stability of the Cu^{2+}:salicylaldehyde base pair was vastly increased when ethylenediamine was added (ΔT_m = +41.3 °C, Table 3).[93] The salicylic aldehyde can condense with ethylenediamine linker producing a metal-salen cross-link between the opposite strands (Figure 12).
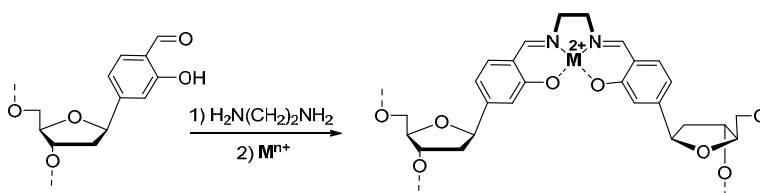
Figure 12. *The metal–salen base pair.*[92]

The salen cross-link in the presence of a metal ion, such as Cu^{2+}, increases the melting temperature immensely, from 45.5 to 82.4°C.[93] In the presence of only ethylenediamine (T_m = 45.5 °C) or just Cu^{2+} ion (T_m = 54.9 °C) the stabilization is more modest. The other metal-ions explored included Mn^{2+}, VO^{2+}, Fe^{3+}, and Ni^{2+}. Mn^{2+}, which oxidized to Mn^{3+} under aerobic conditions, exhibited a higher melting temperature of 68.8 °C (Table 3).[92,93]

As a demonstration of the compatibility of the metallo-salen base pair formation with DNA hybridization, ten of these base pairs were incorporated within a double-helical DNA ON and either Mn^{3+} or Cu^{2+} was used as the bridging metal ion. Formation of the desired assemblies was confirmed by ESI-ICR mass spectrometry (in the presence of Mn^{3+}) or UV spectrophotometric titration (in the prescence of Cu^{2+}).[94]

The capacity of stacking between ten adjacent artificial metallo base pairs within the DNA was studied with different metal ions. To this end, two orthogonal ligands (hydroxypyridone and pyridine) for two different metal ions (Cu^{2+} and Hg^{2+}, respectively) were incorporated into the same DNA ON.[44,49,85,95,96] In another study, ten adjacent or alternating Cu^{2+}-salen and thymine:Hg^{2+}:thymine

base pairs were incorporated next to each other within a DNA oligomer (Figure 13). Coordination of the desired metal ions with correct stoichiometry to the ligands was confirmed by CD-spectroscopic titrations and high-resolution ESI mass spectrometry.
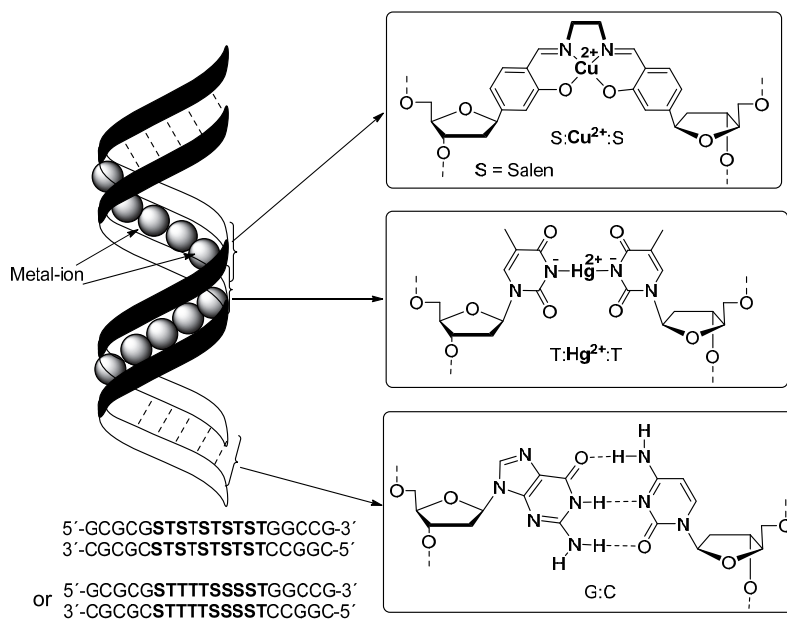
Figure 13. *DNA incorporating several adjacent or alternating Cu²⁺-salen and thymine:Hg²⁺:thymine base pairs.*[48,95]

1.4.4 Metal-ion-mediated base pair with (3+1) coordination

Square-planar geometry around the bridging metal ion can also be achieved through (3+1) coordination, giving rise to metal-ion-mediated hetero-base pairs. In this approach, the metal ion is bound much more strongly by the tridentate than by the monodentate ligand. The first artificial base pair embedded into an ON duplex exploiting this asymmetrical coordination mode was 3-pyridine:2,6-pyridinedicarboxylate (Dipic) (Figure 14A).[46,97] In this case, Dipic formed a planar tridentate chelate with the metal ion, such as: Cu^{2+}, Ag^+, Ni^{2+}, Pd^{2+}, and Pt^{2+}, the monodentate ligand occupying the fourth coordination site. The most stable duplex (**ON14**) was obtained with Dipic:3Py base pair in the presence of Cu^{2+} (Table 4), whereas other metal ions, such as Ce^{3+}, Mn^{2+}, Fe^{2+}, Co^{2+}, Ni^{2+}, Zn^{2+}, Pd^{2+} and Pt^{2+}, did not have any significant affect. Even greater stabilization was observed with the nitrogen analog (Dipam, Table 4) pyridine-2,6-dicarboxamide (Figure 14A).[98] Methylation of the amide nitrogens did not have

any effect on stabilization compared with Dipam and Dipic. When the Dipic and Dipam bases were situated opposite to natural bases, the T_m values ranged from 25.5 to 34.5°C. The most stable mispairs after addition of Cu^{2+} were Dipic:dA ($T_m = 34.1$ °C) and Dipam:dG ($T_m = 34.5$ °C).
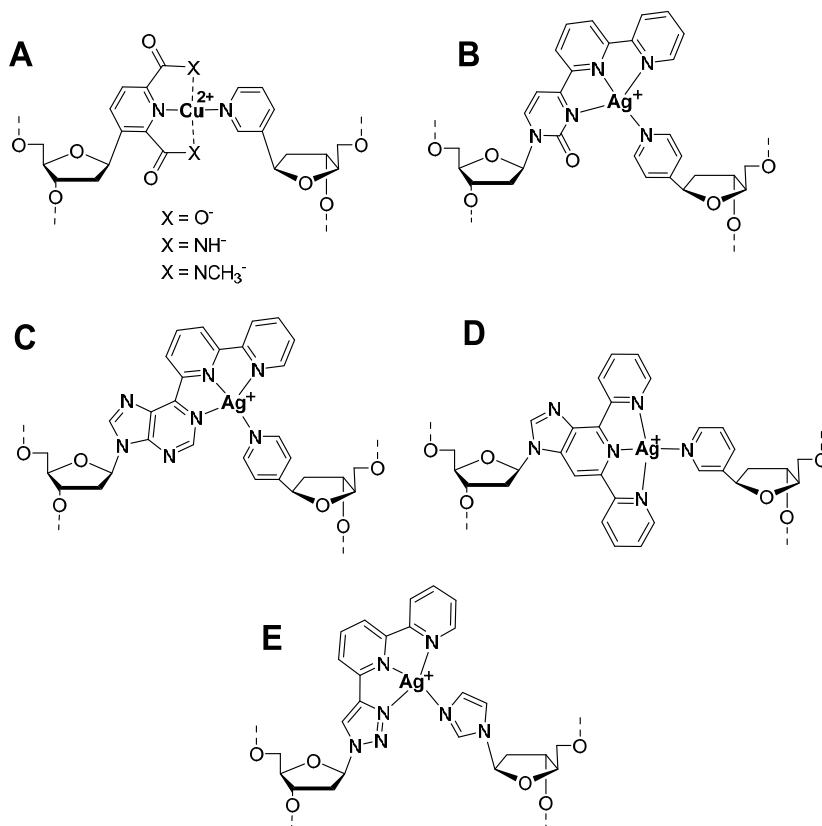
Figure 14. *Metallo base pairs with (3+1) coordination of metal ions.*[46,47,98-100]

Schultz *et al.* succeeded in obtaining the first crystal structure of a self-complementary double-stranded DNA oligonucleotide incorporating two artificial dipic:Cu^{2+}:3Py metallo base pairs (5′-CGCG*Dipic*AT*Py*CGCG-3′).[48,97] This CG-rich palindromic ON crystallized in the unusual Z-conformation. In this Z-type ON, the metallo base pairs have square planar structure and the Cu^{2+} ion is additionally bonded axially with two oxygen atoms from neighboring

nucleosides (the furanose oxygen and guanine-O6), resulting in an octahedral coordination geometry.[97,101]

Another family of modified nucleobases exploiting (3+1) coordination consists of terpyridine (Scheme 2) and its analogs (Figure 14B-E), Bipyridylpyrimidinone base, for example, forms with 4-pyridine (Figure 14B) a stable Ag^+-mediated base pair within double-stranded **ON16** ($Pyr^{Bipy}:Ag^+:4Py$).[99] A 12.9 °C increase in T_m was observed on addition of Ag^+ (Table 4), whereas none of the other metal ions studied (Mn^{2+}, Mg^{2+}, Cu^{2+}, Fe^{2+}, Co^{2+}, Ni^{2+}, Zn^{2+} and Tl^+) showed any significant stabilization.[99] Attachment of either one bipyridyl or two pyridyl rings to purine also affords terpyridine analogs (Pur^{6-Bipy} and $Pur^{2,6-Py}$) and the impact of Ag^+ ion has been explored with these modified nucleobases.[47] The monodentate ligand in these studies was either a natural (A, G, C and T) or another modified (3-Py, 4-Py,) nucleobase. Only the metallo base pairs $Pur^{6-bipy}:Ag^+:4Py$ (Figure 14C) and $Pur^{2,6-Py}:Ag^+:3Py$ (Figure 14D) stabilized duplex **ON16** compared to the Watson-Crick base paired counterpart (C:G, T_m = 38.0 °C).[47] 6-(1*H*-1,2,3-Triazole-4-yl)-2,2′-bipyridine offers yet another example of a terpyridine-type ligand.[100] A Ag^+-mediated base pair between this ligand and imidazole (Figure 14E) was moderately stabilizing: the melting temperature of a double-stranded **ON12** placing these modified nucleosides opposite to each other was increased by approximately 5 °C on addition of Ag^+.

Table 4. The effect of various metallo base pairs with (3+1) coordination on the stability of double helices of complementary oligonucleotides

Mod. base		Metal	ΔT_m						*Ref.*
X	**Y**	**ion**	**X:X**	**X:Y**	**X:A**	**X:C**	**X:G**	**X:T**	
Dipic	3-Py	Cu^{2+}	-	≥10.0	-2.4[a]	-10.5[a]	-7.9[a]	-	46
Dipam	3-Py	Cu^{2+}	-	+15.0	-13.0[a]	-17.5[a]	-8.5[a]	-15.5[a]	98
Pyr^{Bipy}	4-Py	Ag^+	-1.1	+12.9	+5.0	+3.5	+5.4	+2.5	99
Pur^{6-Bipy}	4-Py	Ag^+	+6.7	+11.1	+3.3	+1.1	+5.5	+1.7	47
$Pur^{2,6Py}$	3-Py	Ag^+	+12.0	+16.5	+3.5	+3.8	+12.0	-5.0	47

[a]Comparison with $Dipic:Cu^{2+}:3Py$ metallo mispairs.

1.5. Metal-ion-mediated base-pairing between modified and natural nucleic acids

The first reported metal-ion-mediated base pair between a modified and a natural nucleobase was the Ag^+-mediated pair between 1-deazaadenine and thymine (Scheme 5).[102,103] While 1-deazaadenine (D) is not a natural nucleoside,

nonetheless it closely resembles adenine. Actually 1-deazaadenine and thymine form a Hoogsteen base pair due to the absence of N1 of 1-deazaadenine.[104] When this base pair was incorporated into **ON17** [d(ADADADADA):d(T$_9$)] and **ON18** [d(D$_{19}$A):d(T$_{20}$)] duplexes, the T_m increased from 10 °C in the absence of metal ions Ag$^+$ to 51.2 °C in the presence of 1 equiv. of Ag$^+$.[26] The structure of the duplex was elucidated by CD and UV spectroscopy.[104] The stability of **D**:Ag$^+$:T base pair is comparable to natural ones.
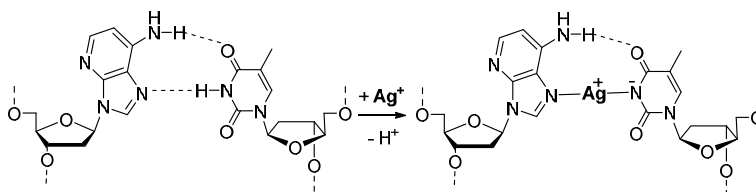
Scheme 5. *1-Deazaadenine:thymine base pair in the absence and presence of Ag$^+$.*[26,104]

Likewise, 1,3-dideaza-6-nitropurine (**I**) has been used as a modified nucleobase, that forms a Ag$^+$-bridged complex with cytosine (Scheme 6).[31] According to CD spectra, this base pair is not formed and the increase in T_m of self-complementary duplex [d(I$_8$C$_8$)] is caused by the formation of C:Ag$^+$:C base pairs.
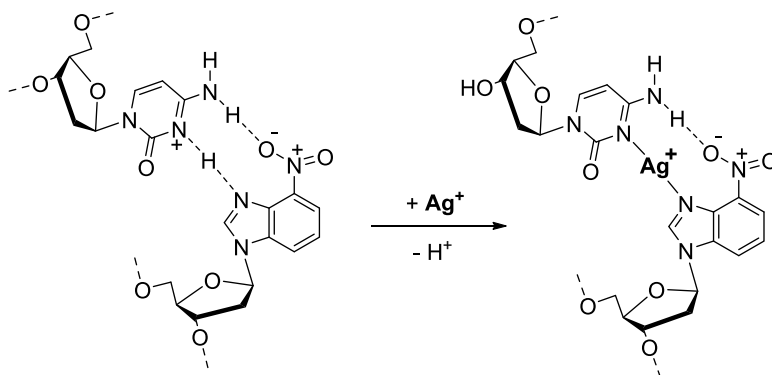
Scheme 6. *Suggested structure of Hoogsteen arrangement of cytosine:1,3-dideaza-6-nitropurine base pair in the absence and presence of Ag$^+$ ion.*[31]

The data on recognition of natural ONs with probes incorporating metal-ion-binding surrogate bases still is limited leaving space for additional studies. The study discussed in the following hopefully is one step on the way to high-affinity-binding probes that still retains sequence selectivity.

2. AIMS OF THE THESIS

MicroRNAs (miRNA) are small non-coding RNAs that have a hairpin structure and usually one or more bulges within the double helical stem.[105] They play, after being processed by the Dicer enzyme, a role in regulation of gene expression, but they are additionally excreted in hairpin form into blood circulation.[106,107] Owing to the fact that the spectrum of miRNAs turns abnormal in severe diseases, such as cancer, they constitute an emerging target for diagnostics and in all likelihood also for chemotherapy.[108-111] One of the problems encountered is that traditional oligonucleotide probes are not able to recognize miRNA by chain invasion, owing to the stable hairpin structure of miRNA. This study is aimed at developing modified oligonucleotides that through metal-ion-mediated base pairing show enhanced and preferably selective affinity to their natural counterparts. Such probes expectedly are useful for recognition of miRNAs and related hairpin-like structural motives of RNA, such as the TAR sequence of HIV.[112-115]

To achieve this general goal

(i) Analogs of purine bases that bind tightly soft and 3d transition metal ions are synthesized and converted to building blocks compatible with solid phase ON synthesis by the phosphoramidite chemistry.

(ii) The metal-ion-binding surrogate nucleosides are incorporated into terminal and non-terminal positions of oligonucleotides and their influence on the duplex stability in the absence and presence of metal ions is studies by UV- and CD-based duplex melting studies. The aim is to learn more about the structural factors that allow in the presence of metal ions high stability and good selectivity.

(iii) The applicability of such metal-ion-binding oligonucleotides as probes with which   to   recognize   structural   motives   of   RNA   is   studied

3. RESULTS

3.1 Synthesis of modified nucleosides and their conversion to phosphoramidite building blocks

3.1.1 Phosphoramidite building blocks derived from 2,6-bis(3,5-dimethylpyrazol-1-yl)-9-(β-D-ribofuranosyl)purine (1) and 2-(3,5-dimethylpyrazol-1-yl)inosine (4)

2,6-Bis(3,5-dimethylpyrazol-1-yl)-9-(β-D-ribofuranosyl)purine (**1**) was prepared by treating commercial 2´,3´,5´-tri-*O*-acetyl-6-chloro-2-iodo-9-(β-D-ribofuranosyl)purine (**2**) with hydrazine hydrate at room temperature to obtain deacetylated 2,6-dihydrazinyl-9-(β-D-ribofuranosyl)purine (**3**) (Scheme 7).[116] Treatment of **3** with pentane-2,4-dione then gave **1**.[117]

2-(3,5-Dimethylpyrazol-1-yl)inosine (**4**) was prepared from **1** by nucleophilic displacement of the 6-(3,5-dimethylpyrazol-1-yl) substituent with ammonia (giving **5**) and subsequent oxidative removal of the 6-amino group with sodium nitrite in aq. acetic acid, giving **4**.

Nucleosides **1** and **4** were finally converted to 3´-(2-cyanoethyl-*N*,*N*-diisopropylphosphoramidite) building blocks compatible with the conventional oligonucleotide synthesis by the phosphoramidite strategy. Accordingly, the 5´-OH of **1** and **4** was protected as a 4,4´-dimethoxytrityl ether, the 2´-OH was silylated with *tert*-butyldimethylsilyl chloride and the 3´-OH was phosphitylated with 1-chloro-1-(2-cyanoethoxy)-*N*,*N*-diisopropylphosphanamine by using conventional methods. The experimental details and characterization of the compounds are given in Publications I and III.[118,119]
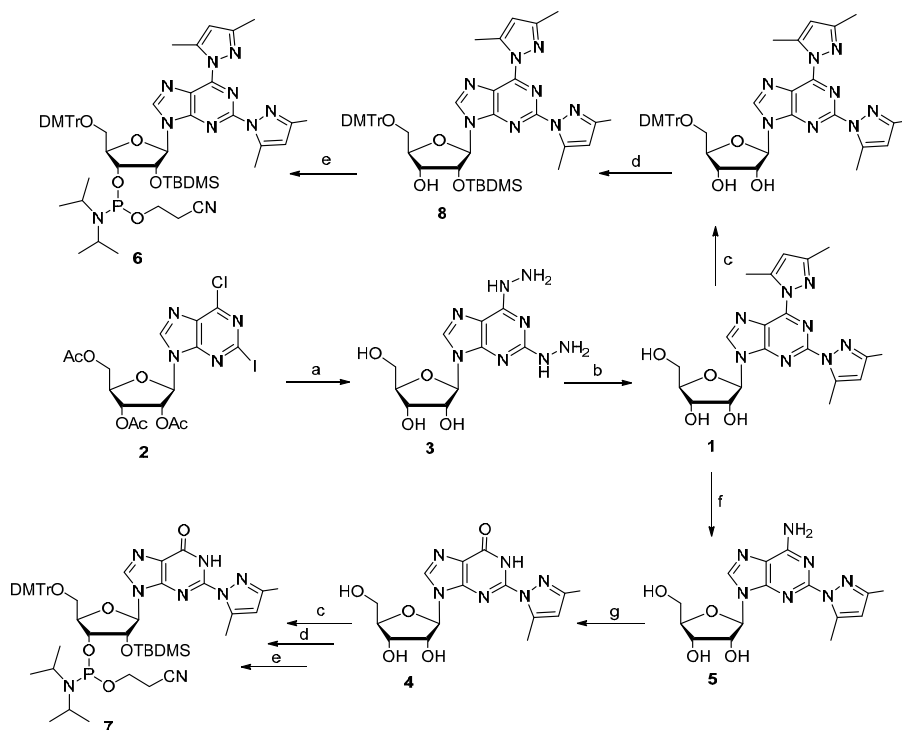
Scheme 7. *Preparation of 2,6-bis(3,5-dimethylpyrazol-1-yl)-9-(β-D-ribofuranosyl)purine (**1**) and 2-(3,5-dimethylpyrazol-1-yl)inosine (**4**) and their conversion to phosphoramidite building blocks. Reagents and conditions: (a) H₂NNH₂•H₂O; (b) pentane-2,4-dione, TFA; (c) DMTrCl, pyridine; (d) TBDMSCl, imidazole, DMF; (e) 1-chloro-1-(2-cyanoethoxy)-N,N-diisopropylphosphanamine, Et₃N, CH₂Cl₂; (f) NH₃, aq. (g) NaNO₂,aq., AcOH.[118,119]*

3.1.2 Phosphoramidite building block derived from 6-(3,5-dimethylpyrazol-1-yl)-9-(β-D-ribofuranosyl)purine (11)

6-(3,5-Dimethylpyrazol-1-yl)-9-(β-D-ribofuranosyl)purine (**9**) was synthesized by first displacing the chloro substituent of 6-chloro-9-(β-D-ribofuranosyl)purine (**10**) with hydrazine and then converting the hydrazinyl substituent to a 3,5-dimethylpyrazol-1-yl group by reacting with pentane-2,4-dione (Scheme 8).[117] The 5′-OH of **9** was then protected as a 4,4′-dimethoxytrityl ether and the 2′-OH was silylated with TBDMSCl. Finally the 3′-OH was phosphitylated as above to yield the phosphoramidite building block **10**.[119] The experimental details are given in Publication III.[119]
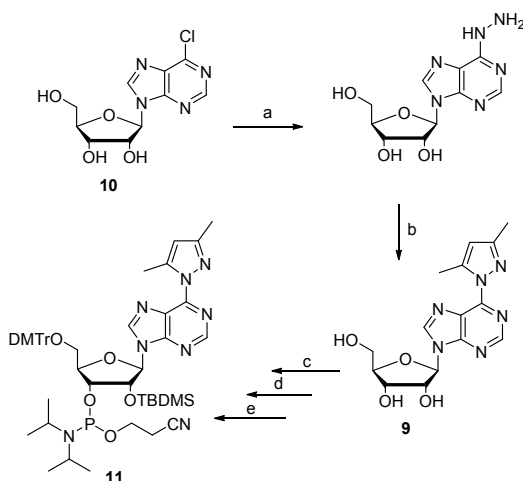
Scheme 8. *Preparation of 6-(3,5-dimethylpyrazol-1-yl)-9-(β-D-ribofuranosyl)purine and its conversion to a phosphoramidite building block. Reagents and conditions: (a) H₂NNH₂•H₂O; (b) pentane-2,4-dione, TFA; (c) DMTrCl, pyridine; (d) TBDMSCl, imidazole, DMF; (e) 1-chloro-1-(2-cyanoethoxy)-N,N-diisopropylphosphanamine, Et₃N, CH₂Cl₂.[119]*

3.1.3 Phosphoramidite building block derived from of 2,6-bis(1-methylhydrazinyl)-9-(β-D-ribofuranosyl)purine (13)

2,6-Bis(1-methylhydrazinyl))-9-(β-D-ribofuranosyl)purine (**12**) was synthesized by treating 2′,3′,5′-tri-*O*-acetyl-6-chloro-2-iodo-9-(β-D-ribofuranosyl)purine (**2**) with *N*-methyl- hydrazine at room temperature,[117] as described above for the reaction with hydrazine. The 1-methylhydrazinyl groups were protected as trifluoroacetamides using ethyl trifluoroacetate as the acylating agent (Scheme **9**). The nucleoside obtained (**14**) was converted to the 3′-phosphoramidite building block (**13**) as described above for **6** and **7**. The experimental details are given in Publication II.[120]
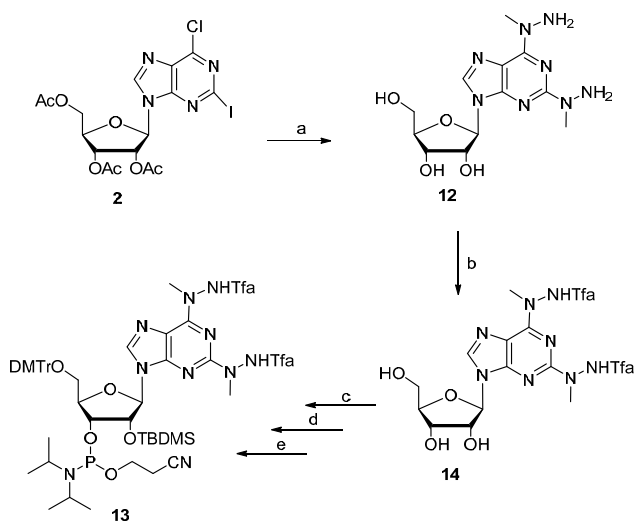
Scheme 9. *Preparation of 2,6-bis(1-methylhydrazinyl)-9-(β-D-ribofuranosyl)purine and its conversion to a phosphoramidite building block. Reagents and conditions: (a) MeNH₂NH₂; (b) ethyl trifluoroacetate, Et₃N, MeOH; (c) DMTrCl, pyridine; (d) TBDMSCl, imidazole, DMF; (e) 1-chloro-1-(2-cyanoethoxy)-N,N-diisopropylphosphanamine, Et₃N, CH₂Cl₂.[120]*

3.2   Synthesis   of   9-[3´-*O*-*tert*-butyldimethylsilyl-5´-*O*-(4,4´-dimethoxytrityl)-2´-*O*-succinoyl-β-D-ribofuranosyl]-2,6-bis (3,5-dimethylpyrazol-1-yl)purine (16) and its immobilization to a solid support

9-[3´-*O*-*tert*-Butyldimethylsilyl-5´-*O*-(4,4´-dimethoxytrityl)-β-D-ribofuranosyl]-2,6-bis(3,5-dimethylpyrazol-1-yl)purine (**15**), obtained as a side product of the synthesis of **8**, was 2´-*O*-succinylated with succinic anhydride (Scheme 10). A lengthy 8 d treatment at 40 to 50 °C was required for complete (97%) the conversion of **15** to **16**.[120]

Compound **16** was immobilized to a long chain aminoalkyl-CPG by conventional HBTU-promoted peptide coupling. The loading of the functionalized CPG was 54 µmol g⁻¹ based on trityl response upon treatment with 3% DCA in CH₂Cl₂.
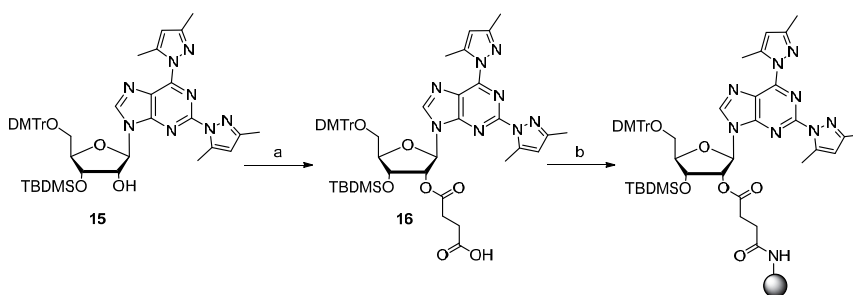
Scheme 10. *Immobilization of 9-[3´-O-*tert-*butyldimethylsilyl-5´-O-(4,4´-dimethoxytrityl)-β-D-ribofuranosyl]-2,6-bis(3,5-dimethylpyrazol-1-yl)purine* (**15**) *to a solid support. Reagents and conditions: a) succinic anhydride, pyridine (dry); b) long chain aminoalkyl-CPG, HBTU, DIPEA.*[120]

3.3 Synthesis of oligonucleotides

3.3.1 Synthesis of unmodified oligonucleotides

The unmodified 2´-*O*-methyl ORNs listed in Tables 5-7 were synthesized from commercial 2´-*O*-methylated RNA phosphoramidite building blocks on an automated RNA/DNA synthesizer. The coupling yields were always > 98 % by the DMTr response. After chain assembly, all ORNs were deprotected and released from the support by standard ammonolysis (33% aq. NH$_3$, 55 °C, 5 h). The crude ORNs then were purified by RP-HPLC and their identity was characterized by electrospray ionization mass spectrometry (ESI-MS).

3.3.2 Synthesis of modified oligonucleotides

The non-terminally modified 9-mers 2´-*O*-Me-ORN, **ON1i** (**I** = **X**, **Q**, **P**, **Y**) (Table 5) incorporating an artificial nucleoside (**1**, **4**, **9** or **14**, respectively) in the middle of the strand were synthesized from commercial 2´-*O*-methylated protected phosphoramidite building blocks on an automated synthesizer with the exception of insertion of the modified building block that was coupled manually using a long coupling time (60 min). The coupling yields for the modified building blocks **1**, **4**, **9** and **14** were 36, 41, 40 and 44%, respectively, while the other couplings proceeded with normal efficiency (approximately 99%). In the case of **ON1Y**, the 1-methyl-2-(trifluoroacetyl)hydrazinyl groups of the modified nucleoside **14** were converted to 2-acetyl-1-methylhydrazinyl groups during the synthesis. Evidently the N2 atom became acetylated during the capping step and

the final ammonolysis removed only the more labile trifluoroacetyl protections (Scheme 11). The 9-mer oligonucleotide **ON1Z**, containing 2-(3,5-dimethylpyrazol-1-yl)adenosine (**5**) in a non-terminal position, was prepared from oligonucleotide **ON1X** in approximately 40% yield by an extended treatment with 33% aq. NH_3 (6 h at 55 °C). Under these conditions, the dimethylpyrazol-1-yl substituents on C6 was displaced by ammonia. The other ONs (**ON1i, i** = **P**, **Q**, **Y**) were released from the support and the phosphate and base protections were removed by conventional treatment with ammonia (33% aq. NH_3, 55 °C, 4-5 h).[119,120]

To estabilish the site of displacement of the dimethylpyrazol-1-yl group within the purine base, a sample of the modified nucleoside (**1**) was kept under the deprotection conditions, *i.e.* in concentrated aq. ammonia (33%) at 55 °C for 5 h. The product mixture formed was then examined by ^{1}H NMR and HMBC which verified that 50% of **1** had been converted to essentially one product. On the basis of HMBC, this was 2-(3,5-dimethylpyrazol-1-yl)adenosine (**5**). The product (**5**) clearly indicated coupling of the C5 atom of the purine ring to the hydrogen atoms of an exocyclic amino group (Figure 15B). This correlation is not observed before ammonolysis (Figure 15A). In all likelihood ammonia had displaced the 3,5-dimethylpyrazol-yl group at a carbon neighboring C5, *i.e.* at C6 (Scheme 12). This reaction seems to occur more readily at the 3´-terminal site than at a non-terminal site.
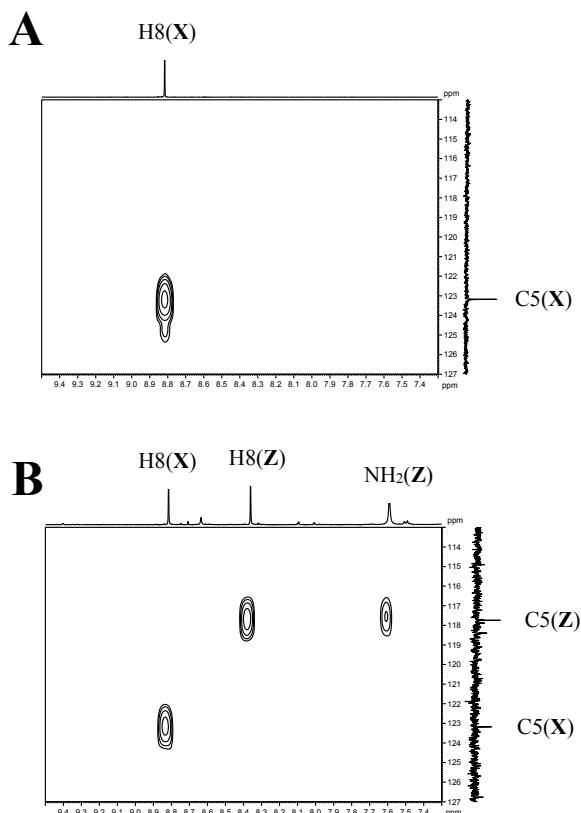
Figure 15. *HMBC spectra of the modified nucleoside **1** (A) before and (**B**) after 5 h incubation in concentrated aq. ammonia at 55 °C. Before ammonolysis, only coupling of C5 to H8 is detected. After ammonolysis, coupling of C5 to NH₂ is additionally seen. The spectra were measured in DMSO-d₆.[120]*

In addition, a modified oligonucleotide, **ON2S,** having an abasic site opposite to the modified nucleoside in **ON1i** (**i = X**, **Z**, **P**, **Q**) was prepared. The abasic site was created with a commercial 2-(hydroxymethyl)tetrahydrofuran-3-ol block (see Table 5).

The modified 6-, 5- and 4-mer 2´-*O*-Me-ORN (**ON4Xi** and **ON5Xi**, where **i = U**, **A**, **G**, **C; ON5Xa, ON5Xb, ON6X**, **ON7X**, **ON8X**, **ON9X** and **ON10X**) bearing the artificial nucleoside **1** at the 3´-terminus were synthesized on the solid support obtained by immobilization of nucleoside **16b**, as discussed above (Scheme 10). The ORNs were assembled on an automated synthesizer, the couplings proceeding with normal efficiency (approximately 99%). As described above for the synthesis of **ON1Z**, the dimethylpyrazolyl group at position 6 of the modified nucleoside **1** was displaced by ammonia during the ammonolysis (33% aq. NH₃, 55 °C, 5 h), affording ONs **ON4Zi** (**i = U**, **A**, **G**, **C**). According to HPLC, 37% of **ON4Xi** oligonucleotides were coverted to their **ON4Zi** counterparts. Oligonucleotides containing an intact modified nucleoside **X** were obtained in good yield by using a shorter ammonia treatment (2 h, at 55 °C).

For all modified ONs, the TBDMS group was removed with 1.53 M triethylamine trihydrofluoride in dry DMSO (2 h at 55 °C). The crude products were purified by RP-HPLC and their identity and purity verified by ESI-MS analysis. The concentrations of the purified products were determined UV-spectrophotometrically at λ= 260 nm using molar extinction coefficients calculated by an implementation of the nearest-neighbors method.[121-123]

Table 5. Structures and *m/z* values[a] of the unmodified and non-terminally modified 9-mer 2´-*O*-Me-ORNs used in the present study.

	Sequence	*m/z* (obsd.)	*m/z* (calcd.)
ON1X	5´-GCGC**X**CCGG-3´	3152.8	3152.7
ON1Y	5´-GCGC**Y**CCGG-3´	3136.6	3136.7
ON1P	5´-GCGC**P**CCGG-3´	3058.6	3058.6
ON1Z	5´-GCGC**Z**CCGG-3´	3073.6	3073.6
ON1Q	5´-GCGC**Q**CCGG-3´	3074.6	3074.6
ON1A	5´-GCGC**A**CCGG-3´	2993.6	2993.8
ON2U	5´-CCGG**U**GCGC-3´	2970.6	2970.8
ON2A	5´-CCGG**A**GCGC-3´	2993.6	2993.8
ON2G	5´-CCGG**G**GCGC-3´	3009.6	3009.8
ON2C	5´-CCGG**C**GCGC-3´	2969.6	2969.8
ON2S	5´-CCGG**S**GCGC-3´	2830.5	2830.6
ON3U	3´-CGCA**U**AGCC-5´	2938.6	2938.8
ON3A	3´-CGCA**A**AGCC-5´	2961.6	2961.8
ON3G	3´-CGCA**G**AGCC-5´	2977.6	2977.8
ON3C	3´-CGCA**C**AGCC-5´	2937.6	2937.8
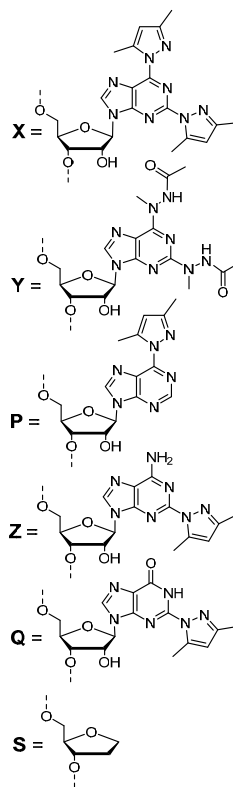
[a] By ESI-MS using a negative ion mode.
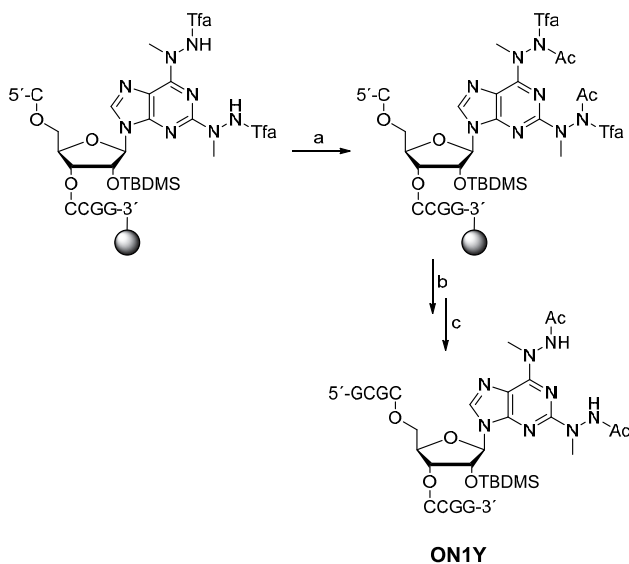
Scheme 11. *Acetylation of the 1-methyl-2-(trifluoroacetyl)hydrazinyl groups of the modified nucleoside **14** during Ac₂O capping and removal of the trifluoroacetyl groups by ammonolysis. Reagents and conditions: a) conventional Ac₂O capping; b) conventional phosphoramidite strategy; c) NH₃, H₂O.*[120]
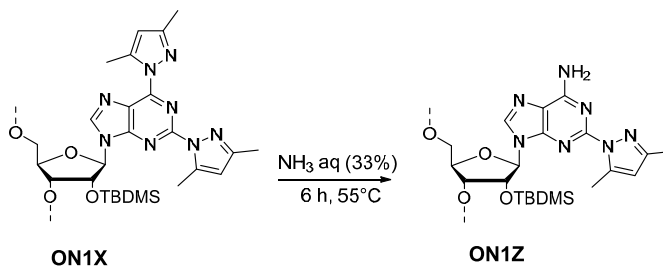
Scheme 12. *Displacement of a dimethylpyrazol-1-yl group with ammonia during deprotection and release of the oligonucleotide from the support.*[120]

Table 6. Structures and *m/z* values[a] of the unmodified and terminally modified 2′-*O*-Me-ORN oligonucleotides used in this study.

	Sequence	*m/z* (absd.)	*m/z* (calcd.)
ON4UA	5′-UGCGCA-3′	1956.4	1956.4
ON4AA	5′-AGCGCA-3′	1979.4	1979.4
ON4GA	5′-GGCGCA-3′	1995.3	1995.4
ON4CA	5′-CGCGCA-3′	1955.4	1955.4
ON4UX	5′-UGCGC**X**-3′	2115.5	2115.5
ON4AX	5′-AGCGC**X**-3′	2138.5	2138.5
ON4GX	5′-GGCGC**X**-3′	2154.4	2154.5
ON4CX	5′-CGCGC**X**-3′	2114.4	2114.5
ON4UZ	5′-UGCGC**Z**-3′	2036.4	2036.4
ON4AZ	5′-AGCGC**Z**-3′	2059.5	2059.5
ON4GZ	5′-GGCGC**Z**-3′	2075.5	2075.5
ON4CZ	5′-CGCGC**Z**-3′	2035.4	2035.4
ON5UA	5′-UGCACA-3′	1940.4	1940.4
ON5AA	5′-AGCACA-3′	1963.4	1963.4
ON5GA	5′-GGCACA-3′	1979.4	1979.4
ON5CA	5′-CGCACA-3′	1939.4	1939.4
ON5UX	5′-UGCAC**X**-3′	2099.4	2099.5
ON5AX	5′-AGCAC**X**-3′	2122.5	2122.5
ON5GX	5′-GGCAC**X**-3′	2138.5	2138.5
ON5CX	5′-CGCAC**X**-3′	2098.5	2098.5
ON5Xa	5′-UCAG**X**-3′	1781.4	1781.4
ON5Xb	5′-UGAG**X**-3′	1821.4	1821.4
ON6X	5′-ACGGC**X**-3′	2139.5	2139.5
ON7X	5′-CGGC**X**-3′	1796.3	1796.4
ON8X	5′-GGC**X**-3′	1477.3	1477.4

[a] By ESI-MS using a negative ion mode.
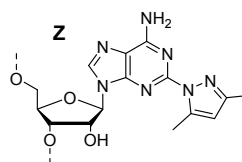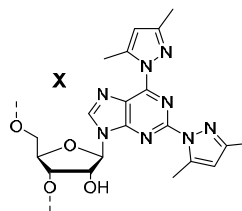
3.3.3 Preparation of pyrrolo-dC-containing RNA targets

The single-strand fluorescent 2′-*O*-Me-ORNs (**ON22**, **ON23**, and **ON2C***) and TAR RNA models (**ON24**, **ON25** and **ON26**) were prepared on an automated synthesizer using commercial pyrrolo-dC phosphoramidite (3-{5′-*O*-(4,4′-dimethoxytrityl-3′-*O*-[(2-cyanoethoxy)(diisopropylamino)phosphanyl]}-β-D-*erthro*-pentofuranosyl)-3,7-dihydro-2*H*-pyrrolo[2,3-d]pyrimidin-2-one) for introduction of the fluorophore (Table 7). Otherwise, commercial 2′-*O*-Me-ORN building blocks were used for the assembly of **ON22**, **ON23** and **ON2C*.** The chain was assembled as described above. The TAR RNA models were assembled from commercial 5′-*O*-DMTr-2′-*O*-TBDMS-protected 3′-phosphoramidite building blocks, but using two consecutive 2′-*O*-methyl ribonucleotides at both ends of the chain to enhance stability of the stem section and to protect the models against cleavage by exonucleases. For the synthesis of single-stranded targets, the 2′-*O*-methylated phosphoramidite building blocks were used exclusively. The

TAR RNA models were deprotected with the mixture of ethanol and 33% aq. NH$_3$ (1:3, *v/v*) at 55 °C for 16 h, followed by removal of the TBDMS groups with 1.53 M triethylamine trihydrofluoride in dry DMSO (2 h at 55 °C). The 2′-*O*-methylated oligonucleotides were ammonolyzed as described above. All the oligonucleotides were purified and characterized, and their concentration was determined as indicated above.[119,120]

Table 7. Structures and *m/z* values[a] of the unmodified and modified RNA oligonucleotides used in fluorometric studies. Lowercase letters refer to ribonucleotide and capital letters to 2′-*O*-Me-ribonucleotide residues. **X** stands for modified nucleoside **1** (see Table 6) and **C**[*] for pyrrolo-2′-deoxycytidine residue.

	Oligonucleotide sequence	*m/z* (obsd.)	*m/z* (calcd.)
ON19	5′-AAUGCAGUGCCGUAA-3′	5008.4	5008.0
ON20	5′-UUACGGCACUGCAUU-3′	4921.7	4921.9
ON21	5′-AAAAAAAAAAAAAAA-3′	5085.5	5085.2
ON22	5′-AAUGCAGUG**C**[*]CGUAA-3′	5015.7	5015.8
ON23	5′-AAUG**C**[*]AGUGCCGUAA-3′	5015.7	5015.8
ON2C*	5′-CCGG**C**[*]GCGC-3′	2978.6	2978.8
ON24	5′-G C **C**[*]a g a^u ^{c}u$_g$ a g c ^{c} ^{u}$_g$ 3′-C G g u c u-------c u c g$_{a\ g}$$_g$	9368.6	9368.2
ON25	$\quad\quad\quad$**C**[*] 5′-G C c a g a^u ^u_g a g c ^{c} ^u_g 3′-C G g u c u------c u c g$_{a\ g}$$_g$	9368.6	9368.2
ON26	5′-G C c a g a^u ^{c}u$_g$ a g c ^{c} ^{u}$_g$ 3′-C G g u c u-----**C**u c g$_{a\ g}$$_g$ $\quad\quad\quad\quad\quad$*	9368.6	9368.1

[a] By ESI-MS using a negative ion mode.

3.4 NMR spectrometric titrations

The binding affinity and selectivity of the modified nucleoside **1** towards a natural uridine nucleoside in the presence and absence of Pd^{2+} was studied by ^{1}H NMR spectrometric titration. The NMR spectra were obtained in a 120 mM deuterated phosphate buffer at pH 7.3, the initial concentration for **1** and uridine being 3.6 mM and that of Pd^{2+} ion 2.5 mM (0.7 equiv.). The titration was performed by stepwise dilution of the sample with buffer until the concentration of uridine and the modified nucleoside **1** was 0.061 mM (Figure 16). At each concentration, two sets of signals for uridine can be clearly distinguished: one referring to the free nucleoside and the other to the putative ternary complex (Figure 16A-D). The two sets were particularly well resolved in the case of the H5 and H1′ resonances of uridine and the integrals of these signals were used to determine the mole fraction of the complex at each concentration (Figure 17).

To ensure that the detected change in the chemical shifts of the H5 and H1′ of uridine was not due to coordination of Pd^{2+} alone, a similar titration was also carried out in the absence of the artificial nucleoside **1** (Figure 16F-I). As seen in Figure 16, the upfield change in the chemical shifts of the H5 and H1′ of uridine in the presence of Pd^{2+} without **1** was in striking contrast to the downfield shift associated with the formation of the assumed ternary complex. Furthermore, the signals of complexes between uridine and Pd^{2+} were much weaker than those of the ternary complex between uridine, Pd^{2+} and **1** under the same conditions. The modified nucleoside **1** exhibited high affinity for Pd^{2+}, as evidenced by the marked downfield shift of the signals of the hydrogens of the pyrazole rings and two of their methyl substituents (Figure 18).

Figure 16. *^{1}H NMR spectra of uridine (H5 and H1′) at various concentrations of uridine, **1** and Pd^{2+} at pH 7.3. (A) [Urd] = [**1**] = 3.6 mM, [Pd^{2+}] = 2.52 mM; (B) [Urd] = [**1**] = 1.49 mM, [Pd^{2+}] = 1.04 mM; (C) [Urd] = [**1**] = 0.57 mM, [Pd^{2+}] = 0.40 mM; (D): [Urd] = [**1**] = 0.061 mM, [Pd^{2+}] = 0.042 mM; (E): [Urd] = [**1**] = 13.84 mM, [Pd^{2+}] = 0; (f)[Urd] = 3.6 mM^1, [Pd^{2+}] = 2.52 mM; (g) [Urd] = 1.49 mM, [Pd^{2+}] = 1.04 mM; (h) [Urd] = 0.57 mM, [Pd^{2+}] =0.40 mM; (i) [Urd] = 0.061 mM.[118]*

Figure 17. *Mole fraction of uridine engaged in the complex* **1***:Pd*$^{2+}$*:U as a function of the concentration of uridine and* **1***;* pH = 7.3.[118]

Figure 18. ^{1}*H NMR spectra of the artificial nucleoside* **1***; A: [***1***] = 3.6 mM, [Pd*$^{2+}$*] = 2.52 mM; B: [***1***] = 3.6 mM, [Pd*$^{2+}$*] = 0; The spectra were measured in a 120 mM deuterated phosphate buffer at pH 7.3.*

As seen in Figure 16A-D, dilution of the sample was accompanied by decrease of the signals of the ternary complex relative to those of free uridine, but even at the

lowest concentration used (61 µM), the mole fraction of the complex was more than 80% of the saturation level observed at high concentration (Figure 17). In contrast, no complex was formed between uridine and **1** in the absence of Pd^{2+} even at relatively high (13.84 mM) concentration of the nucleosides (Figure 16E).

Accordingly, on the basis of ^{1}H NMR titration, Pd^{2+} forms a (1+3) type ternary complex, **1**:Pd^{2+}:U, by binding to N1 of the purine ring and N2 of the pyrazolyl moieties of the modified nucleoside **1** and to N3 of uridine. Rotation around the Pd^{2+}-N3(uridine) bond allows the minimization of steric crowding with the pyrazolyl methyl groups (Figure 19).[124]   In this regard, the most stable conformation is when the bases are perpendicular to each other (Figure 19B).[26] In the double helix due to base stacking, on the other hand, coplanar geometry is favored (Figure 19A).[38,39]

Figure 19. *Ternary complex between artificial nucleoside **1**, Pd^{2+} and uridine and rotation around the Pd^{2+}-N3(U) bond in.[119]*

3.5 Melting temperatures of oligonucleotide duplexes incorporating metal-ion-mediated base pairs

2´-*O*-Me-ORNs were used as mimics of RNA in the present study, because they are hydrolytically much more stable than native ORNs. The temperature is increased above 90 °C during the measurements of duplex melting temperatures and, hence, the risk of metal ion promoted cleavage of phosphodiester linkages is real. The length of ONs was adjusted such that the melting temperature in all cases would be between 20 and 80 °C. The shorter ONs (6-mer-RNA, Table 6) were designed to form homoduplexes bearing two terminal metallo base pairs, which were anticipated to stabilize the double helix more than a single non-terminal modification.

3.5.1 Impact of a single metallo base pair in a non-terminal position within the duplex

The melting temperatures (T_m) of the duplexes between modified (**ON1i; i = X**, **Y**, **Z**, **P**, **Q**) and unmodified (**ON2i**, **i = U**, **A**, **G**, **C**) 9-mer 2´-*O*-Me-ORNs were measured in the presence and absence of divalent metal ions. For comparison, the T_m values of the duplexes of unmodified **ON1A** (containing A instead of the modified nucleoside with the unmodified oligonucleotides **ON2i** (**i = U**, **A**, **G**, **C**) were also determined (Table 8). To find out, whether increasing flexibility in the vicinity of the metallo base pair stabilizes the duplex, a mismatch was introduced to both sides of the metallo base pair. In other words, T_m values were measured for the duplexes that **ON1X** and **ON1A** formed with their mismatched 2´-*O*-Me-ORNs (**ON3i**, **i = U**, **A**, **G**, **C**) in the presence and absence of metal ions (Table 9). To distinguish between the contributions of base pairing and stacking to RNA stabilization by a metallo base pair, respective measurements were performed using **ON2S** as the complementary strand with an abasic site in duplexes formed with modified ONs (**ON1i**, **i = X**, **Z**, **P**, **Q**).

Table 8. Melting temperatures for the duplexes between non-terminally modified 2´-*O*-Me-ORNs (**ON1i** containing a modified nucleoside N^2 = **X**, **Y**, **Z**, **P**, **Q** in a central position) with unmodified 2´-*O*-Me-ORNs (**ON2i** containing any nucleoside, N^1 = **U**, **A**, **G**, **C**, opposite to the modified one in **ON1i**). The values in parentheses refer to the change in T_m on introduction of metal ions. pH = 7.4 (20 mM cacodylate buffer); [oligonucleotides] = 3.0 µM; [metal ions] = 0 or 3.0 µM; I(NaClO$_4$ = 0.10 M).

$$5´\text{-G C G C } N^2 \text{C C G G-}3´ \quad (\textbf{ON1i}; N^2\text{= X,Y,A,P,Q,Z})$$
$$3´\text{-C G C G } N^1 \text{G G C C-}5´ \quad (\textbf{ON2i}; N^1\text{= U,A,G,C,S})$$

M^{2+}	N^2	U	A	G	C	S
				N^1		
no metal	X	61.8 ± 0.4	61.4 ± 0.4	61.6 ± 0.3	60.7 ± 0.2	69.2 ± 0.3
	Y	42.5 ± 0.4	44.9 ± 0.2	45.4 ± 0.2	47.2 ± 0.3	-
	A	75.1 ± 0.3	56.3 ± 0.2	61.2 ± 0.3	59.0 ± 0.2	55.6 ± 0.3
	P	51.9 ± 0.4	53.1 ± 0.4	53.0 ± 0.4	50.1 ± 0.5	58.3 ± 0.2
	Q	67.0 ± 0.6	66.5 ± 0.8	66.1 ± 0.8	66.3 ± 0.6	69.3 ± 0.4
	Z	63.4 ± 0.9	62.7 ± 0.6	63.8 ± 2.1	63.4 ± 0.7	69.6 ± 0.7
Cu^{2+}	X	68.3 ± 0.2 (+6.5)	70.9 ± 0.7 (+9.5)	64.4 ± 1.6 (+2.8)	74.1 ±0.1(+13.4)	70.2 ± 0.5(+1.0)
	Y	43.2 ± 0.8 (+0.7)	44.5 ± 0.5 (-0.4)	45.3 ± 0.3 (-0.1)	50.7 ± 3.0 (+3.5)	-
	A	75.8 ± 0.1 (+0.7)	58.8 ± 0.3 (+2.5)	62.5 ± 0.1 (+1.3)	61.7 ± 0.2 (+2.7)	55.6 ± 0.2 (+0)
	P	58.7 ± 0.8 (+6.8)	54.5 ± 0.5 (+1.4)	56.3 ± 0.6 (+3.3)	53.3 ± 0.6 (+3.2)	58.0 ± 0.3 (-0.3)
	Q	72.2 ± 0.3 (+5.2)	75 ± 2 (+8.5)	72 ± 1 (+5.9)	73 ± 2 (+6.7)	69.6 ± 0.4(+0.3)
	Z	64.8 ± 1.0 (+1.4)	N/A^g	N/A^g	70.6 ± 1.0 (+7.2)	N/A^g
Zn^{2+}	X	65.0 ± 1.0 (+3.2)	69.9 ± 3.0 (+8.5)	63.6 ± 0.8 (+2.0)	68.3 ± 2.0 (+7.6)	69.1 ± 0.4 (-0.1)
	Y	42.3 ± 0.4 (-0.2)	45.7 ± 0.2 (+0.8)	45.7 ± 0.6 (-0.3)	45.7 ± 0.3 (-1.5)	-
	A	76.0 ± 0.3 (+0.9)	56.4 ± 0.2 (+0.1)	62.3 ± 0.1 (+1.1)	61.4 ± 0.1 (+2.4)	55.4 ± 0.2 (-0.2)
	P	51.8 ± 0.4 (-0.1)	52.8 ± 0.8 (+0.9)	54.0 ± 0.8 (+1.0)	51.3 ± 0.6 (+1.2)	58.4 ± 0.1(+0.1)
	Q	74 ± 2 (+7.0)	73 ± 2 (+6.5)	73 ± 2 (+6.9)	72 ± 2 (+5.7)	69.4 ± 0.1(+0.1)
	Z	65.8 ± 1.0 (+2.4)	63.6 ± 0.8 (+0.9)	65.5 ± 1.1 (+1.7)	62.5 ± 0.5 (-0.9)	69.5 ± 1.5 (-0.1)
Pd^{2+}	X	60.6 ± 0.6 (-1.2)	61.6 ± 0.1 (+0.2)	60.1 ± 0.6 (-1.5)	59.9 ± 0.4 (-0.8)	-
	Y	42.4 ± 0.5 (-0.1)	47.5 ± 1.6 (+2.5)	45.7 ± 0.9 (+0.3)	50.7 ± 3.2 (+3.5)	-
	A	73.7 ± 0.1 (-1.4)	56.3 ± 0.1 (+0)	60.4 ± 0.1 (-0.8)	58.8 ± 0.2 (-0.2)	-

^{g} No sigmoidal melting curve was obtained.

Table 9. Melting temperatures for the mismatched duplexes of non-terminally modified 2′-*O*-Me-ORNs **ON1i** (**N² = X** or **A**) with 2′-*O*-Me-ORNs (**ON3i**; **N¹ = U**, **A**, **G**, **C**) containing any nucleotide opposite to **X** or **A** in **ON1i**. The values in parentheses refer to the change in T_m values on introduction of metal ions. pH = 7.4 (20 mM cacodylate buffer); [oligonucleotides] = 3.0 μM; [metal ions] = 0 or 3.0 μM; I(NaClO$_4$ = 0.10 M).

<div align="center">

5′-G C G C N²C C G G-3′

3′-C G C A N¹A G C C-5′

</div>

M²⁺	N²	U	A	G	C
no	**X**	60.4 ± 0.3 (-1.4)	61.0 ± 0.9 (-0.4)	61.8 ± 0.4 (+0.2)	60.3 ± 0.5 (-0.4)
metal	**A**	26.9 ± 0.3 (-48.2)	43.6 ± 0.7 (-12.7)	44.3 ± 0.3 (-16.9)	45.7 ± 0.8 (-13.3)
Cu²⁺	**X**	72.6 ± 0.2 (+12.2)	71.9 ± 0.9 (+10.9)	72.6 ± 0.6 (+10.8)	72.4 ± 0.3 (+12.1)
	A	28.6 ± 0.1 (+1.7)	43.8 ± 0.5 (+0.2)	43.8 ± 0.5 (-0.5)	41.3 ± 0.5 (-4.4)
Zn²⁺	**X**	64.4 ± 0.3 (+4.0)	63.8 ± 0.6 (+2.8)	62.8 ± 0.2 (+1.0)	63.9 ± 0.8 (+3.6)
	A	26.7 ± 0.4 (-0.2)	41.7 ± 0.3 (-1.9)	51.2 ± 0.2 (+6.9)	42.8 ± 0.2 (-2.9)
Pd²⁺	**X**	60.4 ± 0.1 (+0)	61.7 ± 0.9 (+0.7)	60.1 ± 0.2 (-1.7)	61.1 ± 0.3 (+0.8)
	A	27.6 ± 0.1 (+0.7)	44.3 ± 0.6 (+0.7)	43.5 ± 0.9 (-0.8)	43.9 ± 0.7 (-1.8)

Header row over columns U, A, G, C: **N¹**

In all cases, the T_m values were measured in a 20 mM cacodylate buffer at pH 7.4 in the presence and absence of Cu²⁺, Zn²⁺ ions. In the case of **ON1X**, **ON1Y** and **ON1A**, measurements were additionally carried out in the presence of Pd²⁺. The ionic strength was adjusted to 0.1 M with NaClO$_4$ and the concentration of the each ON was 3.0 μM. The concentration of CuSO$_4$, Zn(NO$_3$)$_2$ or K$_2$PdCl$_4$ was either 0 or 3.0 μM.

All results of UV thermal denaturation experiments with 9-mer **ONs** are summarized in Tables 8 and 9. In the absence of divalent metal ions, the most stable duplex was formed between unmodified ONs **ON1A** and **ON2U**, having a Watson-Crick A:U base pair in the middle of the sequence (Table 8). None of the modified ORNs displayed duplex stability of the same magnitude. However, while a non-complementary base (A, C or G) opposite to A diminished T_m by 14 -20 °C, the modified nucleosides were insensitive to the identity of the opposing nucleoside; no selectivity was observed. In fact, hybridization with **ON2S,** containing an abasic site opposite to the modification, was more efficient, whereas omission of the opposing base destabilized the duplex with **ON1A** more markedly than any of the mismatched bases.

Addition of 1 equiv. of Cu²⁺ changed the situation completely: the duplexes formed by **ON1X** and **ON1Q** were stabilized, whereas the duplexes formed by **ON1A** remained essentially unaffected. In particular, all duplexes of **ON1Q**, except **ON1Q**:**ON2S**, were approximately as stable as the fully matched unmodified duplex **ON1A**:**ON2U**. The duplexes formed by **ON1P** and **ON1Z**

were stabilized to a much lesser extent. Interestingly, **ON1X** showed some base selectivity, the ΔT_m values obtained for opposing bases (compared to the situation in the absence of metal ions) being 13.4, 9.5, 6.5, 2.8 and 1.0 for C, A, U, G and abasic site, respectively. With the other modified nucleosides studied, the selectivity was weaker. The effect of Cu^{2+} was not observed at all with duplexes formed by **ON2S**.

Zn^{2+} stabilized the duplexes of **ON1Q** approximately as efficiently as Cu^{2+}. With **ON1X**, Zn^{2+} was somewhat less stabilizing than Cu^{2+}, but retained the base-selectivity for A and C . Only very modest stabilization, if any, was observed with the other modified ORNs. None of the duplexes with **ON2S** was stabilized by Zn^{2+}.

Somewhat unexpectedly, Pd^{2+} ion had virtually no effect on recognition of unmodified ORNs (**ON2i**) with modified ORNs, **ON1X** and **ON1Y**.

The metal-ion-binding base surrogates used in the present study are rather bulky, which may hinder their accommodation inside the rigid base-stacked area between two fully matched base pairs. To make the structure more flexible, one mismatch was introduced on both sides of the metallo base pair. The melting temperatures were measured for duplexes formed by **ON1X** and **ON1A** with their mismatched complements **ON3i** (**i** = **U**, **A**, **G**, **C**) under the conditions indicated above for the duplexes with **ON2i** (**i** = **U**, **A**, **G**, **C**) (Table 5 and 9).

The effect of two mismatches is evident with the duplexes formed by the unmodified oligonucleotide **ON1A**; the melting temperatures dramatically decrease both in the absence or presence of divalent metal ions. In contrast, hybridization of **ON1X** in the absence of divalent metal ions was unaffected by the neighboring mismatches and addition of Cu^{2+} greatly enhanced the stability. Unfortunately, the hybridization did not show any base selectivity. The ΔT_m was (11 ± 1) °C independently of the identity of the opposing base. Only a very modest effect was observed with Zn^{2+} and no effect at all with Pd^{2+}.

3.5.2 Impact of two terminal metallo base pairs

To minimize the steric constraint of the neighboring Watson-Crick base pairs, the metal-ion-mediated base pairing was next studied in a terminal position: the T_m values were measured for self-complementary 6-mer 2´-*O*-Me-ORNs bearing the modified residue at the 3´-terminus. Both matched ONs (**ON4Xi** and **ONZi**, **i** = **U**, **A**, **G**, **C**) and mismatched ONs (**ON5Xi**, **i** = **U**, **A**, **G**, **C**) were studied in the absence and presence of divalent metal ions under the conditions used above with non-terminally modified ORNs. For comparison, the corresponding

unmodified matched (**ON4Ai**, **i** = **U**, **A**, **G**, **C**) and mismatched (**ON5Ai**, **i** = **U**, **A**, **G**, **C**) 2′-*O*Me-ORNs were measured under the same conditions. The T_m values obtained are summarized in Table 10 and 11.

Table 10. Melting temperatures for the duplexes formed by the self-complementary modified (**N²** = **X**, **Z**,; **N¹** = **U**, **A**, **G**, **C**) and unmodified 6-mer 2′-*O*-Me-ORNs (**N²** = **A**; **N¹** = **U**, **A**, **G**, **C**). The values in parentheses refer to the change in T_m on introduction of metal ions; pH = 7.4 (20 mM cacodylate buffer); [oligonucleotides] = 3.0 µM; [metal ions] = 0 or 3.0 µM; I(NaClO$_4$ = 0.10 M).

$$5'\text{-}\mathbf{N^2}\ \mathbf{G}\ \mathbf{C}\ \mathbf{G}\ \mathbf{C}\ \mathbf{N^1}\text{-}3'$$
$$3'\text{-}\mathbf{N^1}\ \mathbf{C}\ \mathbf{G}\ \mathbf{C}\ \mathbf{G}\ \mathbf{N^2}\text{-}5'$$

M^{2+}	N^2	U	A	G	C
				N¹	
no metal	X	44.2 ± 0.6	43.9 ± 1.5	46.9 ± 0.2	44.1 ± 0.5
	Z	53.5 ± 0.1	54.0 ± 0.3	55.7 ± 0.3	51.8 ± 0.2
	A	39.2 ± 0.6	36.8 ± 0.5	37.8 ± 0.2	36.8 ± 0.1
Cu^{2+}	X	71.8 ± 0.5 (+27.6)	62.5 ± 0.3 (+18.6)	69.4 ± 0.3 (+22.5)	62.7 ± 0.2 (+18.6)
	Z	68.7 ± 0.3 (+15.2)	59.2 ± 0.7 (+5.2)	64.4 ± 0.1 (+8.7)	62.0 ± 0.5 (+10.2)
	A	43.0 ± 0.3 (+3.8)	38.9 ± 0.6 (+2.1)	38.3 ± 0.4 (+0.5)	36.7 ± 0.8 (-0.1)
Zn^{2+}	X	51.8 ± 1.0 (+7.6)	50.3 ± 1.8 (+6.4)	52.4 ± 0.1 (+5.5)	48.1 ± 0.5 (+4.0)
	Z	54.3 ± 1.2 (+0.8)	54.4 ± 1.0 (+0.4)	55.2 ± 0.4 (-0.5)	52.9 ± 0.3 (+1.1)
	A	40.0 ± 0.3 (+0.8)	36.6 ± 0.3 (-0.2)	37.0 ± 0.4 (-0.8)	37.1 ± 0.4 (+0.3)
Pd^{2+}	X	54.3 ± 0.7 (+10.1)	44.5 ± 0.8 (+0.6)	41.0 ± 0.4 (-5.9)	38.6 ± 1.6 (-5.5)
	Z	56.2 ± 0.8 (+2.7)	56.8 ± 0.2 (+2.8)	57.0 ± 2.0 (+1.3)	51.5 ± 0.4 (-0.3)
	A	39.4 ± 0.3 (+0.2)	36.1 ± 0.3 (-0.7)	35.8 ± 0.6 (-2)	35.1 ± 1.2 (-1.7)

As seen in Table 10, the modified self-complementary 6-mer 2′-*O*-Me-ORNs form significantly more stable duplexes than their unmodified counterparts, even in the absence of divalent metal ions, in striking contrast to the results of **ON1i** where the modification is non-terminal (see Table 8). In particular, the duplexes of **ON4Zi** (**i** = **U**, **A**, **G**, **C**) having 2-(3,5-dimethyl-pyrazol-1-yl)adenine (**5**) as the modified nucleoside are remarkably stable.

Addition of Cu^{2+} stabilized the duplexes **ON4XU** and **ON4XG** by nearly 28 and 23 °C, respectively. By contrast, only a modest increase in T_m was observed with the unmodified counterparts **ON4AU** and **ON4AG**. The stabilization was base-selective with both **X** and **Z**. The **Z** containing ONs **Z** exhibited higher U-selectivity although they formed weaker duplexes. Accordingly, with the 6-mer duplexes bearing terminal modifications, the metal-ion-mediated binding is U-rather than C-selective, while non-terminal modifications of the 9-mer duplexes favor C over U. The influence of Zn^{2+} ion is modest and not selective. Another

marked difference compared to the behavior of the non-terminally modified 9-mers is that the presence of Pd^{2+} significantly and selectivity enhances the thermal stability of **ON4XU** duplex by increasing the melting temperature by 10 °C.

The greatly enhanced hybridization of the self-complementary 6-mer oligonucleotides bearing terminal metallo base pairs could have been achieved at the cost of reduced base-selectivity in the central part of the duplex. In other words, the thermal stability of these duplexes might solely result from exceptionally high stability of the metal-ion-mediated base pairs. To investigate this possibility, melting temperatures of a series of 6-mer 2′-*O*-Me-ORNs with two consecutive mismatches in the middle of the sequence (**ON5Xi** and **ON5Ai**, **i** = **U**, **A**, **G**, **C**) were measured under the conditions used for the other ONs (Table 10). As seen by comparison of the values in Tables 10 and 11, the T_m values of the mismatched duplex (Table 11) are from 25 to 61 °C lower than those of their matched counterparts (Table 10), irrespective of the presence of divalent metal ions. Obviously even the short metallo oligonucleotides retain the sequence selectivity of the unmodified sequence, regardless of strong stabilization by the two terminal metallo base pairs.

Table 11. Melting temperatures for the duplexes formed by the self-complementary modified (N^2 = **X**; N^1 = **U**, **A**, **G**, **C**) and unmodified (N^2 = **A**; N^1 = **U**, **A**, **G**, **C**) mismatched 6-mer 2′-*O*-Me-ORNs. The values in parentheses refer to the change in T_m on introduction of metal ions. pH = 7.4 (20 mM cacodylate buffer); [oligonucleotides] = 3.0 μM; [metal ions] = 0 or 3.0 μM; I(NaClO$_4$ = 0.10 M).

5′-**N²** G C A C **N¹**-3′

3′-**N¹** C A C G **N²**-5′

		N^1			
M^{2+}	N^2	U	A	G	C
no	**X**	11.2 ± 0.2	14.3 ± 0.3	N/A^g	N/A^g
metal	**A**	10.9 ± 0.1	10.3 ± 0.1	12.0 ± 0.5	12.4 ± 0.4
Cu²⁺	**X**	10.6 ± 0.3	11.7 ± 1.2	10.7 ± 0.5	10.3 ± 0.1
	A	10.3 ± 0.1	10.4 ± 0.1	12.3 ± 1.3	13.7 ± 0.8
Zn²⁺	**X**	10.4 ± 0.2	10.7 ± 0.5	10.1 ± 0.1	10.2 ± 0.2
	A	10.3 ± 0.1	10.3 ± 0.1	10.5 ± 0.1	10.6 ± 0.3
Pd²⁺	**X**	10.6 ± 0.3	10.5 ± 0.2	10.7 ± 0.4	10.9 ± 0.5
	A	10.4 ± 0.1	10.2 ± 0.1	10.3 ± 0.2	10.5 ± 0.4

^{g} No sigmoidal melting curve was obtained.

3.6 CD spectroscopic studies for hybridization properties

To obtain additional information about the helicity of the oligonucleotide duplexes formed in the presence of divalent metal ions, CD spectra[121] for all the duplexes were measured over a wide temperature range from 6 to 94 °C under the conditions that were used for T_m measurements.
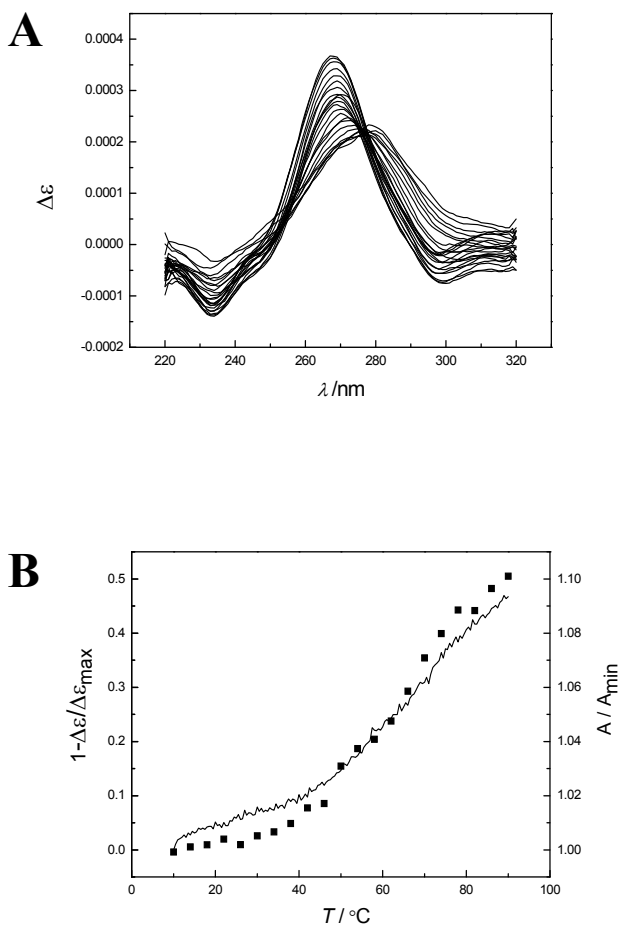
Figure 20. *(A) CD spectra of the **ON1Z**:**ON2C** duplex in the presence of Cu^{2+}, recorded at 4 °C intervals between 6-94 °C and (**B**) thermal hyperchromicity at 260 nm (solid line) and loss of ellipticity (■) of the same duplex; [**ON1Z**] = [**ON2C**] = [Cu^{2+}] = 3.0 μM; I(NaClO₄)=0.1M; pH = 7.4.[119]*

The CD spectra of both the 9-mer (Figure 20A) and 6-mer (Figure 21A) oligonucleotides were at low temperatures characteristic for an A-type duplex. Gradual diminishing of the CD signal was detected on increasing the temperature, *i.e.* upon dissociation of the duplex.[125-127]
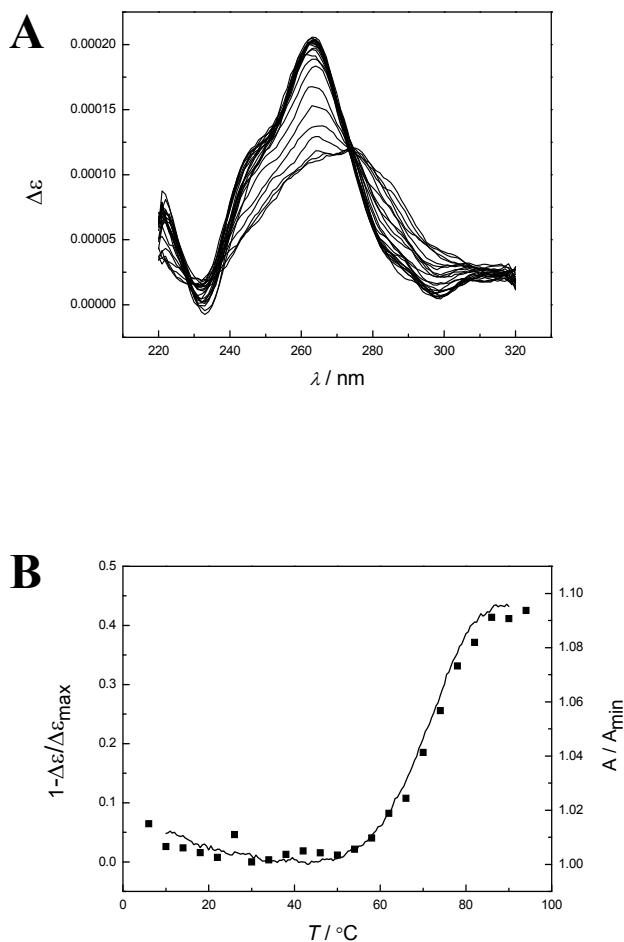
Figure 21. (A) CD spectra of the duplex formed by the self-complementary modified oligonucleotide ON4UX in the presence of Cu^{2+}, recorded at 4 °C intervals between 6-94 °C and (B) thermal hyperchromicity at 260 nm (solid line) and loss of ellipticity (■) of the same duplex; [ON4UX] = [Cu^{2+}] = 6.0 μM; I(NaClO$_4$)=0.1M; pH = 7.4.[120]

As illustrated in Figures 20B and 21B, the loss of ellipticity of CD spectra depended sigmoidally on temperature exhibiting the same inflection point as the UV-melting curves.

3.7 Fluorescence spectrometric studies

In this study, the hybridization of modified metal-ion-binding oligonucleotides with their natural counterparts was examined by using a fluorescent pyrrolocytosine nucleobase (3,7-dihydro-2*H*-pyrrolo[2,3-d]pyrimidin-2-one) as an indicator of hybridization.[128,129] The reason for utilization of fluorescence intensity as the detection method was that the purpose was to examine the interactions with the motives of TAR secondary structure. The fluorescent pyrrolo-dC nucleoside was incorporated within a TAR RNA model. TAR structure includes several double-helical regions, which gives extremely complicated UV melting profiles, therefore the pyrrolo-dC nucleoside was also incorporated in two different sites within a 15-mer 2′-*O*-Me-ORN (Figure 22).

A

ON20	5′-U U A C G G C A C U G C A U U-3′
ON8X	5′-G G C **X**-3′
ON7X	5′-C G G C **X**-3′
ON6X	5′-A C G G C **X**-3′
ON22	3′-A A U G C C **C̊** G U G A C G U A A-5′

B

ON20	5′-U U A C G G C A C U G C A U U-3′
ON6X	5′-G G C **X**-3′
ON7X	5′-C G G C **X**-3′
ON6X	5′-A C G G C **X**-3′
ON23	3′-A A U G C C G U G A C G U A A-5′

◯ = Cu^{2+} **C̊** = Pyrrolo-dC   **X** = Modified nucleoside **1**
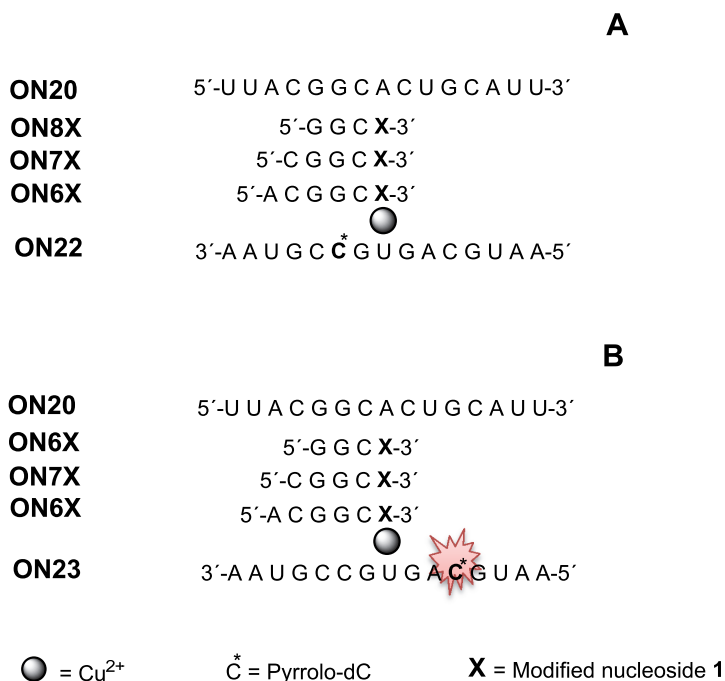
Figure 22. *Metallo base pair formation between the single-stranded oligonucleotides* ***ON22*** *(A) and* ***ON23*** *(B), containing pyrrolo-dC nucleoside in different places within the strand, with short modified (****ON6X****,* ***ON7X*** *and* ***ON8X****) and fully complementary (****ON20****) oligonucleotides. With* ***ON22****, the pyrrolo-dC fluorescence is excepted to be quenched on hybridization with the short oligonucleotides.[128]*

As a proof of concept, the fluorometric studies were first performed with 15-mer 2′-*O*-Me-ORNs containing the fluorescent pyrrolo-dC in two different sites within the ON strand (Figure 22).

3.7.1 Fluorescence spectroscopy results of metal-ion-mediated base-pairing with single-stranded oligonucleotides

The intensity of fluorescence emission of **ON22** and **ON23** as single strands and hybridized with their short modified 6-, 5- and 4-mer complements (**ON6X**, **ON7X** and **ON8X**, respectively) in the presence or absence of 1 equiv. of Cu^{2+} was recorded. The excitation and detection wavelengths were 337 nm and 460 nm, respectively (Figure 23). For maximal quenching of pyrrolo-dC fluorescence, the measurement was also carried out by using the full length **ON20** as a complement. In addition, the fluorescence emission intensity of **ON22** and **ON23** was measured in the presence of a 15-mer oligo(A), used as a model of a non-complementary ON (Table 7). The fluorescence spectra were obtained in a 20 mM cacodylate buffer at pH 7.4, where ionic strength was adjusted with $NaClO_4$ to 0.10 M. The concentration of the oligonucleotides and Cu^{2+} (as $CuSO_4$) was 2.0 μM. The fluorescence emission intensities for the various oligonucleotide assemblies in the presence and absence of Cu^{2+} are presented in Figure 23. Furthermore, the effect of transient intramolecular base-stacking or base-pairing of the single-stranded ONs (**ON22** and **ON23**) on the fluorescence of pyrrolo-dC was estimated by measurements under the same conditions in the presence of formamide (40%, *v/v*) as a denaturant.

In the absence of divalent metal ions, oligonucleotides **ON22** and **ON23** exhibited strong emission at 460 nm. In both cases, the emission was substantially quenched upon formation of a duplex with a full length complementary **ON20**. This behavior was expected since the fluorescent pyrrolo-dC nucleoside became engaged in a double helix. The quenching was somewhat more efficient with **ON23** than with **ON22**. The mismatched oligonucleotide **ON21,** in turn, had no influence on the fluorescence emission of **ON22** and **ON23.**

On using shorter complementary ONs (**ON6X, ON7X, ON8X**) that still hybridized with a sequence containing pyrrolo-dC in **ON22**, the quenching gradually decreased with decreasing the length of the complementary ON. In the case of **ON23**, where the pyrrolo-dC residue is placed outside the sequence engaged in the double helix with these short ONs, the fluorescence emission remained unchanged or was even increased on hybridization. With the 6-mer **ON6X** the emission was increased**,** with the 5-mer and 4-mer it remained

approximately at the level of single-stranded **ON23**. It is worth noting that a marked increase in fluorescence intensity of both **ON22** and **ON23** was detected in the presence of formamide. This suggests that the fluorescence of pyrrolo-dC was also quenched to some extent within a single-stranded ON, most likely due to base-stacking.
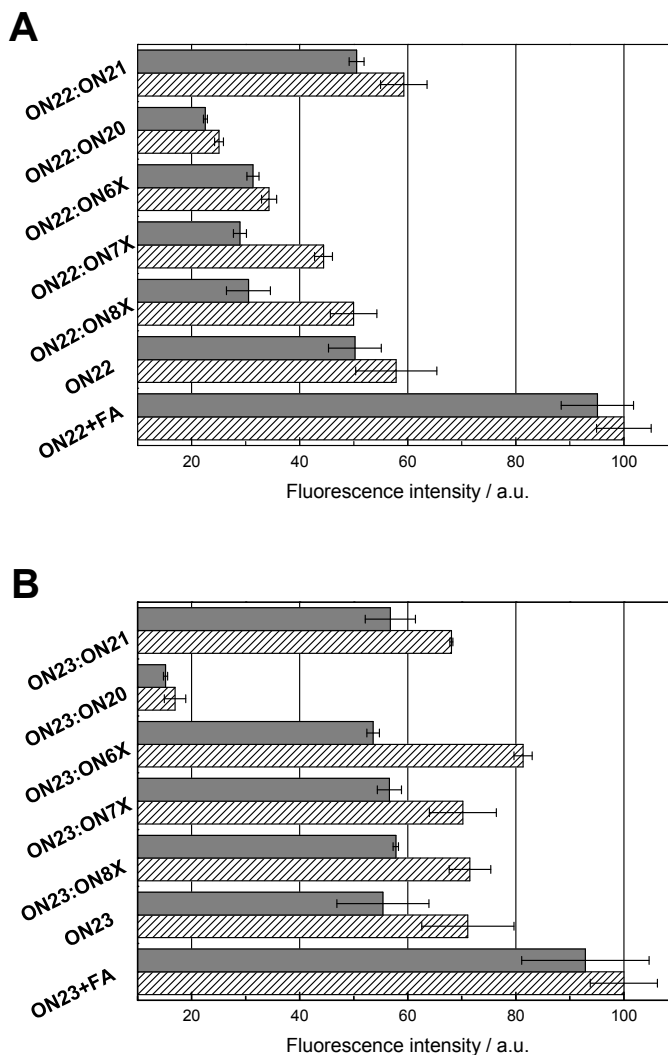
Figure 23. Fluorescence intensity of the pyrrolo-dC residue contained by **ON22**(A) and **ON23** (B) and their duplexes with **ON6X**, **ON7X**, **ON8X**, **ON21** and **ON22** in the absence (hashed bars) and presence of Cu^{2+}(gray bars); $T = 25\ °C$; $pH = 7.4$ (20 mM cacodylate buffer); $I(NaClO_4) = 0.10\ M$; [oligonucleotides] = 2.0 μM; $[Cu^{2+}] = 0$ or 2.0 μM; $\lambda_{ex} = 337\ nm$; $\lambda_{em} = 460\ nm$. FA= formamide.

Addition of 1 equiv. of Cu^{2+} quenched the fluorescence of both **ON22** and **ON23**, as well as their duplexes with the short 4-, 5-, and 6-mer ONs by 10-15%. This change may well be attributed to the coordination of Cu^{2+} ion with pyrrolo-dC base, which to some extent quenches the fluorescence emission.

In addition to this common reduction in fluorescence, the fluorescence of **ON22**:**ON6X**, **ON22**:**ON7X** and **ON22**:**ON8X** was still additionally quenched by 20-30%, most probably because of stabilization by a metal-mediated base pair. In striking contrast to the situation in the absence of Cu^{2+}, the shortest modified ON (**ON8X**) in the presence of Cu^{2+} quenched the fluorescence by 40%, approaching the quenching obtained with the fully complementary duplex **ON22**:**ON20**. A similar enhanced quenching was not observed upon hybridization of **ON6X**, **ON7X** and **ON8X** with **ON23**, having pyrrolo-dC outside the double helical region.

Formation of a Cu^{2+}-mediated base pair may result in a bathochromic shift in the UV absorbance, which might lead to absorption at the excitation wavelength and, hence, quenching. To clarify this issue, the titration analysis of the UV spectrum of modified nucleobase **X** by $CuSO_4$ was performed (Figure 24).
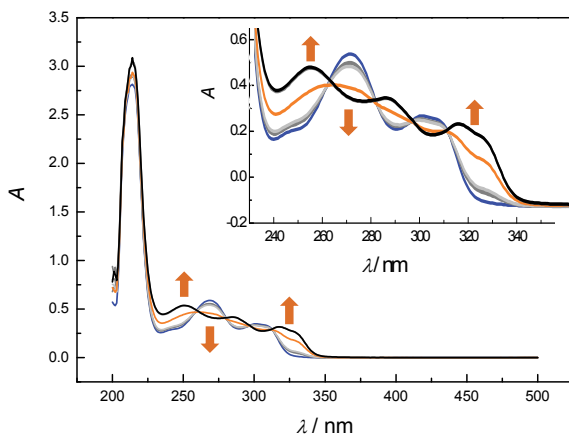
Figure 24. *UV spectrum of the modified nucleoside **X** (10 μM) in the presence Of 0 (blue line), 0.5, 1.0, 1.5, 2.0, 5.0 and 10.0 equiv.(black line) of $CuSO_4$; T = 25 °C; pH = 7.4 (20 mM cacodylate buffer); I(NaClO_4) = 0.10 M.[128]*

As seen, hyperchromic changes at 250 and 330 nm and hypochromic change at 270 nm were detected on addition of Cu^{2+}. The same investigation was also performed with **ON19**:**ON6X** with identical results. According to these results, the absorption by the Cu^{2+}-mediated base pair at 337 nm under the conditions of

the fluorometric measurements has only a negligible influence on the results (approximately 0.01 AU).[128]

The data obtained by fluorescence spectroscopy for hybridization of the linear ONs of various lengths was verified by comparative melting temperature measurements for all duplexes under the conditions used in the fluorescence emission studies. The results are summarized in Table 12.

Table 12. Melting temperatures of the hybridization of the fluorescent oligonucleotides **ON22** and **ON23** with the short metal-ion-chelating oligonucleotides **ON6X**, **ON7X** and **ON8X** and the fully complementary unmodified oligonucleotide **ON20** in the presence and absence of Cu^2; [oligonucleotides] = 2.0 μM; $[Cu^{2+}]$ = 0/2.0 μM; $I(NaClO_4)$ = 0.1 M; pH = 7.4 (20 mM cacodylate buffer).

	ON22		ON23	
	Without Cu^{2+}	**With Cu^{2+}**	**Without Cu^{2+}**	**With Cu^{2+}**
ON8X	10.8 ± 0.5	28.6 ± 0.4 (+17.8)	11.1 ± 0.7	29 ± 3 (+17.9)
ON7X	27.6 ± 1.3	51.5 ± 0.3 (+23.9)	25.3 ± 0.8	51.9 ± 0.5 (+26.6)
ON6X	42.9 ± 0.2	54.6 ± 1.6 (+11.7)	41.9 ± 0.3	55.3 ± 0.4 (+13.4)
ON20	74.0 ± 0.3	74.6 ± 0.2 (+0.6)	70.9 ± 0.3	71.9 ± 0.1 (+1.0)

The results were consistent with the previous observations on short self-complementary oligonucleotides containing the metal-ion-binding nucleoside-**X** at the 3´-end (Table 10). The T_m values expectedly rose with the increasing length of the short modified oligonucleotides. Nearly similar results were obtained with **ON22** and **ON23**, as expected for two almost identical oligonucleotides differing only in the place of the pyrrolocytosine base. The pyrrolocytosine base well imitates the native cytosine in Watson-Crick base pairing. To verify this, the T_m was measured for duplex **ON19**:**ON20**, with canonical C nucleoside instead of pyrrolo-dC. The T_m value obtained (75.5°C) was very close to the one of **ON22**:**ON20** (74.0 °C).

The influence of Cu^{2+}-mediated base pairing of pyrrolocytosine on its fluorescence was also studied with ONs containing the Cu^{2+}-binding nucleoside **X** and pyrrolo-dC in a complementary non-terminal position. The fluorescence intensity measurements were carried out for duplex **ON1X**:**ON2C***** (Figure 25). The stability of a similar duplex containing C in place of C* had been previously studied by T_m measurements (Table 8).
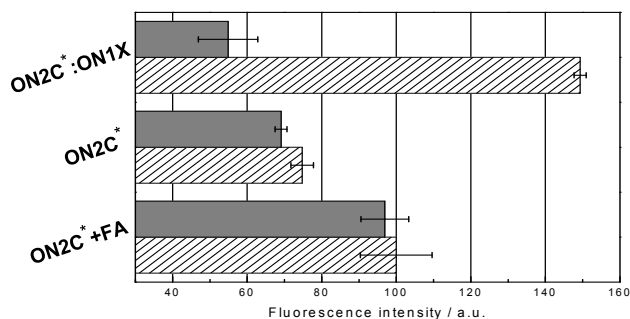
Figure 25. *Fluorescence intensity of the pyrrolo-dC nucleoside in middle of **ON2C****and its duplex with **ON1X** in the absence (hashed bars) and presence of Cu^{2+}(gray bars); T = 25 °C; pH = 7.4 (20 mM cacodylate buffer); $I(NaClO_4)$ = 0.10 M; [oligonucleotides] = 2.0 μM; $[Cu^{2+}]$ = 0 or 2.0 μM; λ_{ex} = 337 nm; λ_{em} = 460 nm. FA= formamide.*

The fluorescence emission of **ON2C*** was similar to that of the single-stranded 15-mer oligonucleotides **ON22** and **ON23**, both in the presence and in the absence of Cu^{2+} (Figure 25). The fluorescence of the duplex **ON1X**:**ON2C*** was, in turn, very different, the emission being more than two times as high as that of single-stranded **ON2C***. The probable explanation for this large increase of emission is that the bulky 2,6-bis(3,5-dimethylpyrazol-1-yl)purine base forces the pyrrolocytosine out of the double helix, exposing it even more than in single-stranded **ON2C*** (Scheme 13). The same effect has been observed for complexes of the methyl-specific endonuclease McrBC with unnatural pyrrolo-dC-containing ONs, in which case flipping out of the cytosine base was also proved by X-ray crystallography.[130] Addition of Cu^{2+} quenched markedly the fluorescence intensity, comparable to the level observed with **ON22**:**ON6X**, **ON22**:**ON7X** or **ON22**:**ON8X** (see Figure 23A). Evidently through formation of the Cu^{2+}-mediated base-pair between pyrrolocytosine and **1**, the pyrrolocytosine becomes part of the base stack again (Scheme 13).
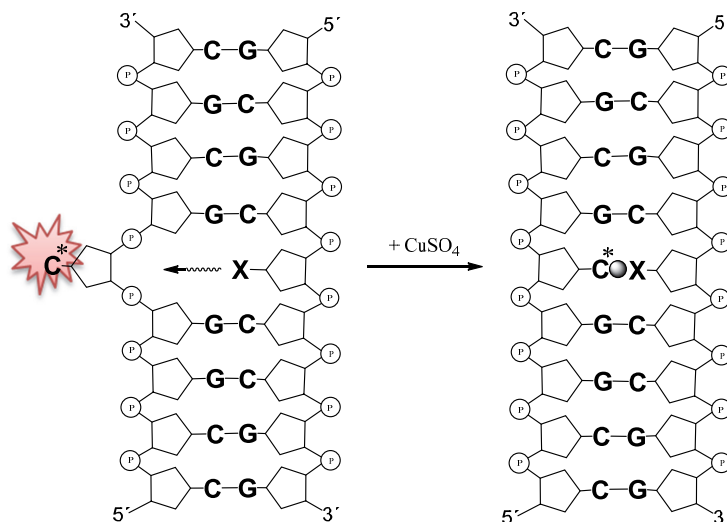
Scheme 13. *Pyrrolocytosine deflected out of the double-strand because of bulkiness of artificial nucleoside X and again accommodated in the double helix by Cu^{2+}-mediated base pairing between C^* and X.*

3.7.2 Hybridization and recognition of the bulge motif of TAR RNA by short metallo oligonucleotides

To study the hybridization selectivity of short metal-ion-binding ONs towards the bulge region (UCU) of TAR RNA, the fluorescence of the three models (**ON24**, **ON25** and **ON26**) with a different placement of the pyrrolo-dC residue were measured in the presence and absence of 5-mer 2′-*O*-Me-ORNs, **ON5Xa** and **ON5Xb** under the conditions used above for the single-stranded targets (Figure 26 and Scheme 14). In **ON25** target model, the pyrrolo-dC was located in the bulge region (UC*U), while in **ON24** and **ON26** it was placed within the double-helical stem. Therefore, only **ON25** was expected to show a clear drop of fluorescence emission upon hybridization with fully complementary **ON5Xa** or partly complementary **ON5Xb** incorporating a GG-mismatch.

A

5´-G C C*a g a $^{u^{c}u}$ g a g c $^{c u}$ g
    : : : : : :   : : : :   g
3´-C G g u c u------- c u c g $_{a g}$

ON5Xa
            3´-**X**GACU-5´

ON24
5´-G C C*a g a $^{u^{c}u}$ g a g c $^{c u}$ g
: : : : : :   : : : :   g
3´-C G g u c u------- c u c g $_{a g}$

B

5´-G C c a g a $^{u^{c}u}$ g a g c $^{c u}$ g
    : : : : : :   : : : :   g
3´-C G g u c u------ c u c g $_{a g}$

            3´-**X**GACU-5´

5´-G C c a g a $^{u^{c}u}$ g a g c $^{c u}$ g
: : : : : :   : : : :   g
3´-C G g u c u------ c u c g $_{a g}$
         ON25

C

5´-G C c a g a $^{u^{c}u}$ g a g c $^{c u}$ g
    : : : : : :   : : : :   g
3´-C G g u c u------ **C**$_{*}$u c g $_{a g}$

ON5Xb
            3´-**X**GAGU-5´

ON26
5´-G C c a g a $^{u^{c}u}$ g a g c $^{c u}$ g
: : : : : :   : : : :   g
3´-C G g u c u------ **C**$_{*}$u c g $_{a g}$

⬤ = Cu^{2+}

C* =

X =
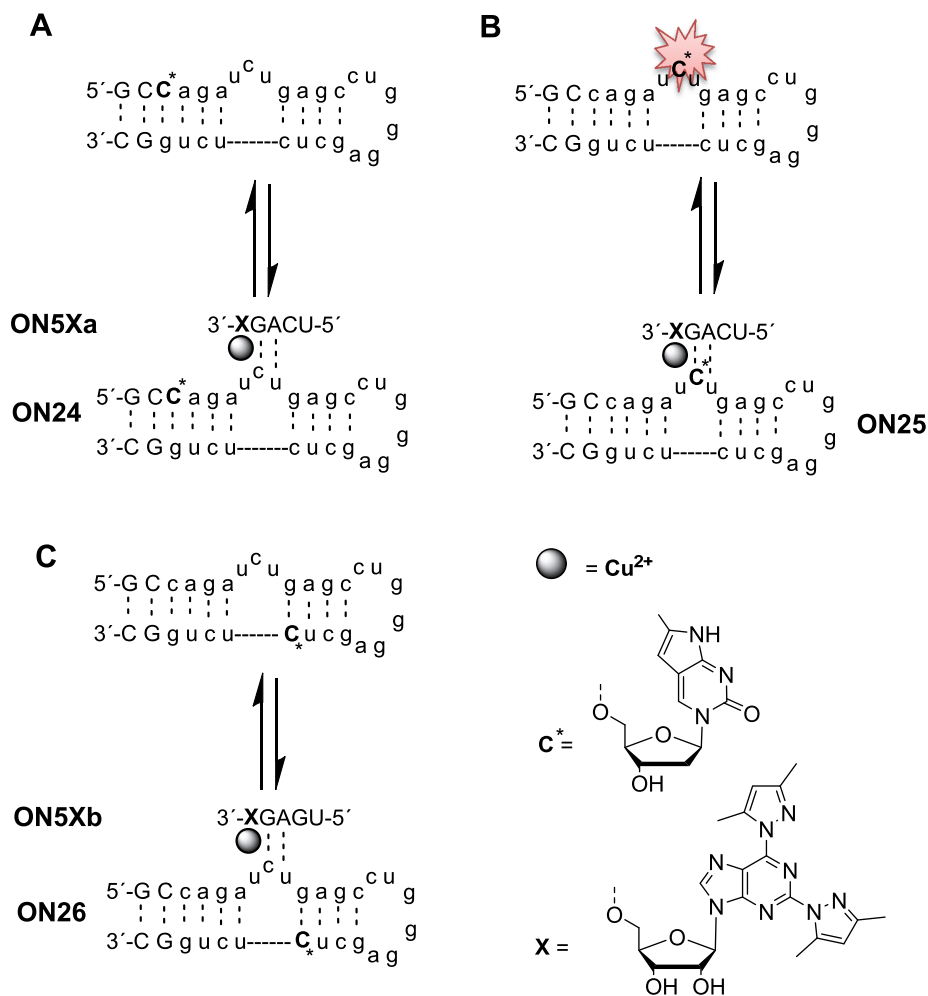
Scheme 14. *Metal-ion-chelation between short modified oligonucleotides and the bulge (UCU) region of TAR RNA. A pyrrolo-dC nucleoside is incorporated in different places of the TAR RNA models. The lowercase letters refer to ribonucleotide and capital letters to 2´-O-methylribonucleotide residues, respectively. Pyrrolo-dC in the duplex part is expected to be only weakly fluorescent (A and C), whereas pyrrolo-dC in the bulge region is expected to emit relatively strongly (B).*
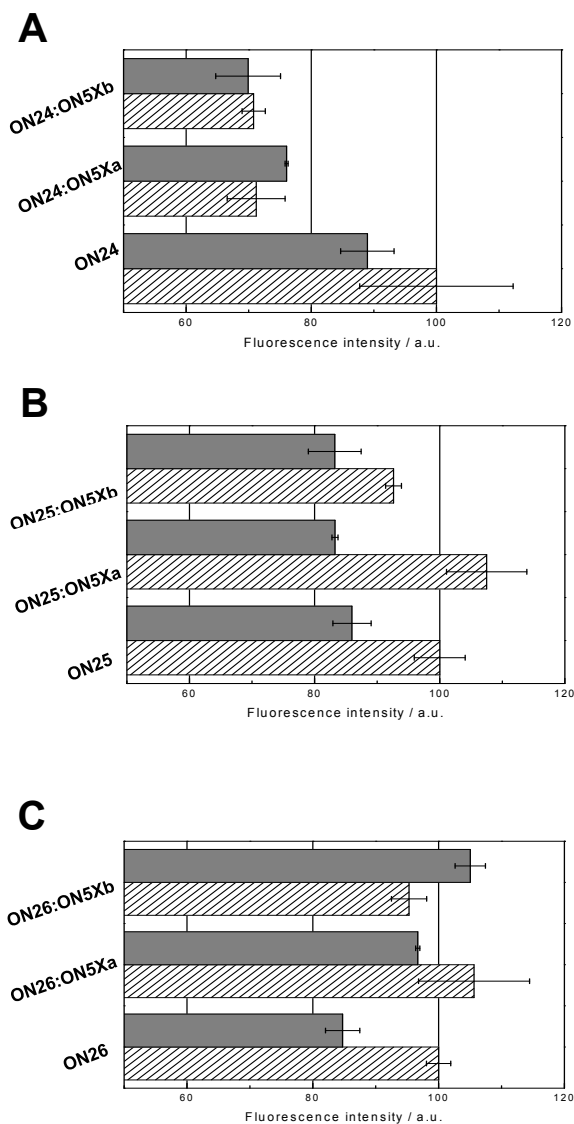
Figure 26. *Fluorescence intensity of the pyrrolo-dC probe in **ON24** (A), **ON25** (B) and **ON26** (C) and their duplexes with **ON5Xa** and **ON5Xb** in the absence (hashed bars) and presence of Cu^{2+}(gray bars); T = 25 °C; pH = 7.4 (20 mM cacodylate buffer); $I(NaClO_4)$ = 0.10 M; [oligonucleotides] = 2.0 μM; $[Cu^{2+}]$ = 0 or 2.0 μM; λ_{ex} = 337 nm; λ_{em} = 460 nm.*

The fluorescence emission of **ON24**, **ON25** and **ON26** turned out to be similar in the absence of Cu^{2+}, in spite of the fact that pyrrolo-dC is in **ON25** situated within a single stranded bulge and in **ON24** and **ON26** engaged in a double

helix. The situation changed when the short fully complementary **ON5Xa** was added: the intensity of **ON25** and **ON26** was slightly increased, whereas the fluorescence of **ON24** was unexpectedly decreased by 30% (Figure 26). Addition of partly complementary **ON5Xb** was quenching with all the three models: 30, 8 and 5% with **ON24**, **ON25** and **ON26**, respectively.

On addition of Cu^{2+}, the fluorescence emission of **ON25**:**ON5Xa** and **ON25**:**ON5Xb** was reduced by 25% and 17%, consistent with more efficient binding of fully complementary **ON5Xa**. Among other duplexes, **ON26:ON5Xa** experienced 9% quenching, while the fluorescence of the rest of the duplexes remained almost unchanged or modestly increased. These results are consistent with the expectations, but the observations that addition of Cu^{2+} markedly reduces the fluorescence of all the targets (**ON24**-**ON26**) in the absence of **ON5Xa,b** severely questions the reliability of this approach. In addition, the fact that the fluoresence emission of **ON24** is markedly reduced by hydridization with **ON5Xa,b** in the absebce of Cu^{2+} is difficult to explain. In summary, the expected strong and selective quenching of the fluoresecence of **ON25** in the presence of **ON5Xa** did not come true. The three base bulge (Scheme 14) may still be structurally so ordered that its interactions with short probes cannot be fully compared to interactions of relaxed single strands.

3.8 Hydrolytic stability of the modified oligonucleotides

During the release of oligonucleotides **ON1X** and **ON4Xi** (i = **U**, **A**, **G**, **C**) from the support and deprotection of the base moieties by concentrated aq. NH_3, some displacement of the pyrazolyl substituent at position 6 of the modified nucleoside **X** by NH_3 took place (Scheme 12). This questioned the hydrolytic stability of ORNs containing the modified residue **X** at the high temperatures used in the T_m measurements. Although water is a weaker nucleophile than NH_3, coordination of a metal ion to N2 of the pyrazole ring may render the purine ring more susceptible to nucleophilic attack.

To assess the extent of hydrolysis of the modified oligonucleotides under conditions of the melting temperature studies, the samples were analyzed by HPLC and ESI-MS before and after the measurement (3 cycles from 0 to 90 °C and back, with 0.5 °C min^{-1}). The **ON1Z**, **ON1P** and **ON1Q** oligonucleotides were shown to be fully stable. **ON1X** had, however, been partially converted to the hydrolysis product **ON1Q** in the presence of Cu^{2+} (Scheme 15). In other words, the 2,6-bis(3,5-dimethylpyrazol-1-yl)purine (**X**) base had been converted to 2-(3,5-dimethylpyrazol-1-yl)hypoxanthine (**Q**).
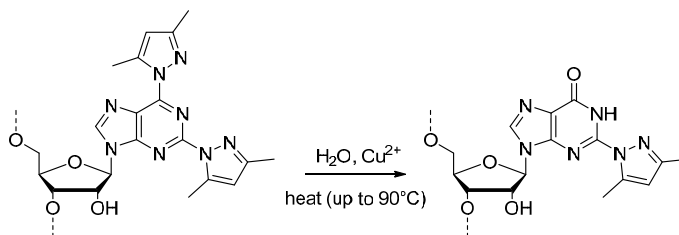
Scheme 15. *Hydrolytic conversion of 2,6-bis(3,5-dimethylpyrazol-1-yl)purine residue to a 2-(3,5-dimethylpyrazol-1-yl)hypoxanthine residue.*[119]

This transformation was not observed in the presence of Zn^{2+} or in the absence of divalent metal ions with the 6-mer ONs containing **X**.
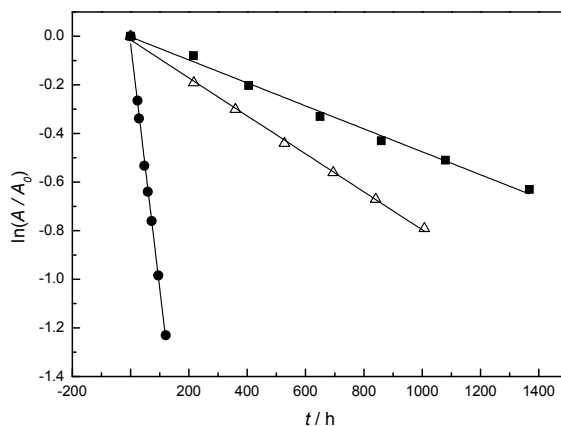
Figure 27. *Logarithmic time profiles for the decomposition of **ON5Xa** in the absence (■) and presence of Cu^{2+} (●) or Zn^{2+} (△); [**ON5Xa**] = [$CuSO_4$] = [$Zn(NO_3)_2$] = 2.0 μM; $I(NaClO_4)$ = 0.1 M; pH = 7.4; T = 37 °C.*[119]

To obtain more quantitative data on the hydrolytic stability of oligonucleotides containing the modified nucleoside **X**, kinetic studies were performed with a 5-mer oligonucleotide, **ON5Xa** (Figure 27). The reactions were carried out in 20 mM cacodylate buffer (pH = 7.4) in the absence and presence of 1 equiv. of either $CuSO_4$ or $Zn(NO_3)_2$ at 37 °C. The ionic strength was adjusted to 0.1 mol L⁻

[1] with $NaClO_4$ and the starting concentration of **ON5Xa** was 2.0 μM for each kinetic run. Potassium 4-nitrobenzenesulfonate was used as an internal standard. Aliquots were withdrawn from the reaction solutions at appropriate time intervals to cover approximately one half-life and analyzed by RP HPLC. The disappearance of the starting material (**ON5Xa**) obeyed first-order kinetics.

In all cases, loss of **ON5Xa** was accompanied by the appearance of a new product, which eluted faster. ESI-MS analysis confirmed the product to be **ON5Q** (Scheme 15). The degradation half-lives of **ON5Xa** in the presence of Cu^{2+} and Zn^{2+} and in the absence of divalent metal ions at 37 °C were 69, 880 and 1500 h, respectively (Figure 27).

4. DISCUSSION

4.1 The effect of metal-ion-binding nucleosides in a non-terminal position on the duplex stabilty

4.1.1 The effect of steric and stacking interactions

Replacement of a non-terminal adenosine with any of the modified nucleosides studied (**X**, **Q**, **P**, **Z**, **Y**) destabilized the double helix with unmodified complementary ONs. With **X**, **Q** and **Z**, the destabilization was, however, lesser than that caused by AA, AG and AC mismatches. Modification **Y** was exceptionally destabilizing. One may tentatively assume that hydrazinyl substituents do not increase the polarizability of the purine π-electron system as much as the aromatic pyrazolyl groups and, hence, stacking with the neighboring base pairs is weaker. Destabilization was less prominent when the base opposite to the modified base is removed, evidently owing to reduction of steric repulsion. In fact, ORNs containing **X**, **Q** or **Z** hybridized better than their **A** containing counterpart with the abasic complement **ON2S.** Since 2-(3,5-dimethylpyrazol-1-yl) substituted **Q** and **Z** were as destabilizing as their 2,6-disubstituted counterpart **X**, stacking around the C2 seems to be of particular importance. A mismatch on both sides of surrogate nucleoside **X**, which made the structure more flexible, did not additionally retard hybridization, while the same mismatches on both sides of an AU pair were highly destabilizing.

4.1.2 The effect of metal-ion-mediated base pairing

In the presence of Cu^{2+} (1 equiv.), ORNs containing **X** or **Q** hybridize approximately as efficiently as the fully complementary unmodified ORNs. The fact that the T_m values are 3-13 ºC higher than in the absence of Cu^{2+} may be taken as a strong indication of metal-ion-mediated bonding to the opposing canonical nucleoside. This conclusion receives further support from the fact that duplexes with ORNs bearing an abasic site opposite to the metal-ion-binding nucleobase were not stabilized by Cu^{2+}. Mismatches for both sides of the metallo base pair still slightly increased stability of the duplex, evidently by reducing constraints for formation of the metallo base pair.

The artificial nucleobases of **X**, **P**, **Q** and **Z** most likely offer N2 of dimethylpyrazolyl ring as a donor atom in addition to N1 or N7 of the purine base. The free electron pair on N2 of the pyrazole ring is not part of the aromatic π-electron system and is, hence, readily available for coordination. Tentatively, **X** may serve as a tridentate, and **P**, **Q** and **Z** as bidentate ligands. The most likely

coordination modes are depicted in Figure 28: binding to N1 and pyrazole-N2 for **X**, **Q** and **Z** and to N7 and pyrazole-N2 for **P**. The recent report on Cu^{2+} binding to N7 of 6-furylpurine 2′-deoxyriboside lends support for the suggested binding mode of **P**.[131] The remaining binding sites of Cu^{2+} in **X**, **Q**, **Z** and **P** are presumably occupied by the ring nitrogens of the opposing canonical base or by water. Several IR, EPR and NMR spectrometric and X-ray crystallographic studies have established N1 and N7 of purines[132-143] and N3 of pyrimidines[144-147] as the favored binding sites for Cu^{2+}.[148-152] At physiological pH, adenosine and cytidine coordinate mainly through N7 and N3, respectively, and guanosine and uridine through deprotonated N1 and N3, respectively. The lone electron pair of the oxo substituents is also available for metal ion binding, whereas the lone electron pair of the amino groups is involved in the aromatic π-electron system and, hence coordination to amino nitrogen is only possible by displacement of a proton.[153,154] The behavior of Zn^{2+} largely resembles that of Cu^{2+}, but the binding is weaker.[143,152,155]
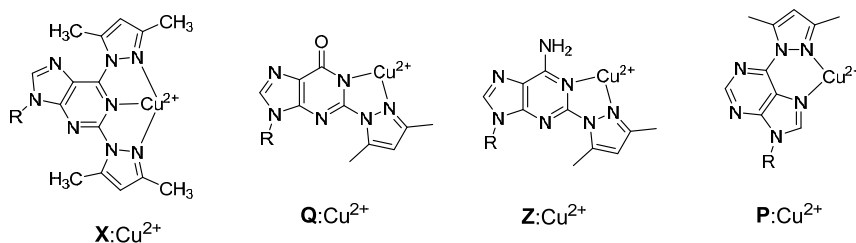
Figure 28. *Coordination of Cu^{2+} by the modified tridentate nucleoside **X**, and bidentate nucleosides **Q**, **Z** and **P**.*

The stability of the metal-ion-mediated base pairs appears to correlate with the potential of either the natural or the surrogate base to serve as an anionic ligand. The greatest elevations in T_m in the presence of Cu^{2+} or Zn^{2+} are observed in cases where at least one member can deprotonate to give an anion. The natural nucleosides guanosine and uridine, and probably the modified nucleoside analog **Q**, may undergo deprotonation upon coordination of Cu^{2+} or Zn^{2+} at physiological pH (Figure 29). The modified oligonucleotide **ON1Q,** hence, formed a stable duplex irrespective of the identity of the opposing base (Figure 29).
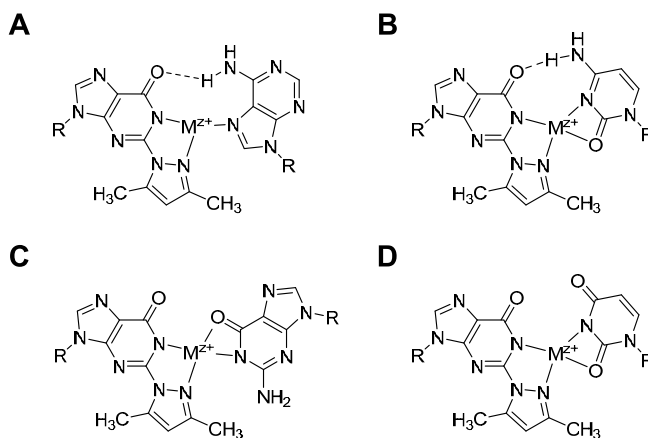
Figure 29. *Suggested metal-ion-mediated base pairs between **Q** and natural nucleosides: (A) adenosine, (B) cytidine, (C) guanosine and (D) uridine.*

Unlike **ON1Q,** modified oligonucleotides **ON1P** and **ON1Z** are not readily deprotonated under the experimental conditions. Accordingly, stable duplexes were formed only with oligonucleotides that contained G or U opposite to the modified base (Figure 30 and 31). **ON1Z** made an exception. C was preferred over U–in the presence of Cu²⁺. T_m value measurements with complements containing A and G failed (no clear inflection point could be obtained), which also questions the credibility of the data obtained with the C and U containing complements.

The tridentate metal chelates of **X** prefer binding to C and A, in contrast to the bidentate chelates of **P** and **Q**. Since **X** is more bulky than **P**, **Q** and **Z** containing only one pyrazolyl substituent, steric factors may play a more important role with this modification. Interactions between the methyl substituents of the pyrazolyl moieties and the opposing canonical bases should be taken into account besides the electronic effects. The structures depicted in Figure 32 do not, however, offer any straightforward explanation for higher stability of planar metal-ion-mediated structures with C and A compared to U and G. As discussed in the section of geometry and coordination of this thesis (1.2.2.), many factors influence on the stability of planar metal-ion-mediated base pairs between tridentate terpyridine and monodentate ligands. Even steric repulsion between hydrogen atoms retards formation of a planar structure (see Scheme 2).[39] One should also bear in mind that in addition of the four donor atoms forming the square planar ligand field,

donor atoms of neighboring base pairs may also contribute to the overall stability by serving as axial ligands. In other words, the ligand field may rather be a distorted octahedron than purely square planar. The alternative that, owing to steric repulsion of the pyrazolyl methyl groups, C (and maybe A) is bound by displacement of one of the amino protons should not be strictly excluded, either. In other words the donor atom would be N4 (with A N6) instead of N3 (Figure 32, A2 and B2). This kind of binding mode is known to occur with cytidine.[156] Interestingly, when the duplex structure was made more flexible by introducing mismached base pairs on both sides of **X**, the C/A-selectivity disappeared.

Figure 30. *Suggested metal-ion-mediated base pairs between **P** and natural nucleosides: (A) adenosine, (B) cytidine,(C) guanosine and (D) uridine.*
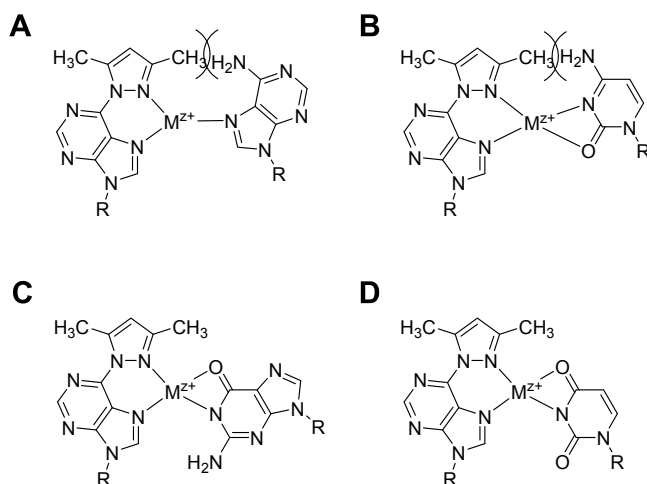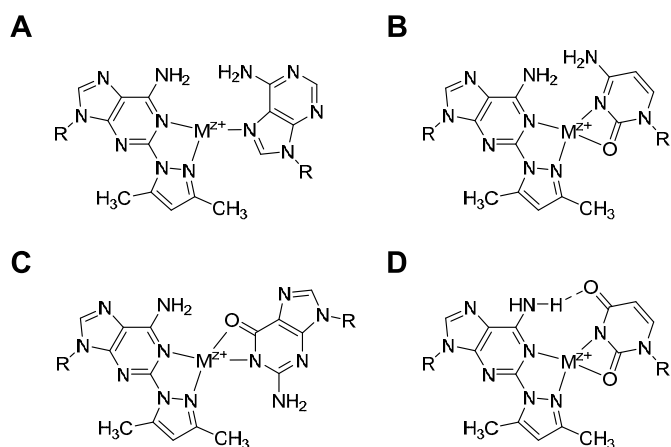
Figure 31. *Suggested metal-ion-mediated base pairs between **Z** and natural nucleosides: (A) adenosine, (B) cytidine,(C) guanosine and (D) uridine.*
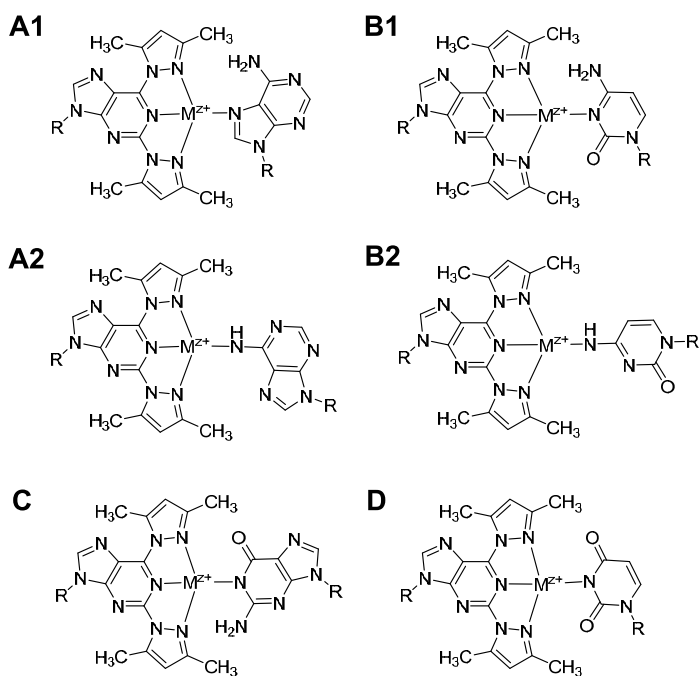
Figure 32. *Suggested metal-ion-mediated base pairs between **X** and natural nucleosides: (A1 and A2) adenosine, (B1 and B2) cytidine, (C) guanosine and (D) uridine.*

Zn^{2+} enhances the hybridization of **ON1X** and **ON1Q** with unmodified targets, but has a minor influence on hybridization of **ON1P**, **ON1Y** and **ON2Z**. **ON1X** shows selectivity towards A and C (as with Cu^{2+}), whereas **ON1Q** exhibits equally high affinity to U, A, G and C containing targets. These findings are noteworthy as Zn^{2+}-mediated base pairs have not been previously described. For example, the stability of a duplex DNA oligonucleotide containing a 3-pyridine:2,6-pyridinedicarboxylate base pair (see Figure 14A and Table 4) was markedly increased by Cu^{2+}, but none of the other metal ion studied, including Zn^{2+}, had any effect.[46] With hydroxypyridone homo-base pairs, as well as hydroxypyridone:pyridopurine base pairs (Figure 11B), stabilization by Zn^{2+} was observed but even in those cases the influence was much less than with Cu^{2+}.[157]

No clear evidence of duplex stabilization by Pd^{2+} was obtained with **ON1X** or **ON1Y**. The latter showed a modest increase in T_m with **ON2A** and **ON2C**. Perhaps the less bulky **ON1Y** is better compatible with relatively bulky Pd^{2+} ion.

4.2 The influence of metal-ion-binding nucleoside in a 3´-terminal position on the duplex stability

4.2.1 The effect of steric and stacking interactions

Only 2,6-bis(3,5-dimethylpyrazol-1-yl)purine riboside (**X**) and 2-(3,5-dimethylpyrazol-1-yl)adenine (**Z**) were studied as modified nucleoside analogues at the 3´-terminus. While replacement of a non-terminal A with either **X** or **Z** markedly destabilized the duplex in the absence of metal ions, the influence in 3´-terminal position was the opposite. **Z** was more strongly stabilizing than **X**. Evidently the steric constraints for proper accommodation of the modified base into the double helical structure are now less demanding.[26,39] The modified self-complementary ORNs (all in **ON4X** series) give higher T_m values compared to their natural counterparts (**ON4A**), most likely due to enhanced stacking of the modified bases. With Z, the stabilization is more prominent than with X (Table 10 and Figure 28). This result is consistent with the observation that the pyrazole ring on C2 is more favorable for stacking than the same group on C6 (see section 4.1.1).

4.2.2 The effect of metal-ion-mediated base pairing

While **X** in a non-terminal position favored binding to C and A in the presence of Cu^{2+}, it exhibited U/G-selectivity when situated in a terminal position. In other words, the selectivity was similar to that of the other modified nucleosides (**P**, **Q**)

in a non-terminal position. The other modified nucleoside, **Z**, studied in a terminal position was also U/G-selective. In summary, the nucleosides being able to bind as anionic ligands seem again to be favored. A possible reason for the different selectivity of **X** in terminal and non-terminal position is that the otherwise preferred binding mode is retarded in a non-terminal position due to difficulties in accommodating the relatively large base moieties within the base-stack of a fully complementary double helix (Figure 4). Such constraints evidently are less stringent in a terminal position. It is worth noting that one mismatch on both sides of a non-terminal **X** abolishes the C/A-selectivity; addition of Cu^{2+} increases the T_m value 11-12 ℃ irrespective of the identity of the opposing base.

The highly stabilizing influence of **X** in a terminal position is not limited to formation of 6-mer duplexes bearing a metallo base pair at both termini. The duplex that pentamer **ON7X** formed with a longer target **ON23** experienced upon addition of Cu^{2+} an increase of 26 ℃ in the T_m value.

The results obtained with Pd^{2+} ion, *viz.* the high stability of the Pd^{2+}-mediated base pairs formed by the modified nucleoside **X** at the monomeric level, and the inability of Pd^{2+} to stabilize oligonucleotide duplexes containing the same residue, are puzzling. Maybe the inert Pd^{2+} binds too strongly to an unwanted place, wherein the thermodynamically most stable product [metallo base pair X:Pd:U(or C,A,G)] can not be formed, however the situation slightly improves at terminal position with 10 ℃ increase in T_m. Although many coplanar Pd^{2+}-chelated base pairs have been reported,[81,86,158] attempts to stabilize ON duplexes with such base pairs have failed.

4.3 Fluoresence spectrometric studies on probing RNA secondary structure by metal-ion-mediated base pairing

Hybridization of short metal-ion-bonding 2′-*O*-Me-ORNs with longer target sequences containing a pyrrolo-dC fluorophore has been shown to be accompanied by marked quenching in the presence of Cu^{2+} in case the pyrrolocytosine base becomes engaged in double helix.

Comparative melting temperature determinations have verified that, the drop of fluorescence intensity upon hybridization correlated well with the thermal stability of the duplex. Attempts to exploit these metal-ion-binding short ORNs for probing of RNA secondary structure have unfortunately been less successful. Marked fluorescence quenching was observed upon Cu^{2+}-mediated binding of the putative probe to the trinucleotide bulge of a TAR RNA model in case the

bulge contained pyrrolo-dC. The quenching was not, however, sufficiently quantitative to allow firm conclusions to be drawn, since addition of ORN probes in the absence of Cu^{2+} or addition of Cu^{2+} in the absence of ORN probe also markedly influenced on the fluorescence intensity. Evidently the three unpaired bases of the bulge are not sufficient for efficient hybridization, even if one of the base pairs participants would be a strong metal-ion-mediated one.

5. CONCLUSIONS

Several Cu^{2+}-mediated base pairs between two bidentate ligands and between one tridentate and one monodentate ligand have been introduced into ONs earlier by others. Markedly increased T_m values have, however, been reported only when both ligands are modified nucleosides.

In our study, the 3,5-dimethylpyrazol-1-yl substituted purine derivatives incorporated into 2´-*O*-Me-ORNs exhibit different preferences in metal-ion-mediated base pairing with natural nucleobases depending on the location of the pyrazolyl substituents. The duplex stability significantly dependent on whether the purine derivative is readily able to participate in the metal-ion-mediated base pair as an anionic ligand. Among all of the modified ORNs studied, this was the case with the ORN containing a 2-(3,5-dimethylpyrazol-1-yl)-6-oxopurine base. This was found in the presence of both Cu^{2+} and Zn^{2+} more efficiently than the other modified ORNs studied exhibiting some base-selectivity.

While 2,6-bis(3,5-dimethylpyrazol-1-yl)purine riboside could not serve as anionic ligand, it still substantially enhanced duplex formation when situated at the 3´-terminus of the ORN. For example, the T_m value of duplexes of a 5-mer ORN with a longer target was increased by 23-26 ºC upon addition of 1 equiv. of Cu^{2+}. This increase of T_m for two terminal **X**:Cu:U and **Z**:Cu:U metal-ion-mediated base pairs are respectively 33 ºC and 30 ºC more than the stabilization with natural A:U. Binding to U and G that may serve as anionic ligands was preferred over C and A. The base-selectivity reversed to favor C and A when bulky 2,6-bis(3,5-dimethylpyrazol-1-yl)purine riboside was situated in a non-terminal position. The difficulty of accommodating modification in the middle of a double helix was also evident from the results of fluorometric studies. When situated opposite to fluorescent pyrrole-dC, (3,5-dimethylpyrazol-1-yl)purine forced the pyrrolocytosine base to flip out, as evidenced by marked increase in fluorescence emission. Addition of Cu^{2+}, however, resulted in formation of a Cu^{2+}-mediated base pair: T_m was increased and fluorescence emission reduced.

The results obtained with the TAR RNA models were not as clear as those obtained with simple duplexes and, therefore, hybridization of the metal-ion-binding oligonucleotides with the desired target site could not be unambiguously established. It seems possible that even with the stabilizing effect of the metal-ion-mediated base pair, the affinity of the modified oligonucleotides for the very short target sequence remains too low.

6. EXPERIMENTAL

6.1 General methods

The modified nucleosides synthesized were characterized by micrOTOF-Q ESI-MS, ^{1}H NMR, ^{13}C NMR and ^{31}P NMR and HSQC (or COSY) spectrometry. The NMR spectra were recorded on a 400 or 500 MHz spectrometer and the chemical shifts are given in ppm. The oligonucleotide products were analysed by HPLC and micrOTOF-Q ESI-MS. All oligonucleotides were prepared on an Applied Biosystems 3400 DNA/RNA synthesizer by conventional phosphoramidite strategy. The synthetic methods for all compounds of this thesis are described in detail in the original publications (I-III).[118-120,128]

6.2 Melting temperature studies

The UV melting curves (absorbance versus temperature) were measured by monitoring the temperature dependence of the absorbance at 260 nm on a Perkin-Elmer Lambda 35 UV-vis spectrophotometer equipped with a Peltier temperature controller. The temperature was changed at a rate of 0.5 °C min^{-1} from 10 to 90 °C. The measurements were carried out at pH 7.4 in 20 mM cacodylate buffer and ionic strength of 0.10 M, adjusted with $NaClO_4$. For all measurements the concentration of the oligonucleotides and $CuSO_4$, $Zn(NO_3)_2$ or K_2PdCl_4 (where applicable) was 3 μM. The T_m values were determined as maximum values of the first derivatives of the melting curves.

6.3 CD measurements

The CD spectra were acquired by an Applied Photophysics Chirascan Spectropolarimeter. The temperature range was from 6 to 94 °C and scan range was between 220 and 320 nm.

6.4 Kinetic measurements

The method of kinetic measurements is reported in detail in the original publication (III).[119] The pseudo first-order rate constants for the disappearance of **ON5Xa** were obtained by applying the integrated first-order rate equation (Eq. 1) to the time-dependent diminution of the relative signal area of the starting material.

$\ln[A1/A2]_t = -kt + \ln[A1/A2]_0$ (1)

The signal area for the starting material (A1) was normalized by dividing it with the signal area of the internal standard (A2) (potassium 4-nitrobenzenesulfonate).

6.5 Fluorometric studies

Fluorescence emission spectra were obtained using a Cary Eclipse fluorescence spectrophotometer between 400 and 600 nm with an excitation wavelength of 337 (1 nm bandwidth). The scan rate of emission excitation spectra was 120 nm min^{-1} with a slit of 5 nm and a PMT voltage of 600 V. The concentration of oligonucleotides and $CuSO_4$ or $Zn(NO_3)_2$ was 2.0 µM and sample buffer and conditions were the same as reported above for the T_m measurements. Before fluorescence measurements all samples were quickly heated to approximately 90 °C and then allowed to slowly cool down in a standard 10 mm, 3.5 mL square Quartz Fluorescence cuvette. The measurements were carried out at room temperature.

7. REFERENCES

1. Huettenhofer, A.; Schattner, P.; Polacek, N. *Trends Genet.* **2005**, *21*, 289.

2. Reidhaar-Olson, J. F.; Rondinone, C. M. *Methods Mol Biol* **2009**, *555*, v.

3. Nelson, K. M.; Weiss, G. J. *Mol. Cancer Ther.* **2008**, *7*, 3655.

4. Ling, H.; Fabbri, M.; Calin, G. A. *Nat. Rev. Drug Discovery* **2013**, *12*, 847.

5. Schoeniger, C.; Arenz, C. *Bioorg. Med. Chem.* **2013**, *21*, 6115.

6. Karolina, D. S.; Jeyaseelan, K.; In Advanced Delivery and Therapeutic Applications of RNAi (Ed. Cheng, K. and Mahato, R. I.), John Wiley & Sons Ltd., Chichester, West Sussex, UK 2013, 439.

7. Ghildiyal, M.; Zamore, P. D. *Nat. Rev. Genet.* **2009**, *10*, 94.

8. Garzon, R.; Marcucci, G.; Croce, C. M. *Nat. Rev. Drug Discovery* **2010**, *9*, 775.

9. Broderick, J. A.; Zamore, P. D. *Gene Ther.* **2011**, *18*, 1104.

10. Condorelli, G.; Latronico, M. V. G.; Dorn, G. W., II *Eur. Heart J.* **2010**, *31*, 649.

11. Swaminathan, S.; Murray, D. D.; Kelleher, A. D. *AIDS* **2012**, *26*, 1325.

12. Ouellet, D. L.; Plante, I.; Barat, C.; Tremblay, M. J.; Provost, P. *Methods Mol. Biol.* **2009**, *487*, 415.

13. Boden, D.; Pusch, O.; Silbermann, R.; Lee, F.; Tucker, L.; Ramratnam, B. *Nucleic Acids Res.* **2004**, *32*, 1154.

14. Nathans, R.; Chu, C.-Y.; Serquina, A. K.; Lu, C.-C.; Cao, H.; Rana, T. M. *Mol. Cell* **2009**, *34*, 696.

15. Scott, G. K.; Goga, A.; Bhaumik, D.; Berger, C. E.; Sullivan, C. S.; Benz, C. C. *J. Biol. Chem.* **2007**, *282*, 1479.

16. Johnson, S. M.; Grosshans, H.; Shingara, J.; Byrom, M.; Jarvis, R.; Cheng, A.; Labourier, E.; Reinert, K. L.; Brown, D.; Slack, F. J. *Cell* **2005**, *120*, 635.

17. Johnson, C. D.; Esquela-Kerscher, A.; Stefani, G.; Byrom, M.; Kelnar, K.; Ovcharenko, D.; Wilson, M.; Wang, X.; Shelton, J.; Shingara, J.; Chin, L.; Brown, D.; Slack, F. J. *Cancer Res.* **2007**, *67*, 7713.

18. Lee, Y. S.; Dutta, A. *Genes Dev.* **2007**, *21*, 1025.

19. Kumar, M. S.; Erkeland, S. J.; Pester, R. E.; Chen, C. Y.; Ebert, M. S.; Sharp, P. A.; Jacks, T. *Proc. Natl. Acad. Sci. USA* **2008**, *105*, 3903.

20. He, L.; He, X.; Lim, L. P.; de, S. E.; Xuan, Z.; Liang, Y.; Xue, W.; Zender, L.; Magnus, J.; Ridzon, D.; Jackson, A. L.; Linsley, P. S.; Chen, C.; Lowe, S. W.; Cleary, M. A.; Hannon, G. J. *Nature* **2007**, *447*, 1130.

21. Weiss, G. J.; Bemis, L. T.; Nakajima, E.; Sugita, M.; Birks, D. K.; Robinson, W. A.; Varella-Garcia, M.; Bunn, P. A., Jr.; Haney, J.; Helfrich, B. A.; Kato, H.; Hirsch, F. R.; Franklin, W. A. *Ann. Oncol.* **2008**, *19*, 1053.

22. Kefas, B.; Godlewski, J.; Comeau, L.; Li, Y.; Abounader, R.; Hawkinson, M.; Lee, J.; Fine, H.; Chiocca, E. A.; Lawler, S.; Purow, B. *Cancer Res.* **2008**, *68*, 3566.

23. Kool, E. T. *Annu. Rev. Biophys. Biomol. Struct.* **2001**, *30*, 1.

24. Turner, D. H.; Sugimoto, N.; Kierzek, R.; Dreiker, S. D. *J. Am. Chem. Soc.* **1987**, *109*, 3783.

25. McGregor, H. C. J.; Gunderman, R. B. *Am. J. Roentgenol.* **2011**, *196*, W689.

26. Müller, J. *Eur. J. Inorg. Chem.* **2008**, 3749.

27. Müller, J.; Böhme, D.; Duepre, N.; Mehring, M.; Polonius, F.-A. *J. Inorg. Biochem.* **2007**, *101*, 470.

28. Zhu, W.; Luo, X.; Puah, C. M.; Tan, X.; Shen, J.; Gu, J.; Chen, K.; Jiang, H. *J. Phys. Chem. A* **2004**, *108*, 4008.

29. Samanta, P. K.; Pati, S. K. *Chem. Eur. J.* **2014**, *20*, 1760.

30. Ahmadi, M. S.; Shakourian-Fard, M.; Fattahi, A. *Struct. Chem.* **2012**, *23*, 613.

31. Megger, D. A.; Müller, J. *Nucleos. Nucleot. Nucl.* **2010**, *29*, 27.

32. Mei, H.; Yang, H.; Roehl, I.; Seela, F. *ChemPlusChem* **2014**, *79*, 914.

33. Tanaka, Y.; Oda, S.; Yamaguchi, H.; Kondo, Y.; Kojima, C.; Ono, A. *J. Am. Chem. Soc.* **2007**, *129*, 244.

34. Lapham, J.; Rife, J. P.; Moore, P. B.; Crothers, D. M. *J. Biomol. NMR* **1997**, *10*, 255.

35. Aich, P.; Labiuk, S. L.; Tari, L. W.; Delbaere, L. J. T.; Roesler, W. J.; Falk, K. J.; Steer, R. P.; Lee, J. S. *J. Mol. Biol.* **1999**, *294*, 477.

36. Martin, R. B. *Acc. Chem. Res.* **1985**, *18*, 32.

37. Lönnberg, H.; Arpalahti, J. *Inorg. Chim. Acta* **1981**, *55*, 39.

38. Wagenknecht, H.-A. *Angew. Chem., Int. Ed.* **2003**, *42*, 3204.

39. Müller, J.; Freisinger, E.; Lax, P.; Megger, D. A.; Polonius, F.-A. *Inorg. Chim. Acta* **2007**, *360*, 255.

40. Böhme, D.; Düpre, N.; Megger, D. A.; Müller, J. *Inorg. Chem.* **2007**, *46*, 10114.

41. Hensel, S.; Megger, N.; Schweizer, K.; Müller, J. *Beilstein J. Org. Chem.* **2014**, *10*, 2139.

42. Richters, T.; Müller, J. *Eur. J. Inorg. Chem.* **2014**, *2014*, 437.

43. Richters, T.; Krug, O.; Kösters, J.; Hepp, A.; Müller, J. *Chem. Eur. J.* **2014**, *20*, 7811.

44. Tanaka, K.; Tengeiji, A.; Kato, T.; Toyama, N.; Shiro, M.; Shionoya, M. *J. Am. Chem. Soc.* **2002**, *124*, 12494.

45. Switzer, C.; Shin, D. *Chem. Commun.* **2005**, 1342.

46. Meggers, E.; Holland, P. L.; Tolman, W. B.; Romesberg, F. E.; Schultz, P. G. *J. Am. Chem. Soc.* **2000**, *122*, 10714.

47. Heuberger, B. D.; Shin, D.; Switzer, C. *Org. Lett.* **2008**, *10*, 1091.

48. Takezawa, Y.; Shionoya, M. *Acc. Chem. Res.* **2012**, *45*, 2066.

49. Clever, G. H.; Kaul, C.; Carell, T. *Angew. Chem., Int. Ed.* **2007**, *46*, 6226.

50. Zimmermann, N.; Meggers, E.; Schultz, P. G. *J. Am. Chem. Soc.* **2002**, *124*, 13684.

51. Tanaka, K.; Yamada, Y.; Shionoya, M. *J. Am. Chem. Soc.* **2002**, *124*, 8802.

52. Takezawa, Y.; Maeda, W.; Tanaka, K.; Shinoya, M. *Angew. Chem., Int. Ed.* **2009**, *48*, 1081.

53. Eichhorn, G. L.; Shin, Y. A. *J. Amer. Chem. Soc.* **1968**, *90*, 7323.

54. Izatt, R. M.; Christensen, J. J.; Rytting, J. H. *Chem. Rev.* **1971**, *71*, 439.

55. Eichhorn, G. L.; Butzow, J. J.; Clark, P.; Tarien, E. *Biopolymers* **1967**, *5*, 283.

56. Jensen, R. H.; Davidson, N. *Biopolymers* **1966**, *4*, 17.

57. Katz, S. *Biochim. Biophys. Acta, Spec. Sect. Nucleic Acids Relat. Subj.* **1963**, *68*, 240.

58. Kosturko, L. D.; Folzer, C.; Stewart, R. F. *Biochemistry* **1974**, *13*, 3949.

59. Johannsen, S.; Paulus, S.; Düpre, N.; Müller, J.; Sigel, R. K. O. *J. Inorg. Biochem.* **2008**, *102*, 1141.

60. Ono, A.; Cao, S.; Togashi, H.; Tashiro, M.; Fujimoto, T.; Machinami, T.; Oda, S.; Miyake, Y.; Okamoto, I.; Tanaka, Y. *Chem. Commun.* **2008**, 4825.

61. Torigoe, H.; Okamoto, I.; Dairaku, T.; Tanaka, Y.; Ono, A.; Kozasa, T. *Biochimie* **2012**, *94*, 2431.

62. Wettig, S. D.; Wood, D. O.; Lee, J. S. *J. Inorg. Biochem.* **2003**, *94*, 94.

63.   Colombier, C.; Lippert, B.; Leng, M. *Nucleic Acids Res* **1996**, *24*, 4519.

64.   Lee, J. S.; Latimer, L. J. P.; Reid, R. S. *Biochem. Cell Biol.* **1993**, *71*, 162.

65.   Fusch, E. C.; Lippert, B. *J. Am. Chem. Soc.* **1994**, *116*, 7204.

66.   Alexandre, S. S.; Soler, J. M.; Seijo, L.; Zamora, F. *Phys. Rev. B: Condens. Matter Mater. Phys.* **2006**, *73*, 205112/1.

67.   Kondo, J.; Yamada, T.; Hirose, C.; Okamoto, I.; Tanaka, Y.; Ono, A. *Angew. Chem., Int. Ed.* **2014**, *53*, 2385.

68.   Ono, A.; Togashi, H. *Angew. Chemie* **2004**, *116*, 4400.

69.   Miyake, Y.; Togashi, H.; Tashiro, M.; Yamaguchi, H.; Oda, S.; Kudo, M.; Tanaka, Y.; Kondo, Y.; Sawa, R.; Fujimoto, T.; Machinami, T.; Ono, A. *J. Am. Chem. Soc.* **2006**, *128*, 2172.

70.   Yamaguchi, H.; Sebera, J.; Kondo, J.; Oda, S.; Komuro, T.; Kawamura, T.; Dairaku, T.; Kondo, Y.; Okamoto, I.; Ono, A.; Burda, J. V.; Kojima, C.; Sychrovsky, V.; Tanaka, Y. *Nucleic Acids Res.* **2014**, *42*, 4094.

71.   Fortino, M.; Marino, T.; Russo, N. *J. Phys. Chem. A* **2015**, *119*, 5153.

72.   Ennifar, E.; Walter, P.; Dumas, P. *Nucleic Acids Res.* **2003**, *31*, 2671.

73.   Gray, D. M.; Hung, S.-H.; Johnson, K. H. *Methods Enzymol.* **1995**, *246*, 19.

74.   Gray, D. M.; Ratliff, R. L.; Vaughan, M. R. *Methods Enzymol.* **1992**, *211*, 389.

75.   Müller, J.; Böhme, D.; Lax, P.; Cerda, M. M.; Roitzsch, M. *Chem. Eur. J.* **2005**, *11*, 6246.

76.   Mandal, S.; Hepp, A.; Müller, J. *Dalton Trans.* **2015**, *44*, 3540.

77.   Kumbhar, S.; Johannsen, S.; Sigel, R. K. O.; Waller, M. P.; Müller, J. *J. Inorg. Biochem.* **2013**, *127*, 203.

78.   Johannsen, S.; Megger, N.; Böhme, D.; Sigel, R. K. O.; Müller, J. *Nat Chem* **2010**, *2*, 229.

79.   Okamoto, I.; Ono, T.; Sameshima, R.; Ono, A. *Chem. Commun.* **2012**, *48*, 4347.

80.   Mei, H.; Ingale, S. A.; Seela, F. *Chem. Eur. J.* **2014**, *20*, 16248.

81.   Tanaka, K.; Shionoya, M. *J. Org. Chem.* **1999**, *64*, 5002.

82.   Tasaka, M.; Tanaka, K.; Shiro, M.; Shionoya, M. *Supramol. Chem.* **2001**, *13*, 671.

83.   Tanaka, K.; Tasaka, M.; Cao, H.; Shionoya, M. *Eur. J. Pharm. Sci.* **2001**, *13*, 77.

84.   Cao, H.; Tanaka, K.; Shionoya, M. *Chem. Pharm. Bull.* **2000**, *48*, 1745.

85.   Tanaka, K.; Tengeiji, A.; Kato, T.; Toyama, N.; Shionoya, M. *Science* **2003**, *299*, 1212.

86.   Takezawa, Y.; Tanaka, K.; Yori, M.; Tashiro, S.; Shiro, M.; Shionoya, M. *J. Org. Chem.* **2008**, *73*, 6092.

87.   Brotschi, C.; Haberli, A.; Leumann, C. J. *Angew. Chem., Int. Ed.* **2001**, *40*, 3012.

88.   Brotschi, C.; Leumann, C. J. *Nucleos. Nucleot. Nucl.* **2003**, *22*, 1195.

89.   Weizman, H.; Tor, Y. *J. Am. Chem. Soc.* **2001**, *123*, 3375.

90.   Switzer, C.; Sinha, S.; Kim, P. H.; Heuberger, B. D. *Angew. Chem., Int. Ed.* **2005**, *44*, 1529.

91.   Kim, E.-K.; Switzer, C. *Org. Lett.* **2014**, *16*, 4059.

92.   Clever, G. H.; Soeltl, Y.; Burks, H.; Spahl, W.; Carell, T. *Chem. Eur. J.* **2006**, *12*, 8708.

93.   Clever, G. H.; Polborn, K.; Carell, T. *Angew. Chem., Int. Ed.* **2005**, *44*, 7204.

94.   Clever, G. H.; Carell, T. *Angew. Chem., Int. Ed.* **2007**, *46*, 250.

95.   Tanaka, K.; Clever, G. H.; Takezawa, Y.; Yamada, Y.; Kaul, C.; Shionoya, M.; Carell, T. *Nat. Nanotechnol.* **2006**, *1*, 190.

96.   Müller, J. *Nature* **2006**, *444*, 698.

97. Atwell, S.; Meggers, E.; Spraggon, G.; Schultz, P. G. *J. Am. Chem. Soc.* **2001**, *123*, 12364.

98. Zimmermann, N.; Meggers, E.; Schultz, P. G. *Bioorg. Chem.* **2004**, *32*, 13.

99. Shin, D.; Switzer, C. *Chem. Commun.* **2007**, 4401.

100. Litau, S.; Müller, J. *J. Inorg. Biochem.* **2015**, *148*, 116.

101. Wing, R.; Drew, H.; Takano, T.; Broka, C.; Tanaka, S.; Itakura, K.; Dickerson, R. E. *Nature* **1980**, *287*, 755.

102. Seela, F.; Wenzel, T. *Helv. Chim. Acta* **1994**, *77*, 1485.

103. Seela, F.; Wenzel, T.; Debelak, H. *Nucleos. Nucleot.* **1995**, *14*, 957.

104. Polonius, F.-A.; Müller, J. *Angew. Chem., Int. Ed.* **2007**, *46*, 5602.

105. Ipsaro, J. J.; Joshua-Tor, L. *Nat. Struct. Mol. Biol.* **2015**, *22*, 20.

106. Li, J.; Tan, S.; Kooger, R.; Zhang, C.; Zhang, Y. *Chem. Soc. Rev.* **2014**, *43*, 506.

107. Shah, M. Y.; Calin, G. A. *Nucleic Acid Ther.* **2013**, *23*, 2.

108. Dong, H.; Lei, J.; Ding, L.; Wen, Y.; Ju, H.; Zhang, X. *Chem. Rev.* **2013**, *113*, 6207.

109. Li, Z.; Rana, T. M. *Nat. Rev. Drug Discov.* **2014**, *13*, 622.

110. Cheng, C. J.; Bahal, R.; Babar, I. A.; Pincus, Z.; Barrera, F.; Liu, C.; Svoronos, A.; Braddock, D. T.; Glazer, P. M.; Engelman, D. M.; Saltzman, W. M.; Slack, F. J. *Nature* **2015**, *518*, 107.

111. Jayaraj, G. G.; Nahar, S.; Maiti, S. *Chem. Commun.* **2015**, *51*, 820.

112. Ouellet, D. L.; Plante, I.; Landry, P.; Barat, C.; Janelle, M.-E.; Flamand, L.; Tremblay, M. J.; Provost, P. *Nucleic Acids Res.* **2008**, *36*, 2353.

113. Klase, Z.; Winograd, R.; Davis, J.; Carpio, L.; Hildreth, R.; Heydarian, M.; Fu, S.; McCaffrey, T.; Meiri, E.; Ayash-Rashkovsky, M.; Gilad, S.; Bentwich, Z.; Kashanchi, F. *Retrovirology* **2009**, *6*, 18.

114. Takahashi, M.; Yamada, N.; Hatakeyama, H.; Murata, M.; Sato, Y.; Minakawa, N.; Harashima, H.; Matsuda, A. *Nucleic Acids Res.* **2013**, *41*, 10659.

115. Deleavey, G. F.; Damha, M. J. *Chem. Biol.* **2012**, *19*, 937.

116. (116) Niiya, K.; Olsson, R. A.; Thompson, R. D.; Silvia, S. K.; Ueeda, M. *J. Med. Chem.* **1992**, *35*, 4557.

117. Brien, K. A.; Garner, C. M.; Pinney, K. G. *Tetrahedron* **2006**, *62*, 3663.

118. Taherpour, S.; Lönnberg, T. *J. Nucleic acids* **2012**, *2012*, 196845.

119. Taherpour, S.; Golubev, O.; Lönnberg, T. *The J. Org. Chem.* **2014**, *79*, 8990.

120. Taherpour, S.; Lönnberg, H.; Lönnberg, T. *Org. Biomol. Chem.* **2013**, *11*, 991.

121. Cantor, C. R.; Warshaw, M. M.; Shapiro, H. *Biopolymers* **1970**, *9*, 1059.

122. Cavaluzzi, M. J.; Borer, P. N. *Nucleic Acids Res.* **2004**, *32*, 1.

123. Tataurov, A. V.; You, Y.; Owczarzy, R. *Biophys. Chem.* **2008**, *133*, 66.

124. Halcrow, M. A. *Coord. Chem. Rev.* **2005**, *249*, 2880.

125. Brahms, J.; Maurizot, J. C.; Michelso.Am *J. Mol. Biol.* **1967**, *25*, 465.

126. Bush, C. A.; Scheraga, H. A. *Biopolymers* **1969**, *7*, 395.

127. Steely, H. T.; Gray, D. M.; Ratliff, R. L. *Nucleic Acids Res.* **1986**, *14*, 10071.

128. Taherpour, S.; Lönnberg, T. *RSC Adv.* **2015**, *5*, 10837.

129. Berry, D. A.; Jung, K.-Y.; Wise, D. S.; Sercel, A. D.; Pearson, W. H.; Mackie, H.; Randolph, J. B.; Somers, R. L. *Tetrahedron Lett.* **2004**, *45*, 2457.

130. Sukackaite, R.; Grazulis, S.; Tamulaitis, G.; Siksnys, V. *Nucleic Acids Res.* **2012**, *40*, 7552.

131. Sinha, I.; Koesters, J.; Hepp, A.; Müller, J. *Dalton Trans.* **2013**, *42*, 16080.

132. Maskos, K. *Acta Biochim. Pol.* **1978**, *25*, 311.

133. Maskos, K. *Acta Biochim. Pol.* **1978**, *25*, 101.

134. Kistenmacher, T. J.; Marzilli, L. G.; Szalda, D. J. *Acta Crystallogr. Sect. B Struc. Sci.* **1976**, *32*, 186.

135. Sletten, E.; Thorsten.B *Acta Crystallogr. Sect. B Struc. Sci.* **1974**, *30*, 2438.

136. Arpalahti, J.; Lönnberg, H. *Inorg. Chim. A-Bioinorg.* **1983**, *78*, 63.

137. Tauler, R.; Rainer, M. J. A.; Rode, B. M. *Inorg. Chim. A-Bioinorg.* **1986**, *123*, 75.

138. Fazakerley, G. V.; Jackson, G. E.; Phillips, M. A.; Vanniekerk, J. C. *Inorg. Chim. Acta* **1979**, *35*, 151.

139. Frøystein, N. A.; Sletten, E. *Inorg. Chim. A-Bioinorg.* **1987**, *138*, 49.

140. Kinjo, Y.; Tribolet, R.; Corfu, N. A.; Sigel, H. *Inorg. Chem.* **1989**, *28*, 1480.

141. Berger, N. A.; Eichhorn, G. L. *J. Am. Chem. Soc.* **1971**, *93*, 7062.

142. Maskos, K. *Acta Biochim. Pol.* **1981**, *28*, 317.

143. Kim, S. H.; Martin, R. B. *Inorg. Chim. A-Bioinorg.* **1984**, *91*, 19.

144. Maskos, K. *Acta Biochim. Pol.* **1979**, *26*, 249.

145. Szalda, D. J.; Kistenmacher, T. J. *Acta Crystallogr. Sect. B Struc. Sci.* **1977**, *33*, 865.

146. Kotowycz, G. *Can. J. Chem.* **1974**, *52*, 924.

147. Marzilli, L. G.; Stewart, R. C.; Vanvuuren, C. P.; Castro, B. D.; Caradonna, J. P. *J. Am. Chem. Soc.* **1978**, *100*, 3967.

148. Chao, Y. Y. H.; Kearns, D. R. *J. Am. Chem. Soc.* **1977**, *99*, 6425.

149. Maskos, K. *Acta Biochim. Pol.* **1974**, *21*, 255.

150. Marzilli, L.; Trogler, W. C.; Hollis, D. P.; Kistenmacher, T. J.; Chang, C. H.; Hanson, B. E. *Inorganic Chemistry* **1975**, *14*, 2568.

151. Eichhorn, G. L.; Clark, P.; Becker, E. D. *Biochemistry* **1966**, *5*, 245.

152. Burger, K. *Biocoordination Chemistry: Coordination Equilibria in Biologically Active Systems*; (Ed. Horwood, E), New York, **1990**.

153. Masoud, M. S.; Soayed, A. A.; Ali, A. E. *Spectrochim. Acta Part A* **2004**, *60*, 1907.

154. Marino, N.; Armentano, D.; Mastropietro, T. F.; Julve, M.; Lloret, F.; De Munno, G. *Cryst. Growth Des.* **2010**, *10*, 1757.

155. McCall, M. J.; Taylor, M. R. *Biochim. Biophys. Acta* **1975**, *390*, 137.

156. Holthenrich, D.; Krumm, M.; Zangrando, E.; Pichierri, F.; Randaccio, L.; Lippert, B. *J. Chem. Soc. Dalton Trans.* **1995**, 3275.

157. Schlegel, M. K.; Zhang, L.; Pagano, N.; Meggers, E. *Org. Biomol. Chem.* **2009**, *7*, 476.

158. Seubert, K.; Böhme, D.; Kösters, J.; Shen, W.-Z.; Freisinger, E.; Müller, J. *Z. Anorg. Allg. Chem.* **2012**, *638*, 1761.